Physical processes and their influence on the biological productivity of Andaman waters during winter monsoon

Thesis submitted to

Cochin University of Science and Technology

in Partial Fulfilment of the Requirements for

the Award of the Degree of

Doctor of Philosophy

in

Physical Oceanography

Under the Faculty of Marine Sciences

By

Salini T. C.
Reg. No. 4009

DEPARTMENT OF PHYSICAL OCEANOGRAPHY
SCHOOL OF MARINE SCIENCES
COCHIN UNIVERSITY OF SCIENCE AND TECHNOLOGY
KOCHI –682 016, INDIA

October 2018

Physical processes and their influence on the biological productivity of Andaman waters during winter monsoon

Ph.D. Thesis in Physical Oceanography under the Faculty of Marine Sciences

Author

Salini T. C.
Research Scholar
Department of Physical Oceanography
School of Marine Sciences
Cochin University of Science and Technology
Kochi – 682 016
e-mail: salinitc@gmail.com

Supervising Guide

Dr. R. Sajeev
Associate Professor & Head
Department of Physical Oceanography
School of Marine Sciences
Cochin University of Science and Technology
Cochin 682 016
Email:rsajeev@yahoo.com

Department of Physical Oceanography
School of Marine Sciences
Cochin University of Science and Technology
Cochin 682 016

October 2018

DEPARTMENT OF PHYSICAL OCEANOGRAPHY
SCHOOL OF MARINE SCIENCES
COCHIN UNIVERSITY OF SCIENCE AND TECHNOLOGY
KOCHI –682 016, INDIA

Dr. R. Sajeev
Associate Professor & Head

Certificate

This is to certify that the thesis entitled **"Physical processes and their influence on the biological productivity of Andaman waters during winter monsoon"** is an authentic record of the research work carried out by **Mrs. Salini T. C.** under my supervision and guidance at the Department of Physical Oceanography, Cochin University of Science and Technology, Cochin 682 016, in partial fulfilment of the requirements for Ph.D degree of Cochin University of Science and Technology and no part of this has been presented before for any degree in any university. All the relevant corrections and modifications suggested by the audience during the pre-synopsis seminar and recommended by the Doctoral committee have been incorporated in the thesis.

Kochi - 16
8th October 2018

Dr. R. Sajeev
(Supervising Guide)

Declaration

I hereby declare that the thesis entitled **"Physical processes and their influence on the biological productivity of Andaman waters during winter monsoon"** is an authentic record of research work carried out by me under the supervision and guidance of Dr. R. Sajeev, Associate Professor, Department of Physical Oceanography, Cochin University of Science and Technology towards the partial fulfillment of the requirements for the award of Ph.D. degree under the Faculty of Marine Sciences and no part thereof has been presented for the award of any other degree in any University/Institute.

Kochi-16 **Salini T. C.**

8th October 2018

Dedicated to...

My Parents & Husband....

Acknowledgement

I am ever grateful to my much loved guide Dr. R. Sajeev for his guidance, encouragement, support, constructive criticism and patience throughout these eight years, which provided me with the motivation and encouragement at the time when I needed it.

In particular, I thank Dr. B. R. Smitha, Scientist, Centre for Marine Living Resources and "Ecology (CMLRE), Kochi for her constant support of scientific merits of this study and extensive knowledge of the field for her interest in this research.

Prof. (Dr). A. N. Balchand (Department of Physical Oceanography) and Prof. (Dr) Chandramohanakumar (Department of Chemical Oceanography) also deserve special thanks as my doctoral committee members and advisors.

I wish to express my sincere thanks to Dr. V. N. Sanjeevan, Former Director, CMLRE (MoES, Govt. of India) for giving me an opportunity to work as a Junior and Senior Research Fellow in the project entitled "Environmental Productivity Patterns of Indian EEZ" and permitting me to take in situ collections from Andaman waters, to which the present thesis is associated.

I extend my sincere thanks to Dr. K.M Santhosh , Dr. P K Saji, Dr. V.Vijith, and Mrs. Thanvi Fathima Rahman, Department of Physical Oceanography, for their timely advice, suggestions and encouragement during the research period. My heartfelt thanks to Late. Prof. (Dr). Raman Laxman for the English correction of my theisis chapters and support during the period of my doctoral research.

Particularly, I would like to thank my friend and classmate Mr. Lix John K., Department of Physical Oceanography for his scientific discussion and support and Mr. Midhunshah Hussain and Mr. Rafeeq M. for generating the plot for the study.

I also thank all institutions around the world that maintain and allow public access to observational, reconstructed, or other data sets used in this thesis and to all people who supported me with this thesis.

It is my pleasure to acknowledge my friends Mr. Vimal Kumar, Dr. Aiswarya Gopal, Mrs. Renjima, Mrs. Remya P. Arjunan and Dr. Prescilla Kurien for their help and encouragement.

My thanks to my lovely son Aadhikesh, daughter Swara, my extended family members especially my mother Rugmany, father Chandran and my sister Charutha for continuing support and tolerance, to my husband Sanjay whose help during all these years cannot be overestimated.

Most importantly, I thank Almighty God for His blessings throughout my life that enabled me to fulfill this endeavour.

Salini T. C.

Preface

The Andaman Sea, eastern part of the Indian Ocean lies between Andaman and Nicobar Islands in the west and Sumatra in the south and Malaysia, Thailand and Myanmar in the north and east. The sea connects with Bay of Bengal through three channels 1) Preparis channel at north, Ten Degree channel at 10°N and Great channel at south. Three rivers entering into the sea are Ayeyarwady, Salween and Sittang play a key role in the dynamics. The sea is connected with South China Sea through the Strait of Malacca at south east.

The ocean dynamics of the area is primarily influenced by the seasonally reversing winds and currents. The area experiences southwest monsoon winds from June through September and the northeast monsoon winds are active from December through February. Circulation pattern in Andaman Sea shows a clockwise gyre during the northeast monsoon and an anticlockwise gyre during the southwest monsoon (Varkey et al., 1996). Many studies have been carried out for understanding the hydrographical pattern and biological production of the Andaman Sea (Rama Raju et al., 1981, Geetha et al., 1997, Varkey et al., 1996). The studies are limited to understand the physical processes, circulation and driving force for the upper layer processes. The role of local/remote forcing in driving the upper layer dynamics needs to be described. The present study is aimed to find out the role of freshwater from Ayeyarwady – Salween system and Malacca Strait water on the hydrography and oceanography of the region and the role of local/remote forcing on the upper layer processes.

The thesis is formulated as five chapters. The first chapter gives an overview of general atmospheric forcing, hydrography, geology, plate tectonics, biological production and a brief description of coral bleaching in Andaman Sea. This chapter contains a brief review of the work carried out in Andaman waters. The chapter also contains scope of study and the specific objectives.

Details on data source and methodology adopted and the analysis made to notice the hydrography, circulation and biological response of Andaman waters are described in the second chapter.

The identification of cold core eddy from in situ and satellite observations, characteristics of the eddy, its influence on the hydrodynamics, the generation mechanism and the biological response are explained in the third chapter.

Chapter four gives a complete depiction of the role of forcing factors controlling the upper layer dynamics using the spatio-temporal analysis of wind, sea surface height anomaly and SST. The chapter also gives the spatial variation of chlorophyll a in Andaman waters.

Major achievements of the present study are summarized in the fifth chapter. Shortfalls and suggestions for future works in the area are also enlisted. The references made during the study are included in the reference section followed by list of publications and reprints of papers published.

Contents

List of Figures

Acronyms and Abbreviations

ADCP	Acoustic Doppler Current Profiler
AS	Arabian Sea
ASCAT	Advanced Scatterometer
AVISO	Archiving Validation and Interpretation of Satellite Oceanography
AWS	Automated Weather Station
BL	Barrier Layer
BoB	Bay of Bengal
BOBMEX	Bay of Bengal Monsoon Experiment
BOPS	Bay of Bengal Process Studies
BV	Brunt Vaisala
CE	Cyclonic Eddy
chl a	Chlorophyll
COARE	Coupled Ocean-Atmosphere Response Experiment
DO	Dissolved Oxygen
EICC	East India Coastal Current
EIO	Equatorial Indian Ocean
ENSO	El-Niño Southern Oscillation
et.al	And others
Fig.	Figure
IIOE	International Indian Ocean Expedition
ILD	Isothermal Layer Depth
IOD	Indian Ocean Dipole
LCS	Linear Continuously Stratified
MLD	Mixed Layer Depth
NEC	North Equatorial Current
NEM	Northeast Monsoon

NOAA	National Oceanic and Atmospheric Administration
OAFlux	Objectively Analysed air-sea Heat Fluxes
OGCM	Ocean General Circulation Model
PODAAC	Physical Oceanography Distributed Active Archive Center
PP	Primary Productivity
psu	practical salinity unit
QuikSCAT	Quick Scatterometer
Ri	Richardson Number
SMC	Southwest Monsoon Current
SSHA	Sea Surface Height Anomaly
SSS	Sea Surface Salinity
SST	Sea Surface Temperature
SWM	Southwest Monsoon
TropFlux	Tropical air-sea Heat Fluxes
VGPM	Vertically Generalised Production Model

.....ꕥ.....

Chapter 1

INTRODUCTION

Contents

1.1 Andaman Sea

Andaman Sea is one of the least explored regions of Indian Ocean. It is positioned along the eastern sides of the North Indian Ocean between 6° to 14°N Latitude and 91° to 99°E Longitude. The sea is bordered by Andaman and Nicobar Islands in the west, which comprises of 572 islands and occupy an area of 8293 km^2 with a coastline of 1962 km and account for 30% of the Exclusive Economic Zone of India (Jeyabaskaran, 1999) and Sumatra in the south and Malaysia, Thailand and Myanmar in

the north and east. It covers an area of 6.02×10^5 km^2 and has 6.6×10^3 km^3 volume and an average depth of 1096m (Fig. 1.1).

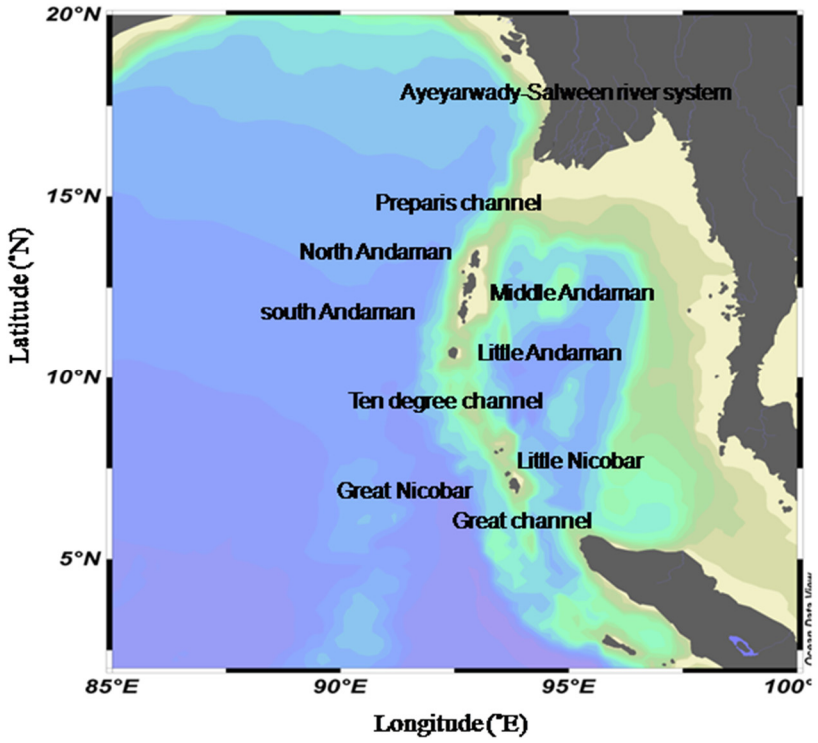

Fig. 1.1: Study Area

A north-south arc of volcanic islands and seamounts, including the Barren and Narcondam islands in the Andaman Sea, demarcates this basin from two smaller basins on the north and south. The sea comprises comparatively wide basin with a maximum depth of 4360m and the eastern side has steeper continental slope compared to western side and erratic bottom topography (Fig. 1.2).

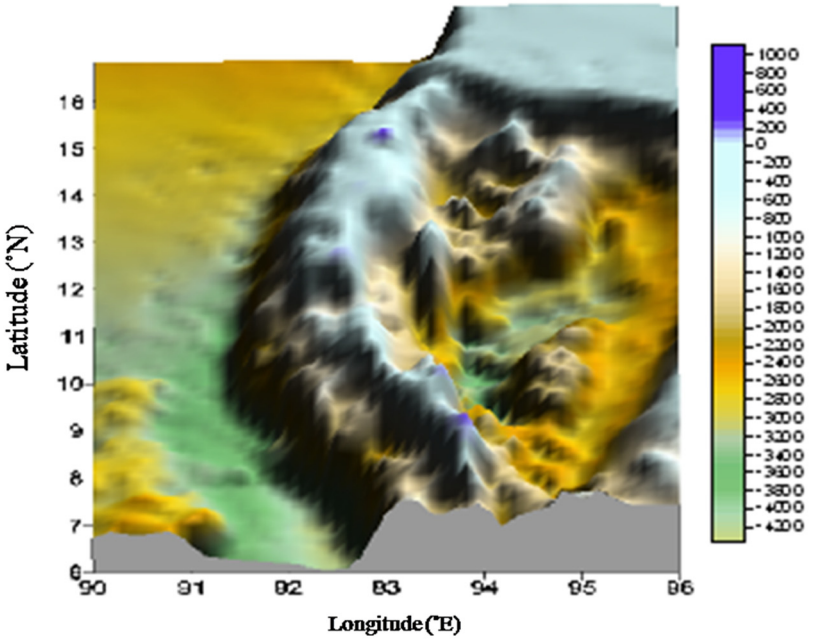

Fig. 1.2: Bottom topography (Sindhu et al., 2007) for the study area derived from NIO's modified datasets

The main source of fresh water to the northeastern part of the sea is from Ayeyarwady (13.6×10^3 m^3/s) and Salween (6.69×10^3 m^3/s) rivers, minor contributions are from Sittang (1.59×10^3 m^3/s) and Tavoy rivers. The anticlinal belt passing from Arakan Yoma in Burma through Andaman and Nicobar Islands and Mentawai Islands west of Sumatra, separate the Andaman Sea from the Bay of Bengal (BoB) by three channels,

1) Preparis channel in the north (200 m)
2) Ten degree channel between Andaman and Nicobar Islands (1800 m) and
3) Great channel between Great Nicobar Island and Sumatra (>1800 m).

The sea is also linked with South China Sea and Pacific Ocean through Malacca Strait in the southeast. Unlike other parts of the coastal India, Andaman and Nicobar area receives enormous rainfall throughout the year except three months. The differential response of the atmospheric forcing exerts major influence on the oceanographical features like sea surface temperature, salinity, stratification, nutrient pattern and biological production including the potential fishery of the region. The following sections explain various features/factors that influence the regulatory mechanism of the ecosystem components and processes of the Andaman waters.

1.2 Atmospheric Forcing

The North Indian Ocean is unique due to the prevalence of reversing monsoon over the area. The winds blow from southwest during summer monsoon (June-Sept) and northeast during winter monsoon (Nov-Feb) and weak winds during the transition period (Mar-May and October), under their influence the circulation reverses twice in a year. During the northeast monsoon (NEM), there is an ingress of lower salinity water mass from the south. This may be attributed to the larger river discharge and introduction of lower salinity water from the South China Sea (SCS). The tremendous influx of fresh water from Ayeyarwady and Salween rivers during the southwest monsoon (SWM) dilutes the waters at the north end of the sea to a salinity of only about 20 practical salinity unit (psu) from June to November. During this period salinity at the southwest end is about 33.5 psu. Winter and spring reflected more normal salinity distribution from 32 to 33.5 psu. The sea surface temperature fluctuates

only very little, from a maximum monthly average of about 30°C in the summer and 27.5°C in the winter.

1.3 Regional circulation pattern

The tropical monsoonal regime is the primary factor regulating the current structure of the Andaman waters. During northeast monsoon, North Equatorial Current (NEC) of 0.3 m/s flows from Malacca Strait to southern SriLanka through Andaman Sea. Southwest monsoon is characterized with the eastward flow of Southwest Monsoon Current (SMC) enters the Andaman Sea via BoB. The surface circulation is a double gyre with anticlockwise flow during the northeast monsoon and clockwise flow in the southwest monsoon. During southwest monsoon, flow enters from BoB, circulates clockwise and exits via the southern Andaman Sea. But during the northeast monsoon, flow enters the Andaman Sea south of the Nicobar Islands and exits south of the Andaman Islands.

Andaman thermohaline stratification is the product of river run off, occurrence of internal waves and exchange of surface water across the shallow passages and the sill depth overflow between Andaman Sea and BoB. During northeast monsoon, upwelling Kelvin waves characterized by low upper layer thickness propagated eastward from equator, impinged on the coast of Northern Sumatra and penetrates into the eastern Andaman Sea. Under favorable wind conditions weak upwelling occurs along the eastern shore of the Andaman Sea.

1.4 Internal waves

Andaman Sea is characterized by extra ordinary large internal wave occurring region in the Indian Ocean (Osborne and Burch, 1980). These waves are the result of interaction of tides with sills and seamounts. In the southern Andaman Sea, these waves propagate several hundreds of kilometers before hitting the Thailand coast. In the northern Andaman Sea, these waves arised when the spring tidal range surpassed 1.5m and the probability increased with increased tidal range. The rippling or choppy water found between Nicobar Islands and north east Sumatra coast are caused by internal solitons. These ripplings cause noise during night time and it beat at the ship's sides. These waves transport momentum and energy within the ocean. The presence of large amplitude internal waves due to non-linear internal tides are reported in Andaman Sea using satellite imagery.

1.5 Geology and Plate tectonics

The geology and plate tectonics of the sea is complex and is linked to the tectonics and geology of Myanmar, Sumatra, Andaman Nicobar Islands and Malay Peninsula (Curray, 2005). The northern side of the basin is shallow and continental shelf off the Myanmar coast extends over 200 km. The continental slope of the eastern shelf is steep between 9°N and 14°N. Due to the silt deposition of Ayeyarwady and Salween river system the northern and eastern parts are shallower than 180 m and the western sides are 900 –3,000 m deep. The major rivers flow into the sea from the north through Myanmar.

The tectonic regions of Andaman Sea can be divided into six (1) The trench-accretionary prism complex including Andaman, Nicobar and Coco Islands in the west (2) Active trans- tensional to strike-slip fault to the east of the accretionary prism complex (the Sumatra Fault Zone and the West Andaman Fault) (3) Alcock and Sewell rises to the east of the strike-slip faults (4) Sediment filled deep water trough called the East Andaman Basin to the east of Alcock and Sewell rises (5) the Mergui Ridge, a basement high which is passing up the continental slope to a drowned shelf in the southern and central part of the eastern Andaman Sea (6) Slope and shelf region of Gulf of Martaban lies in the north of the Alcock Rise, which is the southerly extension of the Myanmar Central Basin.

1.6 Sedimentation

The Ayeyarwady (the fifth largest river in terms of suspended sediment load) together with Salween and Sittang contribute 350 million tons of sediment into the northern Andaman Sea (Robinson et al., 2007). These sediment is transported eastward and deposited in Gulf of Martaban. This sediment transported into the deeper waters of Andaman Sea through the Martaban Canyon is reported by Ramaswamy et al. (2004).

1.7 Tsunami

The tsunami occurred during 26th Dec 2004 due to a massive earthquake near Indonesian island of Sumatra affected the Andaman Nicobar Islands very badly. The Islands were just north of the earthquake epicenter and the tsunami reached a height of 15 m in the southern Nicobar Islands. The worst hit islands are Great Nicobar and Car Nicobar

islands because of its flat terrain. The southernmost point of India and Great Nicobar islands subsided 4.25m in the Tsunami and maximum damage happened in the Nicobar coral reefs than the Andaman reef. The mangroves of Andaman and Nicobar Islands also damaged due to uprooting as well as inundation of sea water.

1.8 Coral reefs and bleaching

Coral reefs termed as earth's marine rainforest play a major role in the coastal biodiversity of India. The estimated coral reefs area in India is 2374.9 km^2 out of which 959.3 km^2 occurring in the Andaman and Nicobar Islands (Jha et al., 2011). The Andaman Sea possesses both fringing reefs as well as barrier reefs (Muley et al., 2000). Various physiological, biological, ecological and anthropological factors cause coral bleaching and ultimately leading to mass mortality of corals. Sea surface temperature (SST) rise and anthropogenic impacts are the primary factors which are active in the Andaman Islands. Increased global warming produces increased SST frequency (Hoegh-Gulberg, 1999). Bleaching was recorded in Andaman Sea in 1998, 2002, 2005 and 2010 (Krishnan, 2011) whereas El- Nino plays a major role in 1998 and 2010 bleaching events at Andaman Sea (Lix et al., 2016).

1.9 Navigation

Navigation in South East Asia is focusing on the Strait of Malacca, which links the Indian and Pacific Oceans and is the most important shipping lanes in the world supporting the east-west trade. It covers 900 km long and 350 km wide.

1.10 Biological Production

Biological productivity is the production of organic matter from inorganic carbon by phytoplankton (suspended plants of ocean). This phytoplankton supply organic matter to zooplankton (floating animals), nekton (fish and marine mammals) and benthos (seafloor organisms). In the marine environment, the phytoplankton are the primary producers, zooplankton composes the secondary producers and fishes comprise the tertiary producers. Primary production is the rate at which biomass produced by phytoplankton through photosynthesis per unit area. The biological production can be computed using primary production. Chlorophyll (chl a) is a main component for the photosynthetic function of phytoplankton and is an indicator of phytoplankton biomass and primary productivity. Thus it is the most important biochemical parameter used in oceanographic study. Chl a variation in ocean illustrates the areas of oligotrophic water (less chl a concentration) to eutrophic water (rich chl a concentration). The Andaman Sea is well known area for tuna fisheries and the eastern side of the Island chain is a trawling ground. The highest pelagic catches comprise sardines, anchovies, carangids, ribbon fishes in Andaman waters.

1.11 Objectives of the study

- To understand the upper layer hydrodynamics and delineation of vertical current pattern using ADCP and SSHA derived geostrophy for the Andaman waters during winter season.
- To understand the multi-scale physical processes and its biological implications in the primary level during this season.

- To explain the spatio-temporal variation of forcing factors regulating the upper layer dynamics based on satellite observations and derived datasets/climatology.

1.12 Scope and Relevance of the study

Andaman water is a part of BoB and most of the earlier research works have been focused in this area, which has a characteristics of seasonally reversing western boundary current [East India Coastal Current (EICC), eddies during entire season and upwelling along the coast during summer season]. Throughout the year, SST of the Andaman waters maintained more than 28° C and is therefore an area of depression, cyclones and strong convective activities.

Though the hydrographical characteristics and the biological production in the region is explained in many studies, a clear understanding of the physical processes and the forcing mechanisms driving the upper layer processes in the region is still lacking. Another gap is in the explanation on the circulation pattern and the driving forces. Role of local versus remote forcing in the upper layer processes needs to be explained properly. The present work is formulated to find out the relative role of local versus remote forcing on the upper layer processes, role of the enormous quantity of freshwater from Ayeyarwady – Salween system and low saline Malacca Strait water on the hydrography and oceanography of the region.

BoB received more attention through Bay of Bengal Monsoon Experiment (BOBMEX) Bay of Bengal Process Studies (BOPS) and the

processes like eddies, coastal upwelling, gyre and the influence of the enormous run off receiving the head bay, have been explained by many authors. Also, the biogeochemistry, primary and secondary production of the region is explained by many properly linking with the physical settings. Oceanic response of the episodic events like cyclones are another key issue and is well understood that such atmospheric disturbances and mesoscale oceanic processes like cold core eddies, influence the biogeochemistry and food web dynamics in the area. However, Andaman waters being the southeast part of BoB, has got least attention as far as oceanographic studies are considered. The Andaman water is not only of great oceanographic interest but also plays a key role in modulating the monsoon.

1.13 Earlier Studies

Oceanographic studies in Andaman waters started in 19th century with Novara expedition (1857-1859). Further, Francis Day visited the Islands in 1869. First observation in deep waters of Andaman was done in Wood Mason expedition (1874) followed by Valdivia (1898-1899). Detailed study of the area for the first time was carried out by Seymour Sewell during 1913-1925. After that Dana expedition (1928-1930) and John Murray expedition (1933) were conducted in the region. Danish Galathea Expedition (1950-1952) during her round-the-world cruise mode took two stations from this region. Galathea followed by R. V. Vityaz in 1956-1960, were taken measurements in the course of her 31-33rd cruises. After Vityaz, the International Indian Ocean Expedition (IIOE) of 1961 gathered information based on biological and hydrological parameters.

The region is under the influence of both southwest and northeast monsoons (Wyrtki, 1973). The rainfall is heavy and prolonged for a long period exceeding 300cm in a year mainly during southwest monsoon prevailing from May-October. The northeast monsoon is active in November-December. February and March are exceptionally dry months (Rao, 2010). Climate is typically tropical with hot and humid conditions, with the atmospheric temperature varying between 25°C and 35°C during the year (Tikedar et al., 1986). The main source of fresh water to the northeast Andaman and Nicobar islands are Ayeyarwady (13.6×10^3 m^3/s), Salween rivers (6.69×10^3 m^3/s) and minor contributions from Sittang (1.59×10^3 m^3/s) and Tavoy rivers (Robinson et al., 2007). Ayeyarwady-Salween river system deposits 350 million tons of sediments into northern Andaman Sea (Ramaswamy et al., 2004 & Robinson et al., 2007). Rama Raju et al. (1981) reported that the northeastern part of Andaman waters are influenced by the water from Ayeyarwady River and the water from Sunda Sea through the Malacca Strait determines the oceanography of southern region. The presence of low saline water and intense evaporation causes temperature inversion in the region. Andaman waters in the western side of the Andaman & Nicobar Islands have similar characteristics of BoB. Heavy run off at the head of the bay get mixed up and transported by the prevailing currents towards the eastern part of the BoB and into the Andaman Sea due to the prevalent clockwise circulation (La Violette 1967). The fresh water flux keeps the water in the near surface layer less saline and retains strong haline stratification (Shetye et al., 1996). This leads to the formation of an intermediate barrier layer (BL) (Lukas and Lindstrom 1991, Thadathil et al., 2007) and BL induce thermal inversion

by trapping the solar radiation (Anderson et al., 1996). This thermal inversion with BL plays a major role in warming the mixed layer (de Boyer Monte'gut et al., 2007b) and is a general feature during winter (Ramesh Babu and Sastry, 1976). With the presence of temperature inversions, the surface ocean may be able to supply abundant heat to the atmosphere quickly by increasing the SST (LI Jian et al., 2012). Thus the area is a spot of deep air-sea interaction and associated convective activities and is marked as cyclone prone area (Varkey et al., 1996).

According to Wyrtki (1961) and Syamsul (2012), the surface circulation in the Andaman waters changes seasonally depending on monsoon seasons. Using multilayer, adiabatic, numerical model Potemra et al. (1991) reported that in the upper layer flow enters the sea south of the Nicobar Islands, circulates counterclockwise around the Andaman Basin and exits south of the Andaman Island from March to July. In the rest of the year the flow enters the basin from the north, circulates clockwise and exits in the south. Based on National Institute of Oceanography (NIO) report (1980), Persian Gulf at a depth range of 200-500m and Red sea water at 500-900m are identified in the region. It is associated with deep mixed layer (75m) and low nutrients concentration. The presence of strong halocline inhibits the heat transfer to deeper layers. Murty et al. (1981) noted that Mixed Layer Depth (MLD) is deeper in the western side of the Andaman and Nicobar Islands compared to east. The shape of the Island and the irregular bottom topography creates turbulence, eddy and modifies the double diffusion. Small anticyclonic eddy around Andaman Sea is documented by Unnikrishnan and Bahuleyan (1991) using two dimensional vertically

integrated model. Winds over the Equatorial Indian Ocean (EIO) play an important role in modulating the circulation features of the BoB and Andaman Sea (Potemra et al., 1991). These winds cause baroclinic mode Kelvin waves which propagate as coastal Kelvin waves into the eastern bay and radiate westward propagating baroclinic mode Rossby waves into the interior (Potemra et al., 1991; Yu, 2003; Rao et al., 2010). The first upwelling Kelvin wave during winter months propagate north and move around the northernmost point of the BoB and tail off on the east coast of India tracking the coastal waveguide before passing Sri Lanka. Near Andaman Sea the wave period becomes more variable, fluctuating between quarter-annual and semi-annual periods possibly due to the effects of westward radiating Rossby waves generated by the coastal Kelvin waves (Subrahmanyam et al., 2001). Wave energy near the Andaman Sea is less at both the semiannual and annual periods due to the energy loss from radiated Rossby waves (Nienhaus et al., 2012).

Andaman Sea is the site where extraordinary large solitons are observed (Osborne and Burch, 1980; Alpers, 1997) which extensively help the mixing characteristics in the sea (Hyder et al., 2005). Osborne and Burch (1980) showed that the waves are generated by tidal flows through the channels in the Andaman and Nicobar island chains and their interaction with shallow bottom topographic features. It is observed that these vigorous tidal and internal wave induced mixing have significant effect on circulation of the region.

Suwannathatsa et al. (2012) reported that local alongshore winds and Ekman current force the southward weak regional currents during

both summer and winter. During NEM, low saline water spread over the eastern side of the islands which originates from the river discharge at north and the intrusion of low saline water from SCS through the Malacca Strait at south (Ibrahim and Yanagi, 2006). According to Sarma and Narvekar (2000), the vertical distribution of temperature and salinity in the eastern BoB is similar to Andaman Sea down to 700-800 m. The relatively high saline Andaman water is intruded into Malacca Strait during SWM (Amiruddin et al., 2011). Burnaprathepratet al. (2010) reported cyclonic eddy in Andaman Sea using satellite altimetry, surface geostrophic currents and chl a. Based on Ocean General Circulation Model (OGCM) and Linear Continuously Stratified (LCS) models, Chatterjee et al. (2017) reported that the circulation around the Andaman Nicobar Islands are forced by equatorial forcing compared to the local wind forcing.

Garg et al. (1968), while explaining the dissolved inorganic nutrients in the region found that the extend and intensity of oxygen minimum layer is more in Andaman waters than Bay of Bengal. Naik and Reddy (1983) reported that the relatively high phosphate concentration found along the western Andaman Island are due to the presence of coral banks in the region. Regarding biological production, the primary production of the area has been studied from the time of IIOE. The IIOE Atlas (Krey and Babenard, 1976) reported higher chl a during November-April period. The sea is oligotrophic with low primary and secondary productivity (Quasim and Ansari, 1981). Sarupriya and Bhargava (1993) stated that the maximum average primary production during SWM is 586.73 mg $C/m^2/d$ followed by NEM with 440.68 mg $C/m^2/d$ and for inter

monsoon spring it is 319.19 mg C/m^2/d. According to Geetha et al. (1997) the most productive season is northeast monsoon (Oct-Jan) followed by the premonsoon (Feb-May). The average secondary production is 49.7 ml/1000m^3 for the region.

Sarojini & Sarma (2001) explained the presence of subsurface phytoplankton abundance in the western side of the Andaman and Nicobar Island is due to the presence of Arabian Sea high saline water and the surface maxima attributed to thicker mixed layer. The southern part of the Andaman has higher zooplankton abundance during northeast monsoon due to wind generated upwelling (Pant, 1992). Later, Tan et al. (2006) reported that this is due to the bloom of phytoplankton from Malacca strait got advected towards Andaman Sea during NEM. Viijayalakshmi & Gireesh (2010) stated that Andaman Sea is a prominent biodiversity hotspot and the diversity increases towards south. Madhupratap et al. (1981) showed that the eastern side of the island has poor biomass due to poorer abundance of decapods. Distribution and abundance of major mesozooplankton groups like amphipods, ostracods, copepods, fish eggs and larvae are explained in many earlier studies (Manickasundaram and Ramaiyan, 1989; Lalithambika et al., 1996; Rosamma and Meenakshikunjamma, 1996; Biju et al., 2010; Honey et al., 2006). Kabanova (1964) found that the primary production in the central part of the Andaman Sea was 114-176 mg C/m^2/d and area was characterized by greater concentration of nitrates than other regions. Madhu et al. (2003) stated that the minimum biomass is confined to 300-Bottom of Thermocline (BT) where oxygen minimum zone is found. The tertiary production and the potential yield tertiary from the

Sea were 0.85×10^6 tons/yr and 0.21×10^6 tons/yr respectively (Goswamy, 2004).

1.14 Expected Outcome of the study

The region is least explored for the ocean dynamics and the prevailing ecosystems compared to other seas in the Indian Ocean. The present study is aimed to explain the physical setup and the surface biological responses addressing the processes and the complex interaction between other components which will be useful in ecosystem based studies. Earlier studies do only explain the relations or responses over other, based on parameter to parameter relations. A detailed understanding on the prevailing processes of a system is required to explain how the atmospheric forcing induces changes in ocean physics, chemistry and then biology and between various components, either biotic or abiotic. The present study attempts to explain the prevailing physical processes during winter monsoon. The results of this study could supplement the ecologist to explain about the spatio-temporal variations in the biotic components of the region which is not established so far. Also, the outputs from the study would be properly used for a better simulation of the available ocean models to explain the basin-scale to mesoscale processes.

Chapter 2

UPPER LAYER CIRCULATION, HYDROGRAPHY AND BIOLOGICAL RESPONSE

Contents

2.1 Introduction

The Andaman waters (surrounding the Andaman and Nicobar islands) occupies the area between 6°-14°N and 91°-95°E in the eastern part of the North Indian Ocean. The northern part of the islands has got the wide continental shelf (170-200 km) and the continental slope along the eastern part of the islands is steeper than western part (Murty et al., 1981) and has erratic bottom topography. Sills are observed in the eastern side due to the sediment accumulation of Ayeyarwady river system (Ramaswamy et al., 2004). The abyssal plain (3000-4180 m) with an even floor is situated along the west coast of Andaman and Nicobar islands. Preparis channel (between Cape Negrais and North Andaman) in the north (200 m, 285 km wide), Ten degree channel (150 km wide) between Andaman and Nicobar Islands (1800 m) and Great channel between Great Nicobar Island and Sumatra (>1800 m and 189 km wide) connects the sea

with Bay of Bengal (Sengupta et al., 1981 and Kamesh Raju et al., 2004). The sea is also linked with South China Sea and Pacific Ocean through Malacca Strait at southeast. The main source of fresh water to the northeast of Andaman and Nicobar Islands are Ayeyarwady (13.6×10^3 m^3/s), Salween rivers (6.69×10^3 m^3/s) and minor contributions from Sittang (1.59×10^3 m^3/s) and Tavoy rivers (Robinson et al., 2007). There is no major perennial fresh water river in these islands except Kalpong in North Andaman, Alexendra, Dagmar and Galathea river in Great Nicobar.

The Andaman waters experience the seasonally reversing Asian Monsoons (Wyrtki, 1973), summer monsoon during May-September and winter monsoon during November-February. During Northeast monsoon, the low saline water spread over the eastern side of the islands originates from the river discharge at north and the intrusion of low saline water from the South China Sea through the Malacca strait at south (Ibrahim and Yanagi, 2006). In addition, during the season, the region experiences strong evaporation of surface water due to cold dry continental air from the north. Thus, the area is a spot of deep air-sea interaction and associated convective activities and is marked as cyclone- prone area (Varkey et al., 1996). The presence of rivers and monsoonal winds influence the regional hydrography and circulation.

In addition to this, internal wave and tidal induced elevated vertical mixing is likely to influence the regional stratification and circulation pattern. The region is one of the sites where extraordinary large solitons have been observed (Osborne, 1990 and Hyder et al., 2005). Internal waves of extraordinary amplitude of 60 m, wavelength of 6-15 km and speed >2 m/s

were noticed in this region (Alpers et al., 1997). This, together with longer period internal oscillation in the Northern Andaman Sea, produced the downward perturbation of the pycnocline. This also endorsed eastward-propagating Kelvin wave parallel to the continental slope. Such wave helped the mixing processes in the Andaman Sea (Hyder et al., 2005).

However, this region is least explored with regard to the oceanographic processes and the related biological impacts. Ramesh Babu and Sastry (1976) studied the hydrography of the sea during late winter. Small anticyclonic eddy around the Andaman Sea during premonsoon season (March) is reported by Unnikrishnan and Bahulayan (1991) using a two dimensional vertically integrated model. Potemra et al. (1991) analysed the seasonal circulation of the Andaman Sea using multilayer, adiabatic, numerical model and pointed out the propagation of Kelvin waves in Andaman Sea. Kelvin waves originating in the equatorial Indian Ocean follow the coastal waveguide counter clockwise around the perimeter of the Bay of Bengal (BoB) after reaching the Sumatra coast (Ninenhaus et al., 2012).

Regarding biological production, the primary production of the area has been studied from the time of IIOE. The region is characterized as oligotrophic when comparing the other areas of Indian Ocean (Bhattathiri and Devassy, 1981) and maximum average column production is noticed during the southwest monsoon (586.73 mg $C/m^2/d$) followed by northeast monsoon (440.68 mg $C/m^2/d$) and inter-monsoon spring (319.19 mg $C/m^2/d$) (Sarupriya and Bhargava, 1993). The waters around the Andaman Islands are considered to be one of the major biodiversity hotspots in the Indian

Ocean (Vijayalakshmi and Gireesh, 2010). While studies from Geetha et al. (1997), analyzing the zooplankton of the upper column, explain that the seasonal biological production is high during winter monsoon. Distribution and abundance of major mesozooplankton groups like amphipods, ostracods, copepods and fish eggs and larvae are explained in many earlier studies (Manickasundaram and Ramaiyan, 1989; Lalithambika et al., 1996; Rosamma and Meenakshikunjamma, 1996; Biju et al., 2010; Pillai et al., 2011).

The present study explains the seasonal response of the region to the prevailing physical mechanism, specifically the circulation pattern, hydrography and the associated biology based on in situ and satellite observation during the winter monsoon January 2009 and November-December 2011. The study is formulated in the following aspects: 1) The hydrography and oceanography of the region, 2) The upper layer circulation pattern using ADCP and 3) The physico-biological interactions in the primary level during winter monsoon.

2.2 Data and Methodology

2.2.1 In situ Data

In situ data were collected onboard *FORV Sagar Sampada* during 8-26 January 2009 and 21 November-14 December 2011 (Fig. 2.1). The transect are on the depths of 50, 100, 200 and1000 m and the offshore station for which depth is greater than 1000 m. These datasets are used to understand the hydrography, circulation and the associated biological responses in the Andaman waters. The meteorological parameters like air temperature, air pressure and humidity were collected through the

instruments/sensors attached to the Automated Weather Station (AWS) onboard in one minute interval. Profiles of temperature, salinity, dissolved oxygen and Sigma-t are obtained using SeaBird 911 plus CTD with Niskin water samplers and deck unit for data acquisition. It has four main sensors used to measure temperature, pressure, conductivity and dissolved oxygen. The datasets are processed for 1 m bins. Salinity is also derived from water samples collected through Niskin samplers and using Guildline 8400A Autosal Salinometer to validate the CTD derived data. Mixed Layer Depth (MLD) is derived from CTD profiles as the depth at which the seawater density (Sigma-t) exceeds the surface density by 0.2 kg/m^3 (Sprintall and Tomczak, 1993). The Isothermal Layer Depth (ILD), the depth of the top of the thermocline, is defined as the depth at which surface temperature decreases by 1°C from sea surface temperature (Kara et al., 2000 and Rao and Sivakumar, 2003). The thickness of the barrier layer is computed as the difference between ILD and MLD (Lukas and Lindstrom, 1991).

Vertical sections of currents are derived using hull mounted OS II BB ADCP of 76.8 kHz frequency operated along the ship's track with vertical range of operation between 30 to 400 m. Georeferencing is done in bottom track option along the coastal area (depth < 200 m), whereas navigation mode is opted for deeper areas. Current datasets are acquired using VmDas in 8 m bins and ensemble time of two seconds. The ship heading and navigational informations are also recorded while acquiring the raw data. The first bin record of current started at 16 m depth. The data in earth coordinates were postprocessed using WinADCP, for an ensemble period of 1 minute. Spurious values including the data at 16 m

of currents were discarded from the data. Processed data which have percentage good more than 80% is considered for the analysis. The in situ data are spaced irregularly and are converted to equidistant rectangular grids using VG Gridding for contouring and graphical display.

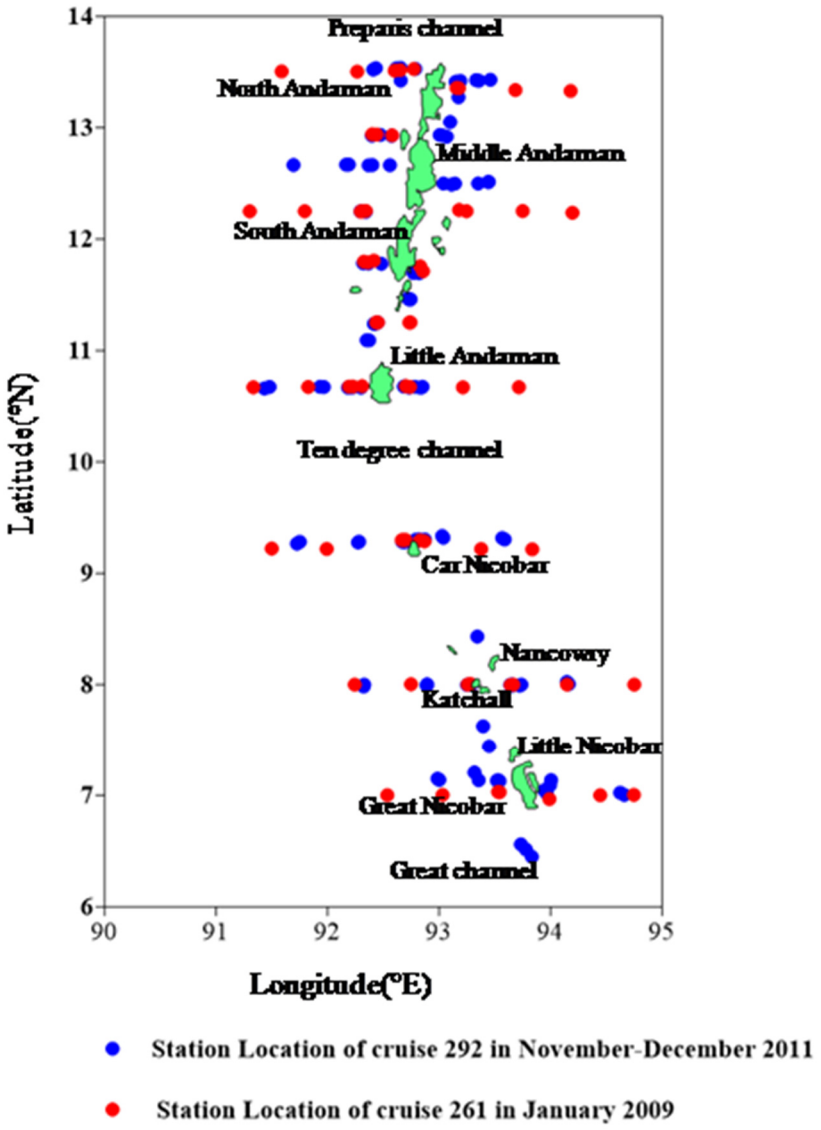

Fig. 2.1: Station Locations

2.2.2 Satellite Measurements

Wind datasets are acquired for the month of January 2009 and November-December 2011 from Advanced Scatterometer (ASCAT)-daily aboard the EUMETSAT METOP satellite. Eight-day composite of the Ocean Color Level 3-binned product derived from MODIS AQUA in 4 km resolution acquired from GSFC NASA which is processed using SeaDAS is used to depict the chl a patterns. TOPEX/POSEIDON (T/P) SSHA data (weekly composite) is obtained from CNES/NASA. Evaporation data is obtained from the Woods Hole Oceanographic Institution (WHOI) Objectively Analyzed air–sea Heat Fluxes (OAFlux) dataset on 1° × 1° grid. Precipitation data came from GPCP (Global Precipitation Climatology Project) version 1.3. Solar radiation flux is obtained from ESRL (Earth System Research Laboratory) NOAA 20th Centuary Reanalysis V2c. The u and v components of the water velocity due to Ekman pumping are computed for the vertical column following Pond and Pickard (1983). The relation is explained as

$$u_E = V_0 \cos(\frac{\pi}{4} + \frac{\pi z}{D_E}) \exp(\pi z / D_E) , v_E = V_0 \sin(\frac{\pi}{4} + \frac{\pi z}{D_E}) \exp(\frac{\pi z}{D_E}) \quad ....(1)$$

$$V_0 = \frac{\sqrt{2}\pi\tau_{yn}}{D_E \rho f} , \text{ total Ekman current, } \quad .....(2)$$

$$D_E = \frac{4.3W}{(\sin\phi)^{\frac{1}{2}}} , \text{ Ekman depth, } \quad .....(3)$$

τ_{yn} is the magnitude of the wind stress on the sea surface, f is the Coriolis parameter, Φ is the latitude and z is the water depth. At the sea

surface, the surface current flows at 45° to the right of the wind direction in the northern hemisphere. Below the surface, the total current speed decreases as depth increases. When $z = -D_E$, at the Ekman depth, the direction of the flow becomes opposite to that at the surface.

The Primary Productivity (PP) of the region during the study was derived using Vertically Generalized Production Model (VGPM) of Behrenfeld and Falkowski (1997) which describes the relationship between the surface chlorophyll from satellite data and depth-integrated primary production. The VGPM is a chlorophyll-based model that estimates Net Primary Production (NPP) from chlorophyll using a temperature- dependent description of chlorophyll-specific photosynthetic efficiency. In the VGPM, NPP is a function of chlorophyll, available light and photosynthetic efficiency.

The core equation describing the relationship is expressed as

$$PP_{eu} = 0.66125 P_{opt}^{B} \frac{E_0}{E_0 + 4.1} C_{SAT} \times Z_{eu} \times D_{IRR} \quad \text{.....(4)}$$

where C_{SAT} is the satellite surface chlorophyll concentration as derived from measurements of water leaving radiance (mg Chl/m^3). VGPM calculations of primary production were based on monthly average C_{SAT}. D_{IRR} is daily photoperiod (in decimal hours) calculated for the middle of the month for each pixel, E_0 is the sea surface daily Photosynthetically Available Radiation (PAR) (mol quanta/m^2/d) and Z_{eu} is the physical depth (m) of the euphotic zone defined as the penetration depth of 1%

surface irradiance based on the Beer-Lambert law. Z_{eu} is calculated from C_{SAT} following Morel and Berthon (1989).

2.3 Results and discussion

The upper column dynamics can be best studied and illustrated based on the changes in the wind and SST pattern and the present study attempts on this approach considering the real time in situ SST from CTD (bulk SST at 5 m) and Scatterometer-derived wind fields for the observation time. Also, the hydrography can be best illustrated based on vertical profiles on temperature, salinity and density and this has been addressed by analyzing the 91 and 44 castings during the two cruises.

2.3.1 Atmospheric forcing

The analysed wind pattern suggested that the area is experienced with cold, dry continental air from northeast and the oceanic region is experienced with evaporative cooling with significant spatial variation (Wang et al., 2006). November-December 2011 characterizes northeasterly wind over the northern region and easterly winds in the southern region (6° to 9°N) with increasing magnitude towards south (Fig. 2.2a). However, during January 2009, the pattern is northeasterly over the entire area with magnitude increasing towards south as observed during November-December 2011 (Fig. 2.2b).

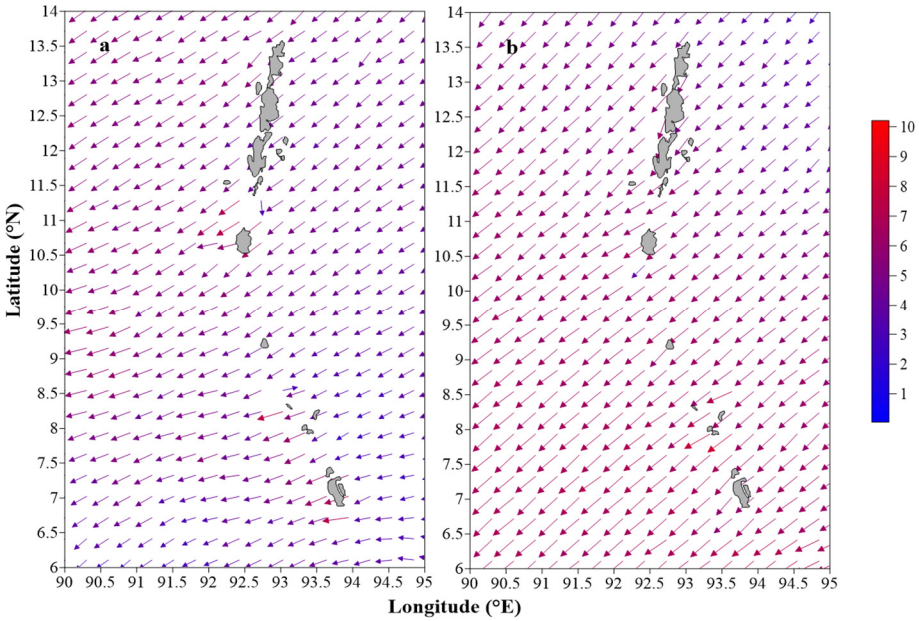

Fig. 2.2: Wind (m/s) during a) Nov-Dec 2011 and b) Jan 2009

2.3.2 Upper layer mixing and hydrography

Immediate response due to atmospheric forcing will be best reflected in the Sea Surface Temperature (SST) pattern and is thus considered as the most important parameter in the air-sea interaction processes (Manikiam, 1988). November-December 2011 is characterized with the prevalence of warmer water (≥ 28.4 °C) extended over the region and the temperature changed from 28.4-29.2 °C (Fig. 2.3a) which is quite different from the expected trend of increasing towards south (Rama Raju et al., 1981). East coast is somewhat cooler than the west, showing similar tendency during January 2009 (Fig. 2.4a). During January 2009, the SST recorded between 27.0 and 28.1 °C with warmer water in the south than the north. The waters along the east coast are comparatively cooler in the range of 28.4-28.9 °C in the November-December 2011 and 27.3-27.6 °C

in January 2009 than that along the west recording 28.5-29.2 °C in November-December 2011 and 27.6-28.1 °C in January 2009. North of Camorta is the coldest point in the November-December 2011 and the northeast in January 2009. The warmest point is northwest (29.2 °C) in November-December 2011 and southeast in January 2009.

From the SST maps, it is evident that the eastern side is more cool than the west. To explore this, the E-P (evaporation- precipitation) is calculated. During November-December 2011, the computed E-P is negative in the southern latitude (up to 8°N) ranges from 101 to 239 cm/year. E-P increases towards north vary from 16 to 158 cm/year. The eastern side is characterised with E-P of –13 to –412 cm/year upto 6.5°N and again increases towards north like the western side (86-128 cm/year). For the period of January 2009, the western side E-P rate varies from –33 to –225 cm/year in the southern latitude (up to 6.5°N) and it increases towards north similar to November 2009 (47-179 cm/year). But in the eastern side, the E-P ranges from –117 to –215 cm/year up to 6°N and the value shoot up from 19 to 201 cm/year towards north. From this, it is evident that the eastern side is cooler than west due to the cold dry continental air from northeast which causes evaporation in the ocean surface.

During November-December 2011, the net solar radiation in the western part of the island chain varies from 160 to 280 W/m^2 and 71 to 260 W/m^2 in the eastern region. During January 2009, the western side receives solar radiation in the range of 142 to 278 W/m^2 and 82 to 258 W/m^2 in the eastern part. The cooling in the eastern side is due to the combined effect of evaporation and reduced solar radiation.

In the Andaman waters, the Sea Surface Salinity (SSS) is low and falls in the range of 31.8-33.4 psu in November-December 2011 (Fig. 2.3b) and 32.05-33.25 psu in January 2009 (Fig. 2.4b) with significant spatial variation in the distribution pattern (Sewell, 1929). Temperature-Salinity (TS) profiles characterize two water types in the northeastern section as warm (27.5-29.0 °C) less saline (32.5-33.5 psu) and less dense (20.2-21.5 kg/m^3) for the upper (5-55 m) and below this level, uniform waters occupied upto 1000 m. Similar trend exists for the southeast also with warm (24.5-29.3 °C), saline (32.3-34.0 psu), less dense water (20.5-23.4 kg/m^3) for the upper (5-80 m) column but the source of water occupying the upper layer is found to be different. For northeast, it is due to heavy runoff from Ayeyarwady-Salween river system, while intrusion of Malacca strait water (Riley and Chester, 1971) in the south defines the watermass (Rama Raju et al., 1981 and Tan et al., 2006). Intrusion of low saline water through the Malacca strait during the active winter as mentioned above is verified based on Levitus climatology for December and January. The western side of island chain exhibits more or less similar pattern and the area is shown to be occupied by BoB waters with temperature 25.0-29.2 °C, salinity 32.1-34.0 psu, σ_t 20.3-22.0 kg/m^3 in the upper column (5-75 m) and below with 5.0-24.9 °C, 34.0-34.9 psu, 22.1-27.3 kg/m^{3}respectively up to 1000 m depth during December and January.

Surface sigma-t also showed the same pattern of SSS and varies from 20.13 to 21.28 kg/m^3 with less dense water in the east than the west in January 2009 (Fig. 2.4c). The density pattern of November-December 2011 (Fig. 2.3c) is entirely different from January 2009 and shows an increasing trend towards south (20.2-20.45 kg/m^3). Northeast part exhibits less density which is corroborated with SSS of the Ayeyarwady region (Wyrtki, 1971).

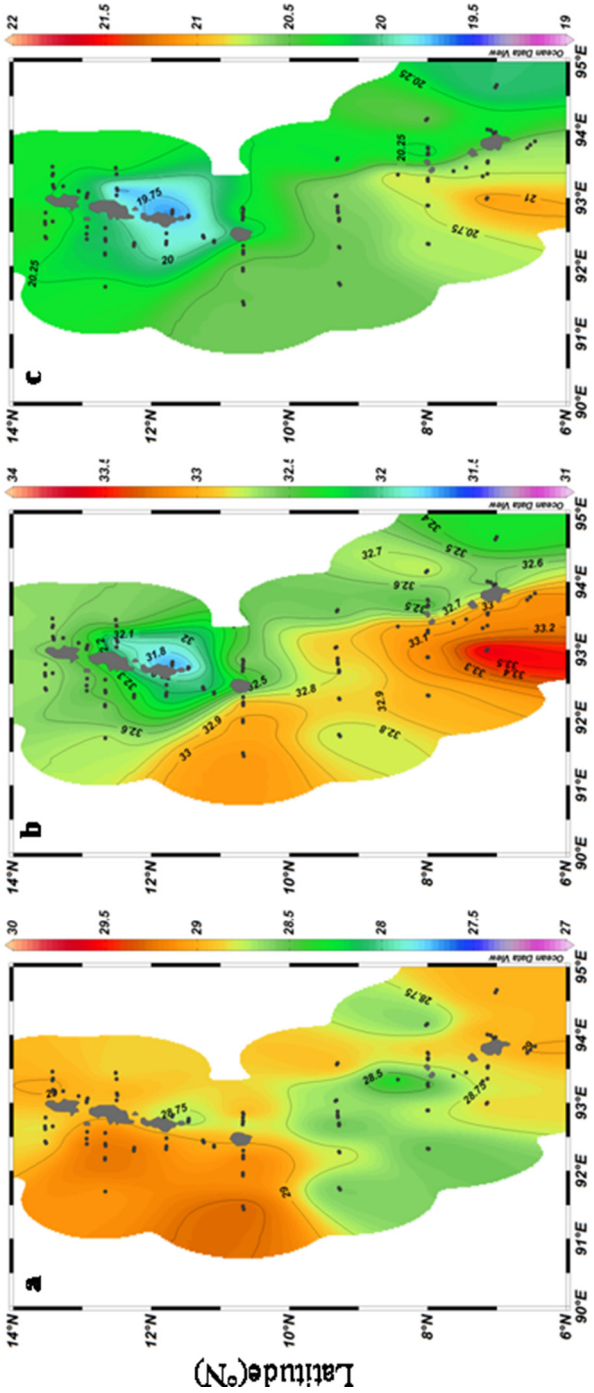

Fig. 2.3: Surface distribution of a) temperature (°C), b) salinity and c) density (kg/m^3) during Nov-Dec 2011

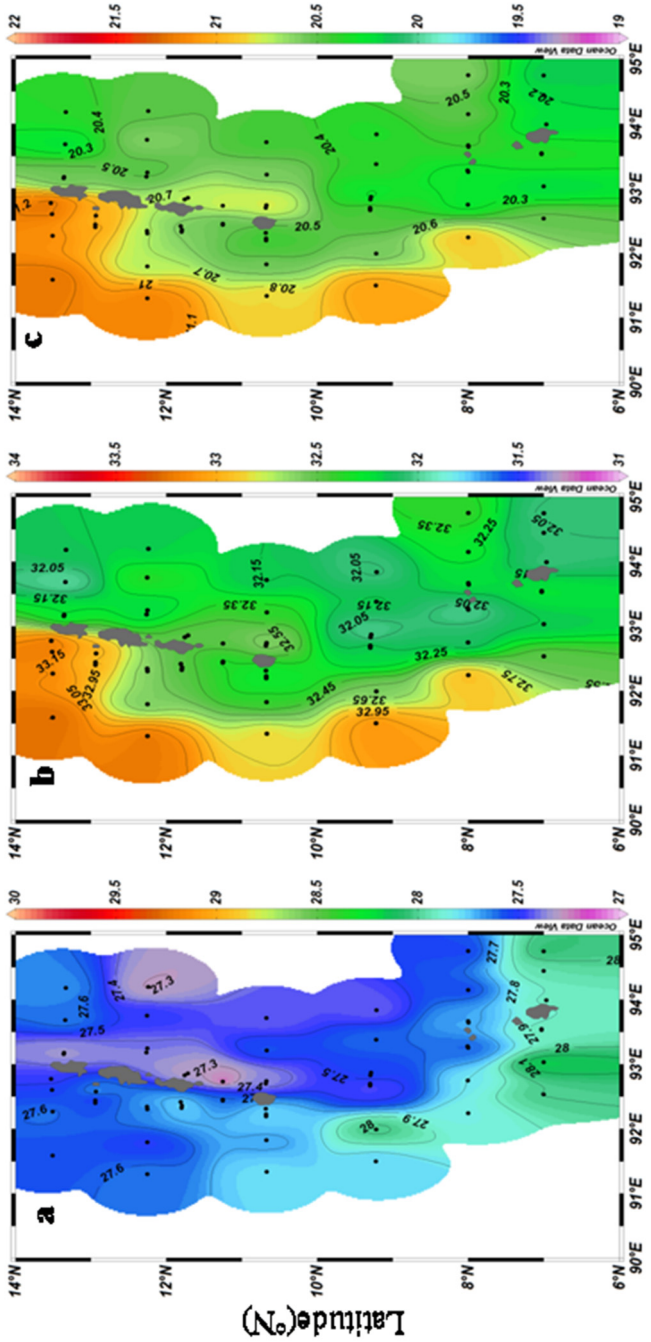

Fig. 2.4: Surface distribution of a) temperature (°C), b) salinity and c) density (kg/m^3) during Jan 2009

Spatial variation in water properties thus subregionalises the sea around Andaman into three, one is along the west, with BoB waters, second is at northeast with the influence of riverine discharge and the third one is in south influenced by the intrusion of less saline water from Malacca Strait.

The extend of vertical mixing is determined by MLD and in the observation, it is found to be ranging between 20 and 44 m with high value at southwest in November-December 2011 (Fig. 2.5a) and 16 and 87m with higher values at north in January 2009 (Fig. 2.6a). In November-December 2011, MLD in the western side of the island chain is 48 m at 7°N and shoals to 24 m at 9°N, again increases to 40 m at 10.5°N and decreases towards north (24 m). In January 2009, MLD in the western side is about 17 m at 7°N, and it deepens to 42m at 8°N. Again, along 8° to 10°N, it varies between 27 and 37 m. MLD shows sharp deepening north of 12°N with maximum value of 77 m at 13.8°N. In the eastern side of islands, MLD is shallow (20-32 m) in November-December 2011 and MLD maximum (72 m) is recorded at 11°N in the offshore waters of Middle and Little Andaman in January 2009. Along the southeast and southwest MLD is shallow and is in the range of 25-30 m in January 2009. From the time series analysis of wind speed in the coastal and oceanic region, the deepening of mixed layer is due to prevailing northeasterly winds and the wind-induced mixing. The shallow mixed layer in the east can be attributed to the presence of low saline water from Malacca strait and Ayeyarwady-Salween river system which might have strengthened stratification resulting weak vertical mixing (Rama Raju et al., 1981). In BoB also, the stratification is

controlled by the fresh water flux, river runoff, mixing and advection (Fousiya et al., 2015).

Another important observation noticed with the vertical distribution is the occurrence of temperature inversion (0.2-0.4 °C) in the upper subsurface layer (17-80 m). This is recorded in almost all the stations except around the Nancowry, Katchal and Camorta Island chain in November-December 2011 and along the middle east Andaman in January 2009 and is significant as the subsurface values exceeded by 0.2 °C from that of surface as explained by Durand et al. (2004), and is a general feature of Andaman Sea during winter (Ramesh Babu and Sastry, 1976).

Strong barrier layer is conducive for the formation of temperature inversion by suppressing the vertical advection processes (Masson et al., 2002). Presence of temperature inversion and shallow mixed layer indicates the existence of intermediate barrier layer, the layer between the base of mixed layer and the top of the thermocline (Lukas and Lindstrom, 1991; Vinayachandran et al., 2002, Rao and Sivakumar, 2003 and Thadathil et al., 2007). Surface layer inversions observed at east may be due to differential mixing of Andaman waters with those coming from the adjacent seas and rivers as mentioned earlier. These low saline waters in conjunction with the intense evaporation contribute the above condition which supports the results from Ramaraju et al. (1981).

It is recorded by de Boyer Monte'gut et al. (2007b) that the thermal inversion supported by barrier layer plays a significant role in warming the mixed layer during winter monsoon by entrainment of warm

subsurface water. In support of these studies in the BoB, the present observations in the Andaman waters show that barrier layer is of 10-47 m thickness in November-December 2011 (Fig. 2.5b) and 10-50 m in January 2009 at most of the stations (Fig. 2.6b). It is more prominent in the southeastern side in November-December 2011 due to the presence of less saline Malacca water in the region. But in January 2009, barrier layer is more in the western side and in a small area along the eastern side of north Andaman Islands. The thickness of barrier layer is less in the northeastern side, which is a heavy fresh water input area as evidenced by the SSS values (32.05-33.25 psu) and may be due to the soliton-induced mixing as reported by Osborne and Burch (1980). It is also observed that the sills and underwater volcanic seamounts in the eastern side of the islands are the potential source of internal waves in the region and contribute substantially to the upper layer mixing (Hyder et al., 2005).

The distribution pattern of barrier layer observed in the region is similar to the observations done by Thadathil et al. (2007), where they explored the seasonal variability of the barrier layer thickness and explains that the layer is more prominent in the Bay during winter monsoon. Also, the surface circulation and the redistribution of low saline (BoB water, freshwater from Ayeyarwady-Salween and less saline South China Sea water from southeast) waters have shown a dominant influence on the distribution of barrier layer thickness (Agarwal et al., 2012). In addition, Ekman pumping and Rossby waves induced by coastal Kelvin waves propagating along the eastern boundary contribute significantly on the barrier layer thickness pattern (Girishkumar et al., 2011).

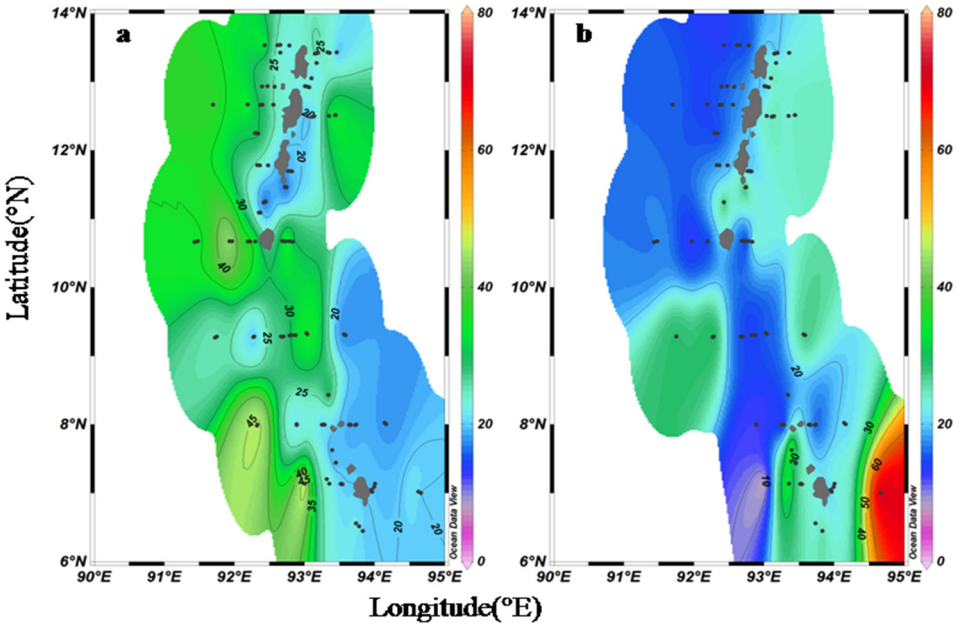

Fig. 2.5: a) MLD (m), b) BLT (m) during Nov-Dec 2011

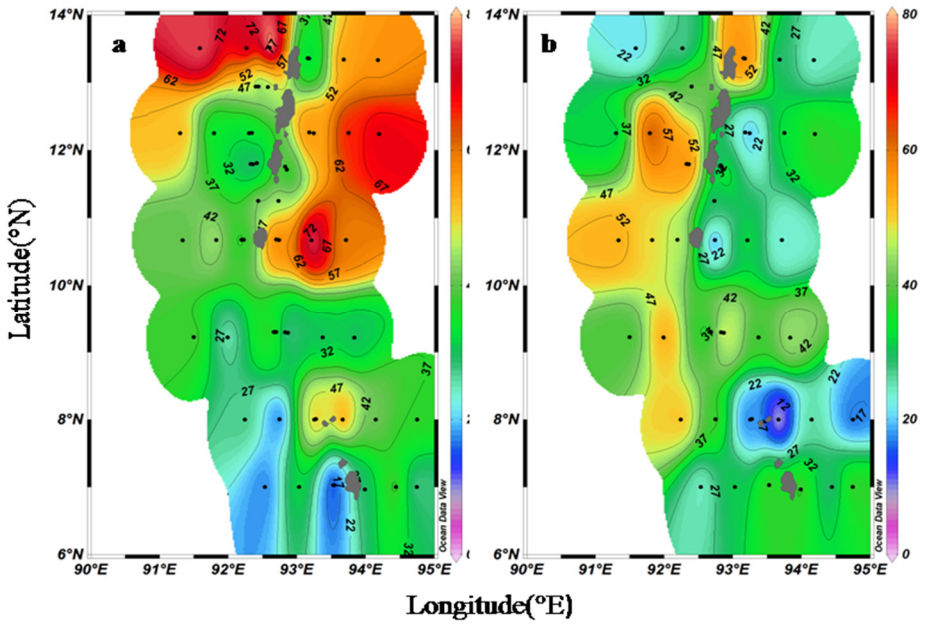

Fig. 2.6: a) MLD (m), b) BLT (m) during Jan 2009

2.3.3 Upper layer circulation

The circulation pattern in the upper layer (16-96 m) is studied using the velocity profiles recorded through the VM ADCP of 76.8 kHz frequency. The analysis is done for different depth strata viz between 24 and 96 m in 8 m intervals. In November-December 2011, the current recorded at 16 m is considered for near surface pattern and this shows the presence of a strong (600-800 mm/s) eastward component from 7°N to 8°N along the western side of the island chain (Fig. 2.7a). Above 8°N, it turns to northeastward direction away from the island chain with decreasing magnitude (200-300 mm/s). Further north (above 9°N), the flow is maintaining the same direction, i.e., northeastward, with a decreasing magnitude of ≤100 mm/s. Along the eastern side, the current is directed towards north and northeastward with reduced speed compared to western side of the island chain. At 32 m, the current shows same trend (Fig. 2.7b) like at surface. The data is analyzed for all 8 m cells up to 88 m depth (Fig. 2.7f) and found to follow the same pattern as that of near surface but with decreasing magnitude.

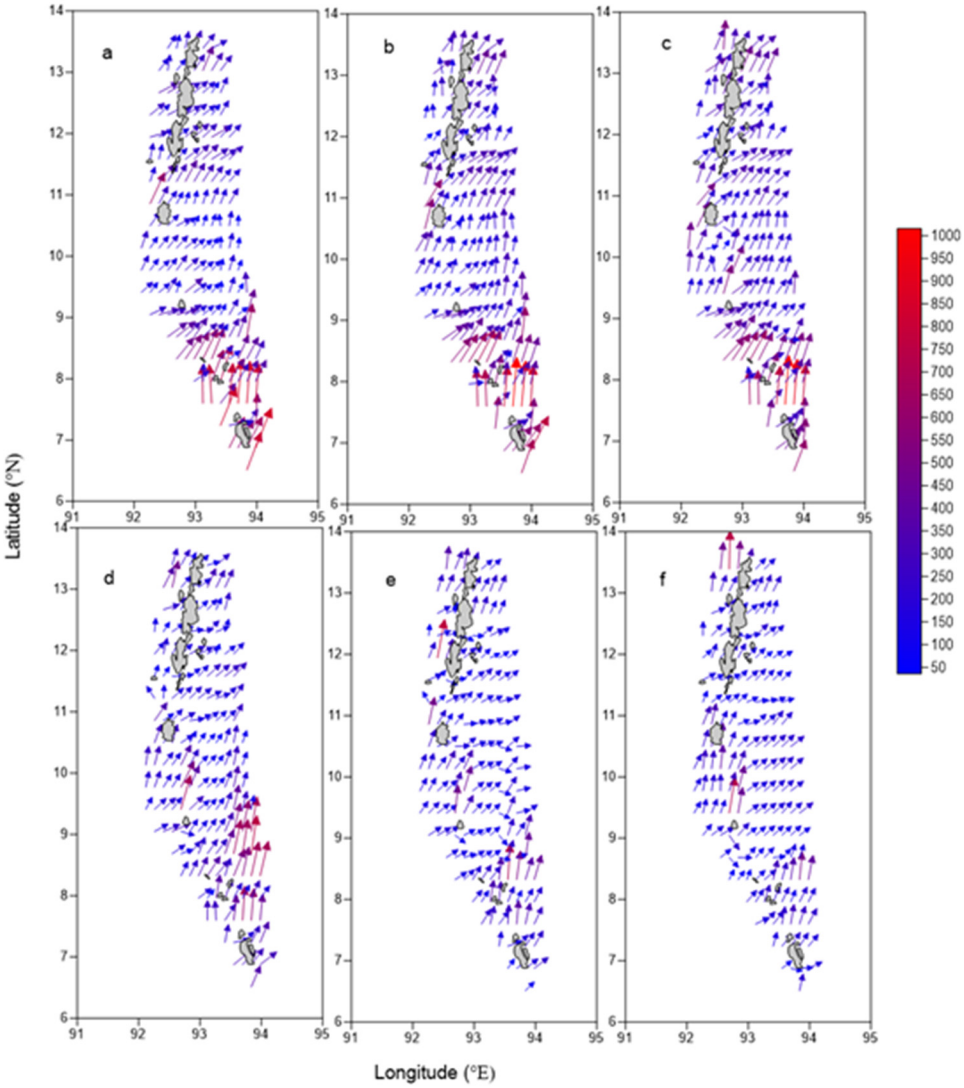

Fig. 2.7: Horizontal map of currents (mm/s) at different depths a) 16m, b) 32m c) 40m d) 56m e) 72m and f) 88m in Nov-Dec 2011

During January 2009, the current recorded at 24 m (Fig. 2.8a) represents near surface pattern and this shows the presence of a strong westward component of 600 mm/s up to 10°N along the western side of the island chain. South to 10°N, it takes southeastward direction towards the Nancowry, Katchal and Camorta Islands with magnitude in the range of 120-700 mm/s. Further south of 7°N, the flow is directed to south, with a strengthening in magnitude (700 mm/s). Along the eastern side, the observations indicates the flow from west to east through the Preparis Channel, which takes an anticyclonic path and reenter to the west via south of Car Nicobar. Overall, pattern is converging in the near surface layer between the latitudes 11-12°N and 93-94°E.

At 32 m depth (Fig. 2.8b), the current pattern shows the same trend as that at the surface with magnitude in the range of 145-775 mm/s. The data is analysed for all 8 m depth cells up to 96 m depth, and it is found that, up to 80 m (Fig. 2.8e), the circulation is in the same pattern as that in the near surface layer. At this level, the magnitude strengthens to 1000 mm/s near to Car Nicobar Island. At 96 m depth (Fig. 2.8f), the current shows irregularity in its direction and the magnitude is maintained in almost the same range. The observations in the upper layer circulation suggest convergence of the water from east and west near the Nicobar and Little Nicobar islands.

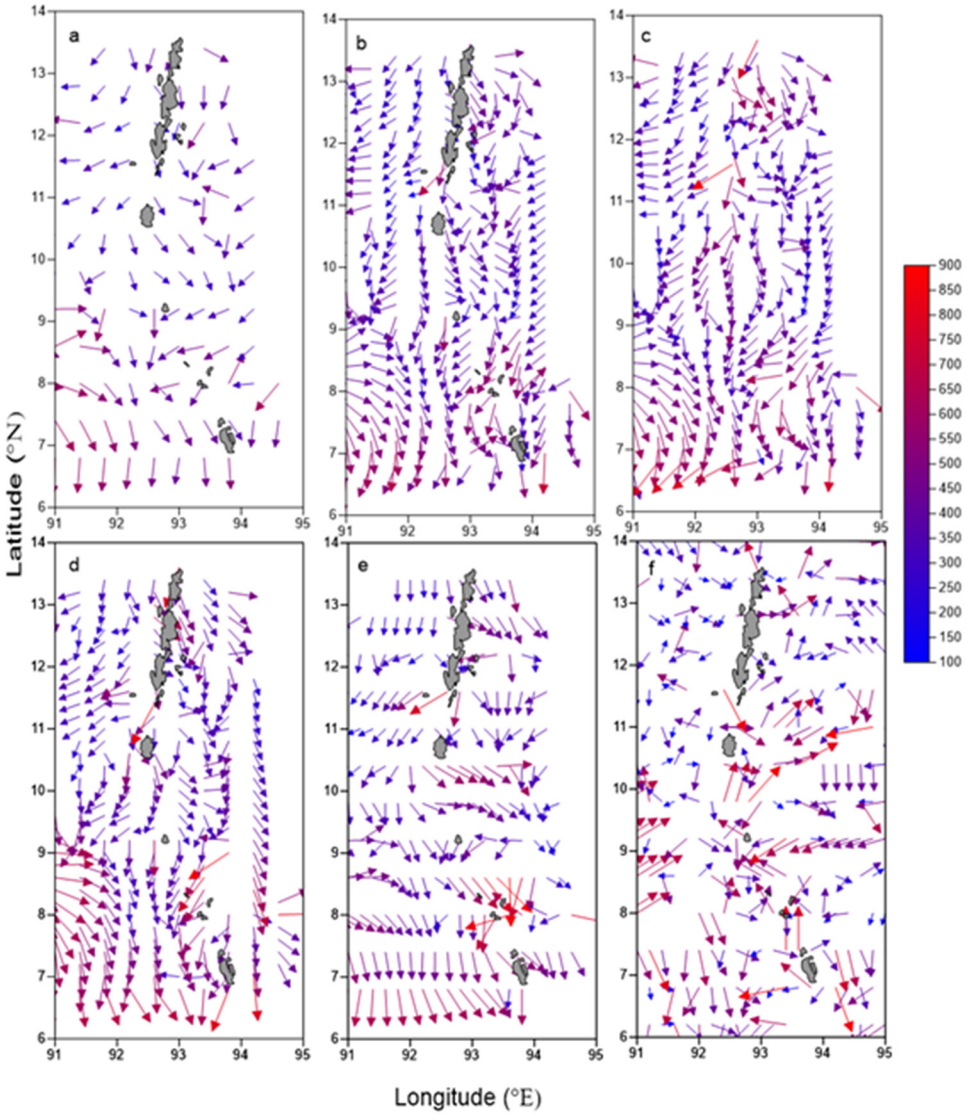

Fig. 2.8: Horizontal map of currents (mm/s) at different depths a) 24m, b) 32m c) 40m d) 56m e) 80m and f) 96m in Jan. 2009

Another important aspect of understanding on seas surrounding the island chain is the Island Mass Effect (IME), which may be reflected as, a change in temperature/salinity/nutrient pattern, eutrophication due to terrigenous discharge, pollution, changes circulation pattern near the

coast, coastal upwelling and eddies. However, in the present study, the near coastal station considered is at 50 m depth contour and found no significant influence in hydrography except for silicate concentration, observed 2-10 µmol/L. However, no significant influence of the same is observed during the survey, except the high biovolume (0.55 ml/m^3) of zooplankton in the west. Other indications of the IME are the weak coastal upwelling observed in the chemical and biological response (Salini et al., 2010) and the irregularities in SSHA pattern as seen in Fig. 2.9c.

To further understand the forcing mechanism which controls the upper layer circulation of the region, the vertical extent of the momentum transfer due to Ekman depth is computed using Pond and Pickard (1983) and on an average, it is 55 m in November-December 2011 and 52 m in January 2009. This strikes contradiction with the ADCP derived current structure, which is uniform up to 88 m in November-December 2011 and 80 m in January 2009, and it explains that some other forcing is also involved other than the Ekman forcing. This supports the observation from Potemra et al. (1991) and Yang et al. (1998) that the propagation of Kelvin waves does play a major role in regulating the upper layer dynamics with clear seasonal variations. According to Chatterjee et al. (2017), the mean circulation within the Andaman Sea and around the islands is primarily driven by equatorial forcing, rather than the local wind forcing which is marginal. The current forced by local winds is weak compared to that remote forcing along the equator. So the present study, based on the in situ vertical profiles on currents and hydrographical parameters, suggests the role of additional factors than the atmospheric momentum transfer due to wind.

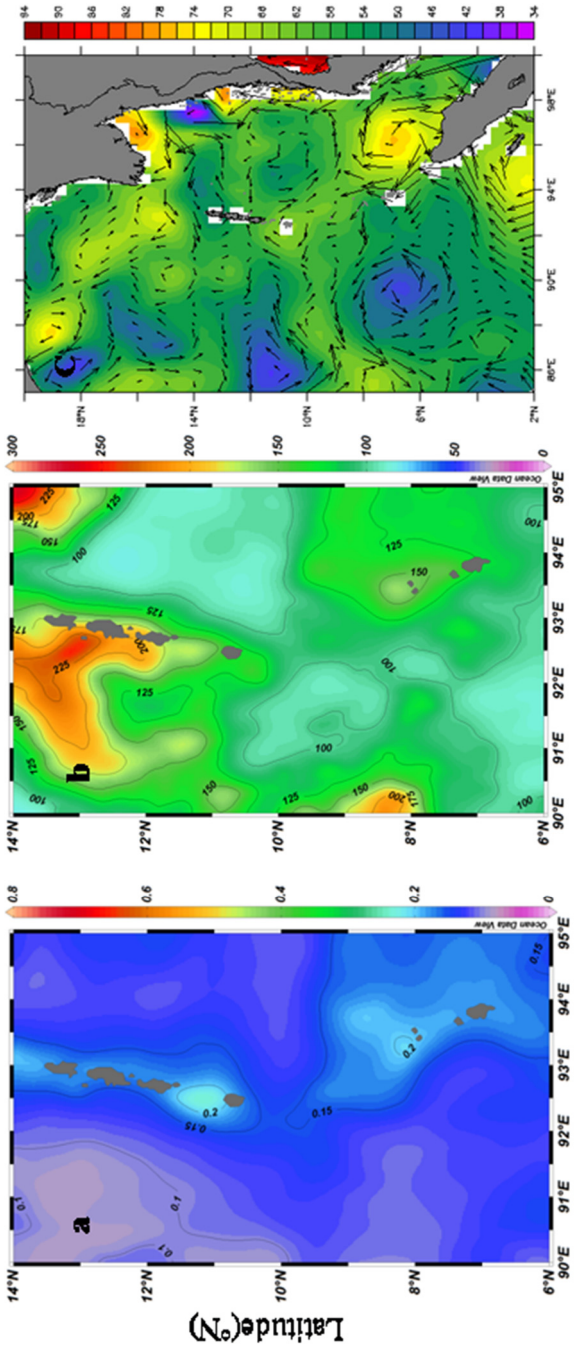

Fig. 2.9: Surface distribution of a) chl a (mg/m^3) b) PP (mgC/m^2/d) and c) SSHA and Geostrophic currents during Nov-Dec 2011

2.3.4 Biological response

Spatial and temporal changes in the physico-chemical characteristics of this region are expected to have great influence in the chl a and phytoplankton distribution. Monthly composite of the surface chl a derived from ocean colour sensor is made use to understand the biological response and it is found that the mean surface chl a varies between 0.1 and 0.4 mg/m^3 in November-December 2011 (Fig. 2.9a) and 0.2 and 0.4 mg/m^3 in January 2009 (Fig. 2.10a) with relatively higher concentration along the south of 10°N (>0.3 mg/m^3) compared to other areas. The high concentration of surface chl a may be due to the inflow from Malacca Strait. Rama Raju et al. (1981) reported the inflow of Malacca Strait into the southern region. The moderate chl a (0.3-0.4 mg/m^3) along the coastal area is mainly due to the presence of the island chain. VGPM-derived column-integrated primary productivity shows variation between 100 and 225 mg C/m^2/d in November-December 2011 (Fig. 2.9b) and 200 and 300 mg C/m^2/d in January 2009 (Fig. 2.10b). Maximum PP is recorded as 300 mg C/m^2/d along the south in January 2009. At some extent, it spreads northward upto 9°N. Again, the higher chl a and PP in the southeastern part are associated with productive environment of Malacca strait. Weak mixing as explained in the upper layer mixing and hydrography between the surface, subsurface and the bottom water may be the reason for low production in the Andaman Sea as suggested by Sengupta et al. (1981). Other than the near coastal area where PP>250 mg C/m^2/d and the southeastern part, the waters are more or less oligotrophic. However, the higher PP (150-200 mg C/m^2/d) during November-December 2011 in the

southeastern and southwestern part is due to the cyclonic circulation, as evidenced from the SSHA pattern (Fig. 2.9c).

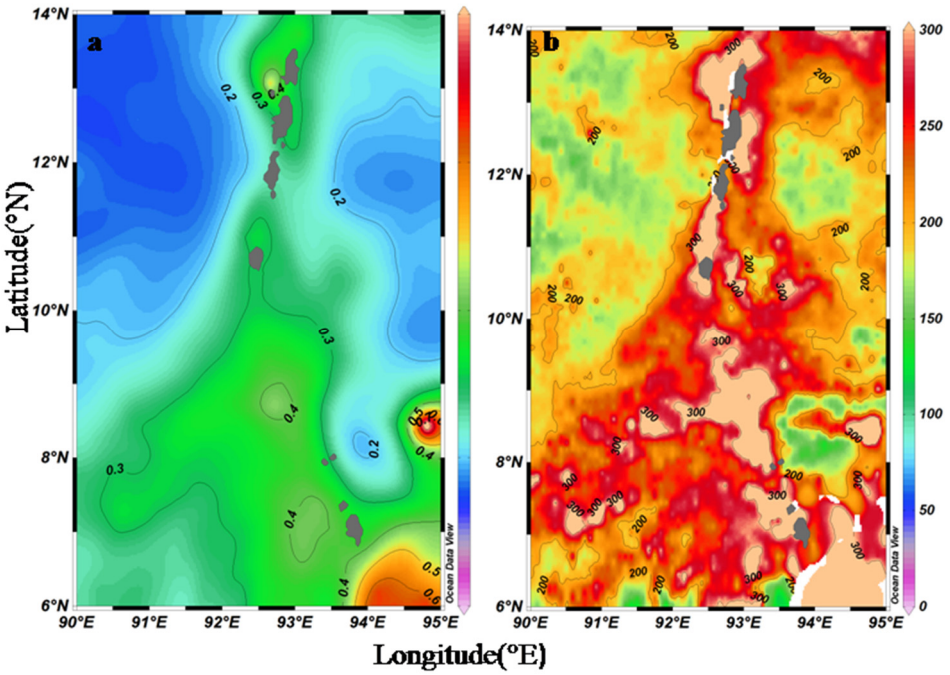

Fig. 2.10: Surface distribution of a) chl a (mg/m^3) b) PP (mgC/m^2/d) during Jan 2009

2.4 Conclusion

Physical forcing and related biological response of Andaman waters is addressed during winter monsoon (November-December 2011and January 2009) based on in situ and satellite measurements. It is found that prevailing northerly and northeasterly winds makes the area cool and, though not intense, influence the upper layer characteristics. Hydrography of the region clearly demarcate the area into three: i) along west showing typical BoB characteristics, ii) along east showing the influence of

riverine input from Ayeyarwady-Salween river system supplemented with weak evaporative cooling and iii) south due to intrusion through Malacca strait. Also, the study reports the upper layer circulation up to 96 m based on in situ current profiles as regulated by both geostrophy and Ekman in a magnitude range of 100-1000 mm/s. The southern area is productive compared to other parts due to the influence of productive environment of Malacca Strait. Overall, the region is oligotrophic in comparison with other seas in the Indian Ocean due to weak mixing between surface and subsurface water. The surface geostrophy and the production pattern evidence the role of local as well as remote forcing in determining the spatial pattern of oceanographic features of the region.

Chapter 3

MESOSCALE PROCESSES REGULATING THE UPPER LAYER DYNAMICS

Contents

3.1 Introduction

The Sea around the Andaman and Nicobar Island chain is influenced by reversing monsoon with moisture rich summer winds and dry continental air flow from north-east during winter (Potemra et al., 1991). The region receives enormous runoff and suspended matter from Ayeyarwady-Salween river system, which has significant influence on the hydro-dynamics and oceanography (Robinson et al., 2007). The region is characterised by strong stratification, prevents vertical mixing, causes nutrient depletion in the upper layers and subsequently leads to oligotrophy. The seasonal winds, moderate or strong, though are experienced during the summer and winter months, are not found to exert any divergence or positive curl and nutrient pumping to enrich biological production is least encountered in these waters. The sea is less productive compared to the Arabian Sea and Bay of Bengal and average primary production during

fall inter-monsoon is 283.19 mg C/m^2/d followed by spring inter-monsoon (249 mg C/m^2/d), summer monsoon (238.98 mg C/m^2/d) and winter monsoon (195.47 mg C/m^2/d) (Sanjeevan et al., 2011). Earlier observations show that the eastern and western part of the island chain is governed by distinct water properties where west shows typical BoB characteristics, northeast is highly influenced by the Ayeyarwady and Salween river system and the southeast by the productive environment of Malacca strait (Salini et al., 2010). The region is least explored for oceanic processes and surveys conducted so far for understanding the biodiversity and the basin scale environment associated with the living resources indicate the absence of any major or seasonal processes that result in nutrient pumping to alter production pattern. However, the emergence of satellite techniques, especially the Altimetry and Ocean Color imageries on mesoscale to basin scale, the understanding of the upper layer dynamics has been strengthened. Explanations have come on such major processes in the BoB, especially on number of eddies and gyres and also the impact of cyclones, which causes enormous mixing in its path. Eddies are mesoscale processes (50–200 km diameter) and ubiquitous feature of the ocean occurs in both clock-wise and anti-clock wise direction, resulting in convergence/divergence at the center.

Mesoscale eddies play a dominant role in transportation of salt, heat and nutrients within the ocean (Dong et al., 2014) and enhance local production in oligotrophic areas (Hyrenbach et al., 2006), ultimately influencing the production pattern in each trophic level (Bakun, 2006). Mechanisms behind the eddy formation has been suggested by many researchers; different driving mechanisms have been

attributed to eddy formation, such as Ekman pumping and remote forcing from the equatorial Kelvin wave reflecting off the eastern boundary as Rossby wave. According to Yu et al. (1999), westward propagating Rossby wave, excited by the remotely forced Kelvin wave, contribute substantially to the variability of the local circulation in ocean. Using the multilayer model, Potemra et al. (1991) described coastal Kelvin wave, which originates at the equator and propagates around the entire western perimeter of the region around both the Andaman Sea and the Bay of Bengal. Mesoscale eddies are observed in the coastal waters of the Andaman and Nicobar Islands (Hacker et al., 1998 and Chen et al., 2013) based on in situ hydrographic measurements. Burnaprathepart et al. (2010) described the presence of eddies in Andaman Sea and its role in enhancing the primary productivity synthesizing number of vertical profiles on chl a, major nutrients, temperature, as well as salinity. Eddies are identified based on SSHA imagery and geostrophic current pattern, indicated by low and anticlockwise circulation pattern resulting in divergence and upsloping in the center. The present study, based on a suit of in situ and satellite measurements on physical, chemical and biological data, explains the characteristics, generation mechanism and evolution of the eddy and its impact on the regional primary production.

3.2 Data and Methodology

In situ measurements were taken onboard FORV *Sagar Sampada* during 21 November –14 December, 2011. The environmental characteristics are understood from station based measurements in the east and west of

the island chain. However, the focus was to obtain a transect with 4 stations (Fig. 3.1) along the eddy.

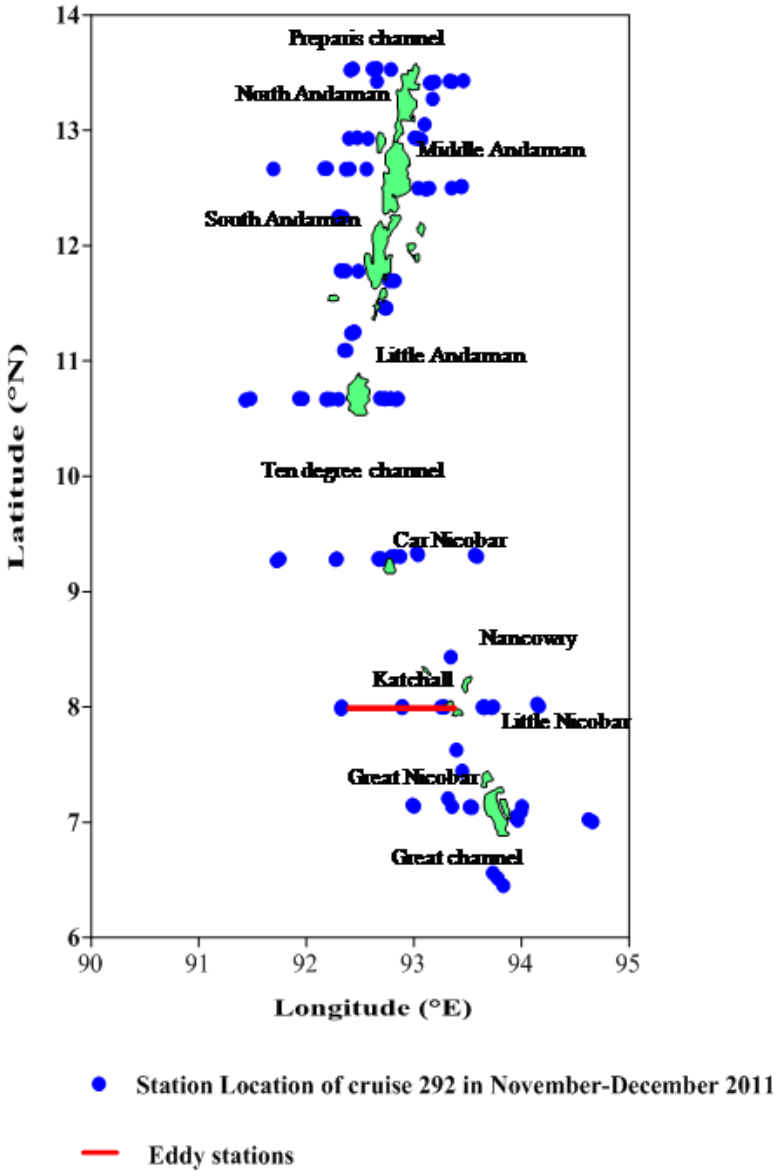

Fig. 3.1: Station Locations

The detailed description of in situ datasets acquired on meteorology/ oceanography parameters are described in Chapter 2. Twelve numbers of 10 liter Niskin water samplers were used to collect water samples from standard depths (surface, 10, 20, 30, 50, 75, 100, 120, 150, 200, 300, 500, 750 and 1000 m) for measurements of dissolved oxygen and nutrients. Temperature-Salinity profiles for water mass characteristics are based on averaged (climatological) data from Levitus et al. (1994). Monthly composite of the chlorophyll data is obtained from the Distributed Active Archive Center (DAAC) of National Aeronautics and Space Administration, NASA. Dissolved oxygen was measured by Winkler titration. Analyses of nitrite, nitrate, phosphate and silicate were performed using a Skalar Analyser.

Bathymetry of the region was analysed using the NIO's modified dataset (Sindhu et al., 2007). NIO modified the original ETOPO5 and ETOPO2v2 bathymetric grids in shallow water regions using the digitized data.

Wind stress curl (daily) data used was taken from ASCAT processed by NOAA/NESDIS utilizing measurements from the Scatterometer instrument aboard the EUMETSAT Metop satellites with a spatial resolution of 25 km; chl a data was taken from MODIS Aqua Level 3 at a spatial resolution of 4 km, downloaded from Ocean Color Website and processed using SeaDas. SST was obtained from MODIS Aqua Level 3 at a spatial resolution of 4 km downloaded from Ocean Color Website, while SSHA data obtained with 7 day temporal resolution from AVISO for the period from January 2003-January 2013. The cold core eddy was recognized through SSHA with geostrophic current imagery obtained

from https://oceanwatch.pifsc.noaa.gov, and was observed to be centered at 7° N and 90° E with current moving in cyclonic direction. Net heat flux, solar radiation, latent heat flux, and specific humidity were obtained from http://oaflux.whoi.edu. The in situ observation at 8° N along 92.5° E-93.5° E was identified as the eastern periphery of the eddy identified.

The eddies are spotted using two ways, first method is using SSHA contours and geostrophic currents, calculated from the following geostrophic equations,

$$u = -\frac{g}{f}\frac{\partial h}{\partial y} \quad \text{.....(1)}$$

$$v = \frac{g}{f}\frac{\partial h}{\partial x} \quad \text{.....(2)}$$

Where u and v are the zonal and meridional components of geostrophic currents, g is the gravitational acceleration, f is the Coriolis parameter, x and y are longitudinal, latitudinal co-ordinates and h is the SSHA.

Second method is using the Okubo-Weiss parameter, OW (Okubo, 1970 and Weiss, 1991) and is defined as

$$OW = s_n^2 + s_s^2 - w^2 \quad \text{.....(3)}$$

Where s_n is the normal strain component, s_s is the shear strain component and w is the relative vorticity.

$$s_n = \frac{\partial u}{\partial x} - \frac{\partial v}{\partial y} \quad \text{.....(4)}$$

$$s_s = \frac{\partial v}{\partial x} + \frac{\partial u}{\partial y} \quad \text{.....(5)}$$

$$w = \frac{\partial v}{\partial x} - \frac{\partial u}{\partial y} \quad \text{.....(6)}$$

If the vortex core is dominated by vorticity, the negative Okubo-Weiss are predictable in the vortex core.

Wavelet transform is an appropriate analysis tool to study multi-scale, non-stationary processes occurring over finite spatial and temporal domain. In this study, the wavelet was used to analyse time series data of oceanographic parameters that contain non-stationary power at many different frequencies. This technique is used to decompose time series into its frequency components based on the convolution of the original time series with a set of wavelet functions, and if possible, determine both the dominant modes of variability, and how those modes vary with time. It expands functions in terms of wavelets, which are generated in the form of translations and dilations of a fixed function called the Mother Wavelet. Meyers et al. (1993) used wavelet analysis to study the propagation of mixed Rossby-gravity waves in an idealized numerical model of the Indian Ocean.

The phase speed for long baroclinic Rossby wave is given by

$$C = \frac{-gH_0\beta}{f^2}, \quad \text{.....(7)}$$

where g is the reduced gravity term (taken as 0.04 m s^{-2} for the first baroclinic mode), H_0 is the thermocline depth (taken as an annual mean depth of 20°C isotherm derived from Levitus and Boyer, 1994), f the Coriolis parameter and $\beta = \frac{\partial f}{\partial \phi}$, where ϕ is the latitude.

3.3 Results and Discussion

3.3.1 Physical characteristics of the eddy region

The region is characterized by warm (27.6–28 °C), humid (72–77%) air and wind is from northeast, suggesting the prevalence of northeast monsoon condition of magnitude in the range of 10–12 m/s with comparatively lower speed (10 m/s) in the western part and higher speed (12 m/s) in the eastern part of the eddy (referred to hereafter as CE1).

The SST varies in the range of 28.4-28.8 °C with lower temperatures near the coastal water compared to offshore; the surface salinity (33.00 psu) and density (20.40 kg/m^3) values, on the other hand, are similar in coastal and offshore waters. Regional water mass characteristics from temperature, salinity, and density profiles show that the area is occupied by BoB waters with temperature ranging from 28.0-28.5 °C, salinity 33.2-33.8 psu, and density 20.6-20.8 kg/m^3 (Salini et al., 2018). Vertical temperature distribution along 8°N (Fig. 3.2b) shows warm (>28.5 °C) and thick isothermal layer (~54 m) in the western part and a gradual decrease towards east (20 m). The most important feature in the thermal structure is the upsloping of isothermal layer, which is prominent in the subsurface (54–220 m) also, and the mixed layer depth (MLD) shoaled from west to east (47–19 m). Vertical salinity and density distribution show the presence of low saline (32.9–33.1psu) water in the upper 30 m, with an upsloping tendency (Fig. 3.2 c, d) as in the case of temperature. Similar pattern is reflected in density characteristics too.

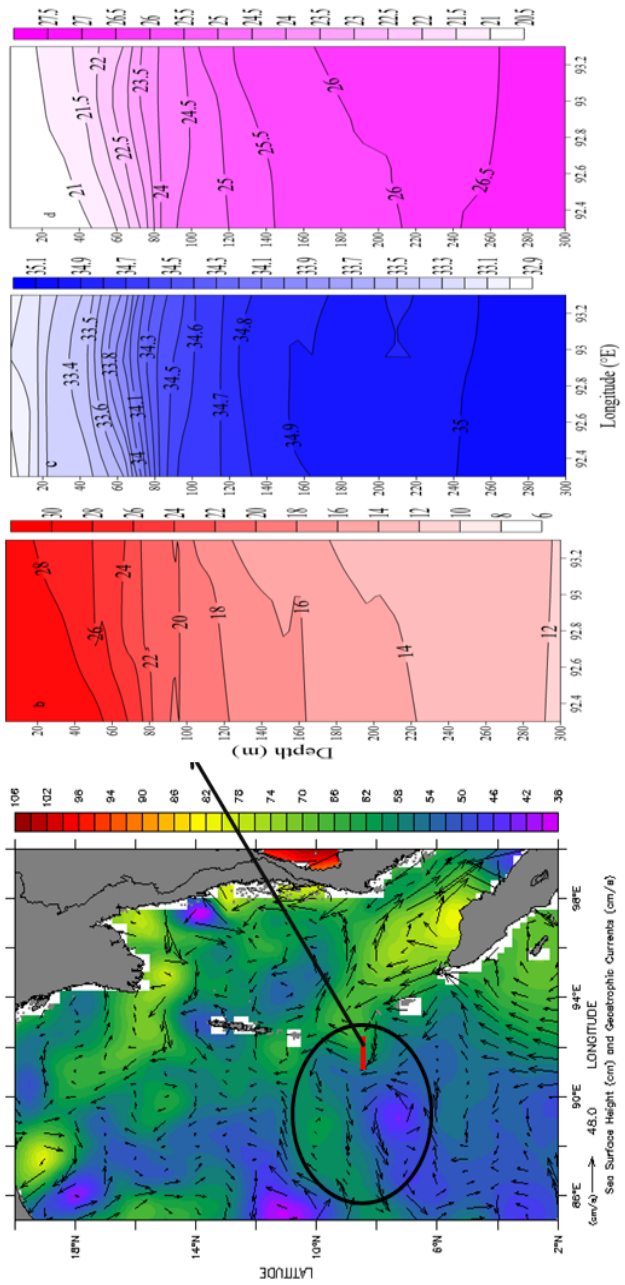

Fig. 3.2: a) Weekly Sea surface height (cm) and geostrophic current (cm/s) from 1-7 Dec, 2011 b) Vertical temperature (°C) c) salinity d) density (kg/m^3) distribution at 8 °N and 92.5-93.5 °E

The vertical current structure at 8° N along 92.5° E to 93.5° E shows irregular current pattern from surface to 90 m (Fig. 3.3). Along the eastern part of the 100 km transect, major flow is towards south (≅30 km), west to it with a narrow and weak northward flow, followed by major southward drift up to 40 m. However, the response to this irregular pattern is insignificant in the T-S profiles and so the eastern part of the transect (~60 km) is not considered for addressing the eddy. In the western flank, the northward and the subsequent flow towards south indicate cyclonic flow direction. The current recorded at 16 m depth is considered for near surface pattern and this shows the presence of a northern component with a magnitude of 0.3 m/s in the eastern part negligible speed in the western part, directed westward. But at 40 m the current magnitude decreases in the eastern flank (0.1 m/s) and increases in magnitude in the western flank (0.1 m/s) with direction changing from northeast to southwest. The current at 88 m also follows the same pattern, but magnitude changes from 0.5 m/s in the western part and 0.4 m/s in the eastern part. The upsloping in the T-S profiles concurrent to this confirms the feature as a subsurface cyclonic eddy. The flow in the eastern flank is towards north (0.3 m/s) and at west it is to the south (0.5 m/s). The data was analyzed for all 8 m cells up to 88 m depth and found to follow the same pattern as that of near surface but with a decreasing magnitude. The dataset was seen to contain spurious values below 88 m and hence discarded.

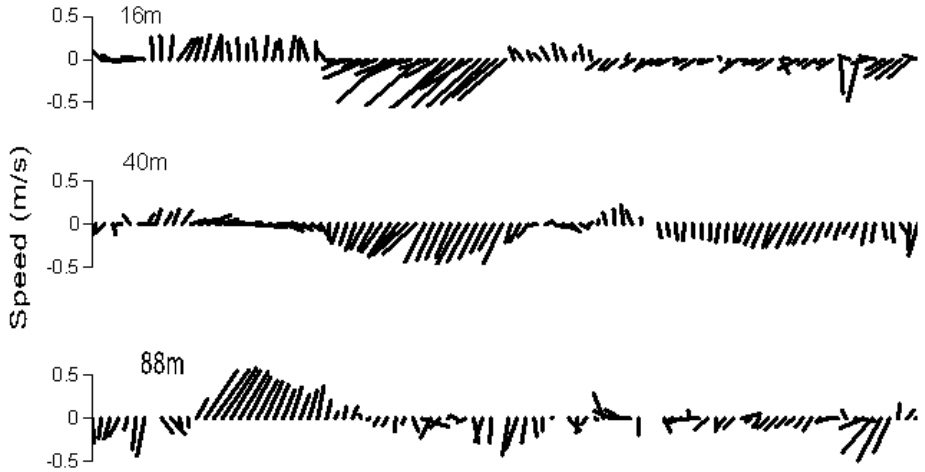

Fig. 3.3: Horizontal current (m/s) pattern at different depth along 8ºN

3.3.2 Eddy Generation Mechanism

The possible physical mechanisms that govern the eddy includes the wind stress curl, topographic instability, shear flows, baroclinic instability and the radiation of Rossby waves from poleward propagating coastal Kelvin waves etc. (White, 1977 and Kessler, 1990). Daily wind stress curl is examined to identify the local forcing that contributes to the formation and sustenance of the eddy. Curl of the eddy region from ASCAT wind data shows negative values in the range of -5.6×10^{-8} and -8.24×10^{-8} Pa/m, indicating convergence and hence the contribution due to wind stress curl is ruled out.

Other possible eddy generation mechanisms are differential mixing of region with the adjacent sea mainly through inflow from Malacca Strait and freshwater influx from adjoining rivers leading to strong density variations in the water column. This variation may reduce or enhance the

mechanical effects in the form of eddy or meanders in the region. This is measured based on the estimated Richardson Number (Ri). According to Miles (1961), the flow is stable if Ri>0.25.

Ri is calculated as $\mathrm{Ri} = \frac{N^2}{(\frac{\partial u}{\partial z})^2}$ .....(8)

where N^2 is the Brunt Vaisala frequency (BV),

$$N^2 = \frac{-g}{\rho_0}\frac{\partial \sigma_t}{\partial z} \quad \text{.....(9)}$$

where g is the gravitational acceleration, $^{\rho}{}_0$ the average sea water density, z the depth, and σ_t is ρ-1000 where ρ is the sea water density. The denominator term $\partial u/\partial z$ in (7) is the velocity gradient, which is an indicator of strength of mechanical generation calculated from vertical current profiles acquired using ADCP.

The low BV (avg. 3.165×10^{-5} s^{-1}) and large velocity gradient (avg. 3.968 s^{-2}) resulted into low Ri (avg. 0.0001), indicating unstable well mixed water column. These lead to instability in the water column and favor eddy-like perturbation in the region.

Instability arises either as a result of mixing of different water masses or due to the shear flows. Mixing with other water masses can be ruled out as there is clear evidence of the presence of BoB water in the eddy region from the T-S profiles. Another possibility is the prevalence of planetary waves that might modulate the horizontal flow and induce shear, thereby causing instability; such instability has been well reported along this region by Schott et al., 2009 and Rao et al., 2010, that planetary

waves influence the near surface circulation through local and remote forcing. The role of such planetary wave influence on eddy generation mechanism was examined using altimeter data and mapping of planetary wave propagation was carried out to identify their influence on regional circulation. Referring to Yu (2003), Hovmuller diagram of SSHA at 8°N along 89°E to 94°E was analyzed to track the planetary wave and are plotted (Fig. 3.4). Low SSHA in this region from mid-November to mid-January indicates the presence of upwelling mode Rossby wave (Girishkumar et al., 2011). Negative SSHA is almost horizontal, indicating a fast propagation of Rossby wave. Further west (nearer to the eddy location), negative SSHA showed a steeper slope, indicating a slower propagation. The westward propagating signal takes about 45-60 days to travel from the coast of Nicobar Island chain (Potemra et al., 1991) to the periphery of the eddy region, which yields phase velocity of the westward signal at 0.20 m/s. The theoretical phase speed of Rossby wave at 8°N that propagates westwards is calculated as 0.21 m/s, suggesting that the signal appearing in the plot is a Rossby wave that is generated on the west coast of Nicobar island chain. The estimated speed of the wave is close to the theoretical wave speed and the estimate also compares well with earlier results of Yang et al. (1998), Yu (2003) and Girishkumar et al. (2011). The Rossby waves were produced by radiation from the west coast of Nicobar Island chain in association with poleward propagating coastal Kelvin waves (Potemra et al., 1991). The baroclinic instability due to the interaction of westward propagating Rossby waves and local wind stress curl cause meanders and eddies in BoB (Nuncio and Prasanna Kumar, 2012). Using a numerical model, Kurien et al. (2010) also

concluded that baroclinic instability plays a key role in meander growth and eddy generation in BoB. Sreenivas et al. (2012) argued that coastal Kelvin waves and the associated radiated Rossby waves from the east play a dominant role in the mesoscale eddy generation in BoB.

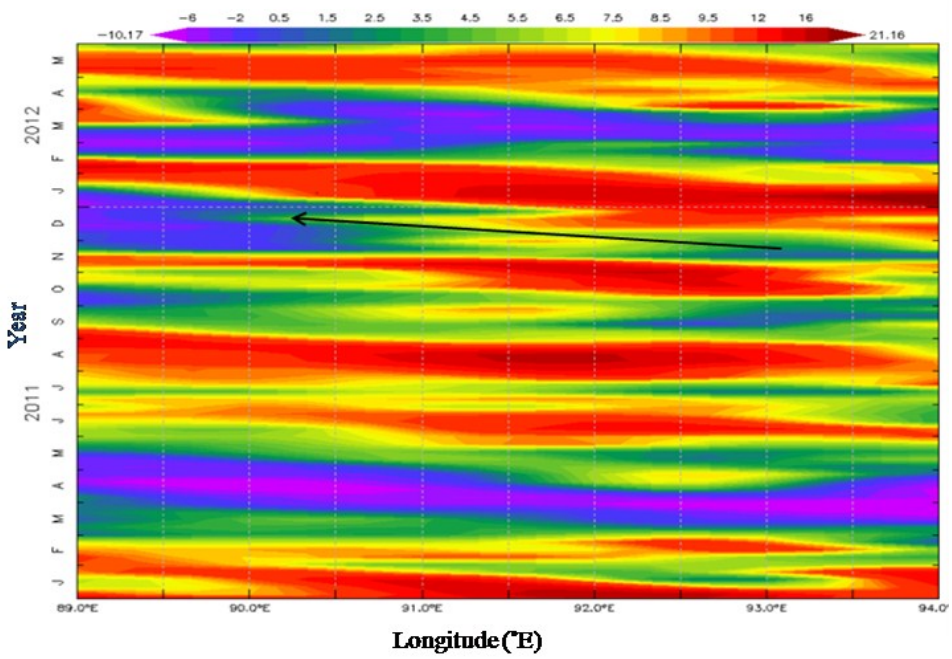

Fig. 3.4: Hovmuller of SSHA along 8ºN

To ascertain the periodicity of SSHA, the data is again subjected to continuous wavelet transforms with Morlet wave as mother wavelet following Torrence and Compo (1998). It is clear from Fig. 3.5 that the dominant mode of variability is semiannual. In the Andaman waters, the wave period is more variable due to the effect of westward propagating Rossby wave from the coastally trapped Kelvin wave (Vialard et al., 2009 and Nienhaus et al., 2012). From power and global wavelet spectrum, the

predominant frequencies are in semiannual and annual modes. The annual mode seems to be reduced in intensity compared to the semiannual mode. On the basis of the results of wavelet analyses, it is clear that the semiannual Rossby waves are significant in the years 2005, 2008, 2010 and 2011, whereas the annual wavelets are significant during 2006-2009. Therefore, we concluded that the westward propagating Rossby wave radiated from the coastal Kelvin wave contribute to cyclonic eddy in the region.

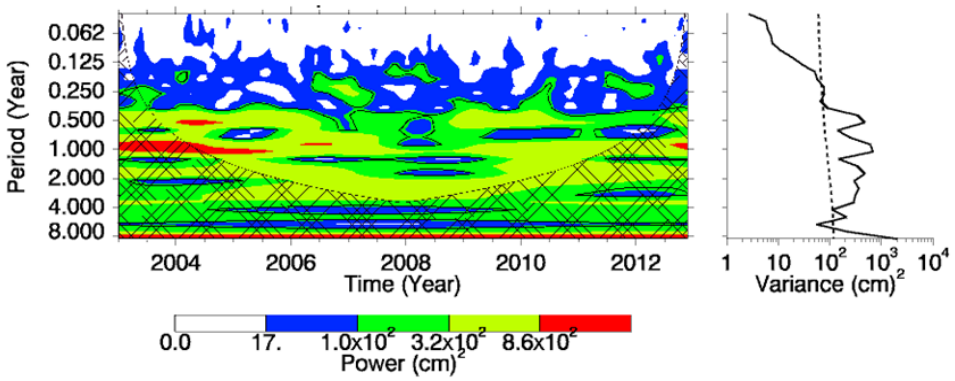

Fig. 3.5: Wavelet power spectra of SSHA along 8ºN

3.3.3 Chemical and biological response of the eddy

Concurrent with the thermohaline oscillations, the vertical structure of dissolved oxygen (DO) also demonstrates fluctuations above 90 m depth. The 4.22 ml/L DO contour shoaled from a depth of about 47 m (92.3°E) to 25-30 m at eastern flank of the eddy (93.3°E). The upper nitrate (NO_3) concentration is in detectable levels (0.67-0.98 µM) and shows slight upsloping towards the eastern flank (93.3°E). The phosphate (PO_4) concentration in the upper water was also at a detectable level and showed a slight upsloping towards the eastern side (0.12 µM at 92.3°E

and 0.27 µM at 93.3°E). Further, the vertical distribution of silicate (SiO_4) showed slight upsloping towards the eastern periphery (0.77 µM at 92.3°E to 1.62 µM at 93.3°E). Hence, concomitant with the thermohaline characteristics, the vertical distribution of nutrients also showed oscillations in the upper water column.

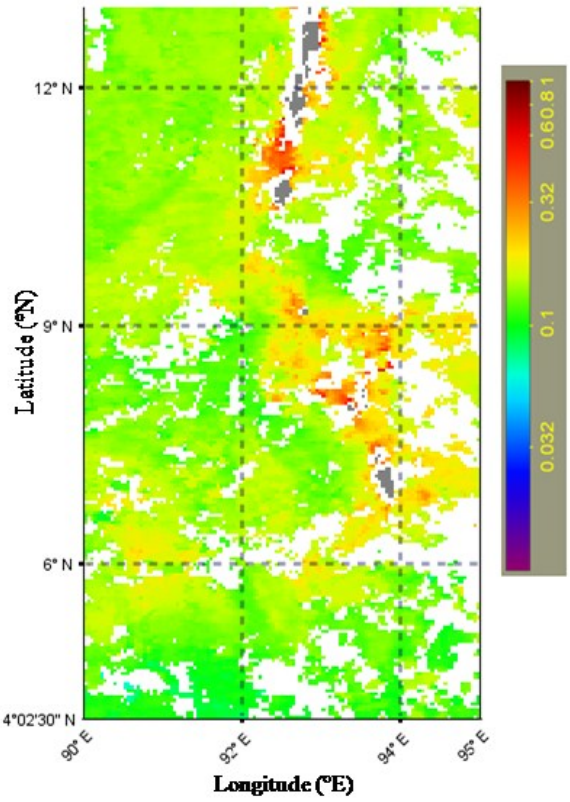

Fig. 3.6: Chl a pattern during insitu observation

The physical and chemical characteristics do reflect on the regional biology and this is well reflected in the surface chl a distribution. Chl a derived from ocean colour imagery (Fig. 3.6) can illustrate the standing stock of the primary consumers for the optical depth and is 0.5 mg/m^3 in

the eddy region compared to the adjacent regions (0.1 mg/m^3). This increases within the eddy in association with the nutrient values explains the impact of churning due to the eddy. This points out the significance of such mesoscale processes that influence the production marginally in the Andaman waters.

3.3.4 Satellite evidence (SSHA based) for cyclonic eddies

The distribution of mesoscale production favourable pockets is examined using monthly SSHA and geostrophic current pattern (Fig. 3.7a-d) for the winter monsoon (November-February, 2011). This evidences the presence of two cyclonic eddies (CE), of which CE1 is the same that encountered during the in situ measurements and CE2 observed at 13°N and 93°E. CE1 was stronger as indicated by negative SSHA between 5°–9°N with core at 7° N latitude and is observed to be propagating from 93°E to 86°E within one month (November to December). The eddy intensity is more during November and December, with a negative value of ¯0.14m. In December CE1 propagates westward to BoB and is observed between 86°-93°E. It is completely replaced from Andaman waters by January and exhibited a positive SSHA (0.18 m). But the low SSHA observed in BoB waters even during February centered at 86° E. The shape of the eddy is elliptical with its axis oriented in east west direction. The eddy CE1 characteristics and generating mechanism is described in the above sections (3.3.1-3.3.3) using in situ as well as satellite observations.

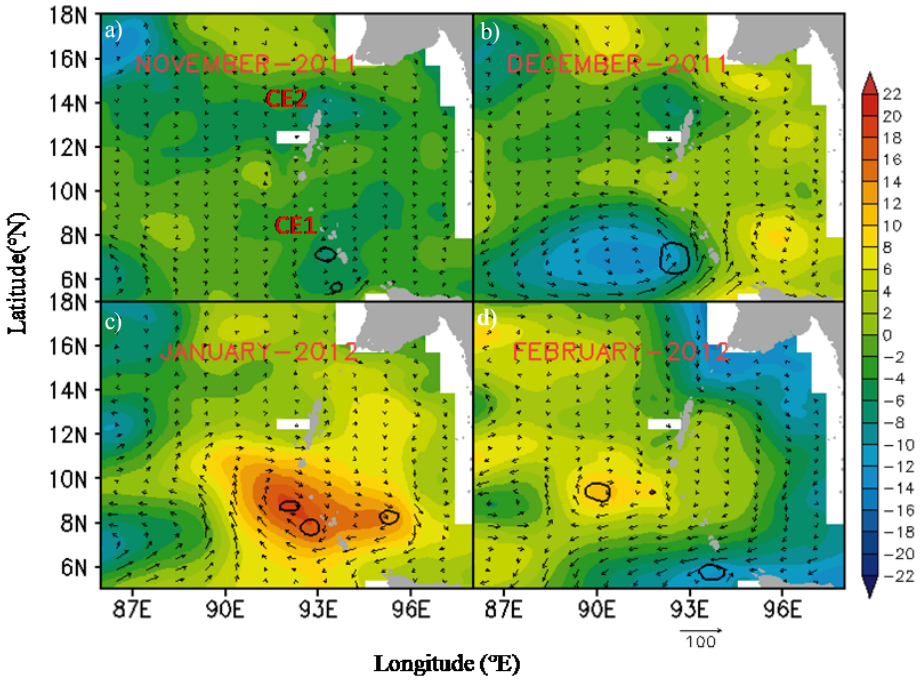

Fig. 3.7: Monthly SSHA (cm), Geostrophic current (cm/s) and Okubo-Weiss paremeter (Black contour of $^{-}2x10^{-11}$ /s^2) from Aviso during a) November b) December c) January d) February

The SSHA maps also revealed a cyclonic eddy located at 13°N and 93°E during November with negative anomaly of ¯0.12m. This eddy is marked as CE2. The negative anomaly is more in November with SSHA of -0.12 m, and the intensity decreases during December with SSHA of 0.10. Negative anomaly is replaced by positive anomaly of 0.16m during January.

In order to identify eddies in a prominent way, Okubo-Weiss (OW) parameter method is also exercised in this study. Eddies are characterized with negative OW parameter at the eddy core due to the dominance of vorticity over strain components; while strain dominated areas have positive OW parameter. According to Isern-Fontanet et al. (2003), closed

contours of OW with a value of -2×10^{-11} /s^2 corresponding to the threshold value for defining eddies. The threshold value was fixed as same as Isern-Fontanet et al. (2003) for defining eddies and finding out the vorticity dominated area. From the Fig. 3.7a-d, the closed contours of OW, and cyclonic current structure confirmed the presence of an intensified cyclonic eddy at 8°N and 93°E. But the area characterized with threshold value less than -2×10^{-11} /s^2, negative SSHA and the cyclonic current structure at 13°N and 93°E indicated the presence of a weak eddy.

Having recognized eddies from SSHA, OW and geostrophic current maps, it is further confirmed the occurrence of prevailing processes using SST and chlorophyll. Cyclonic eddies formed due to the divergent forcing at the center is occupied with sub-surface nutrient rich waters at the core. These areas of negative SSHA are characterised with relatively cool and high chlorophyll concentration.

SST is high during the initial phase of winter months, i.e. in November (Fig. 3.8a), with higher values in the entire region of Andaman waters (28.2-28.8 °C). During December (Fig. 3.8b), the values change to 27.6-28.8 °C. Further, during January (Fig. 3.8c) and February (Fig. 3.8d), the basin wide temperature is in the range to 27-29 °C and 26-29 °C respectively. Though the Andaman waters are warm in general, the cold core eddies identified in this area show relatively cool temperatures owing to the prevalent cyclonic flow associated with it. CE1 records a temperature of 28.6 °C during November, and when the eddy advances to the Andaman waters the surface temperatures begin to cool. SST decreases from 28.6 to 28.2 °C during December; SST again decreases to 27.6 °C in January.

But in February the temperature remains the same as in January. CE2 displays a temperature of 28.6 °C during November; during December, the temperature decreases to 28.2 °C, and decreases further to 27 °C during January and again in February (26.5 °C). The hike in temperature along the eastern Andaman waters might be due to the intrusion of low saline waters through Malacca strait as inferred by Rama Raju et al. (1981) and Tan et al. (2006).

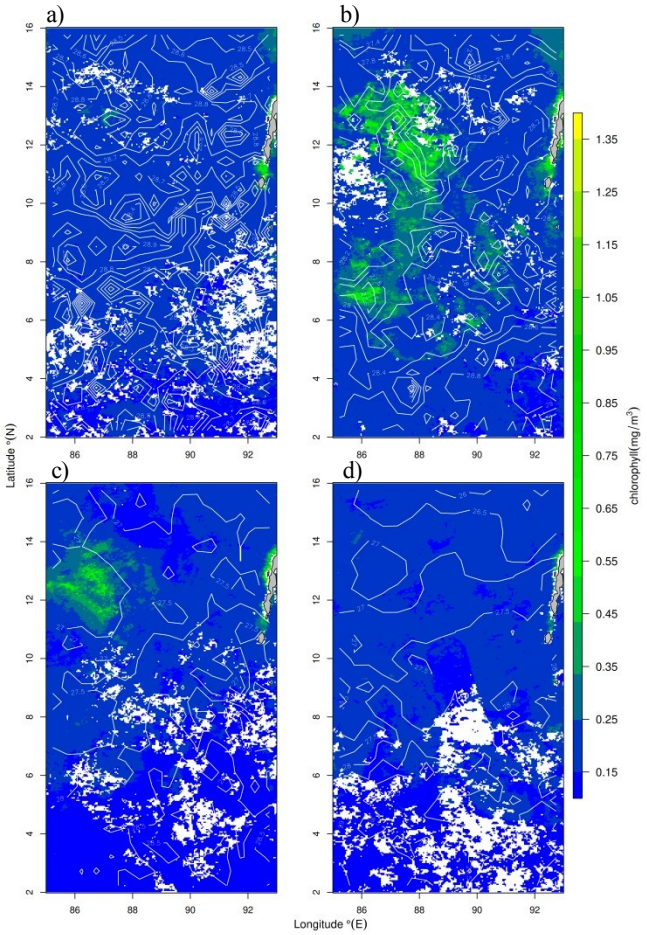

Fig. 3.8: Overlap map of SST and chl a during a) November b) December c) January d) February

High chlorophyll concentration is expected in the eddy region due to enhancement of nutrients at the surface. These cold core eddies are important because they are in the area of high biological activity and these areas are observed to have strong physical and biogeochemical coupling resulting in high chlorophyll concentration. Generally, Andaman waters are oligotrophic in nature with less chlorophyll concentrations (Vijayalakshmi et al., 2010). The existence of cyclonic circulation increases the chl a levels in the eddy region. When the cyclonic flow advances, increased chl a level was observed in the eddy locations at CE1 and CE2. CE1 recorded 0.1 mg/m^3 during November, increased to 0.8 mg/m^3 during December and decreased again to 0.3 mg/m^3 in January (Fig. 7a-d). Chl a level decreased to 0.2 mg/m^3 in February. CE2 revealed a very low value (0.1 mg/m^3) during November; during December, chl a began to increase in the eddy region (0.4 mg/m^3) and in January also the pattern followed with a concentration of 0.4 mg/m^3, which decreased to 0.2 mg/m^3 in February.

The role of wind stress curl on inducing the eddy was verified with weekly progress in the wind stress curl (ASCAT) for the pockets. At CE1 the curl varied from -4.43×10^{-7} to 1.28×10^{-6} Pa/m, but the mode of the signal was -1.47×10^{-7} Pa/m. The wind curl at CE2 showed values between -2.87×10^{-7} and 2.09×10^{-6} Pa/m and mode was -3.25×10^{-8} Pa/m. However, the occurrence of maximum negative values implies that wind is not a dominant causative factor for the generation of eddy.

At CE2, the surface temperature is low (27-27.2 °C) compared to the nearby locations and the MLD is also deeper (>70 m). Wind is

northeasterly, with a magnitude of 4 to 7 m/s. Specific humidity of 14 to 18 g/kg implies dry continental air during the period. Net heat flux varies from −98 to −134 W/m^2 during November-February. This causes heat loss due to evaporation (latent heat flux −220 to −312 W/m^2), resulting in cooling in the sea surface. Solar radiation varies from 114 to 170 W/m^2 in the eddy region. This low solar insolation reduces the SST, resulting densification of water. Thus, the surface water sinks and nutrient rich water entrains from deeper depths. This evidences that the atmospheric forcing causes surface cooling and the resulting convective mixing entrains nutrients into the upper layer which activates the primary production (Prasanna Kumar and Prasad, 1996, Madhupratap et al., 1996). Chatterjee et al. (2017) reported that the equatorial signal of Kelvin comes into the Andaman Sea through the Great Channel, travels along the eastern boundary, and exits to BoB through Preparis Channel, with a smaller part flowing southward along the east coast of the Andaman Islands. In this context it is presumed that the generating mechanism of CE2 is Kelvin. The instability owing to the flow from Ayeyarwady-Salween river system is also supposed to be the reason for CE2 origin.

3.4 Conclusion

The column dynamics, forcing mechanisms, chemical and biological responses of cyclonic eddies are explained for the Andaman waters based on a suit of in situ and satellite datasets. The eddies are tracked using Okubo-Weiss parameter and the eddy CE1 is strong compared to CE2 based on the threshold Okubo-Weiss parameter of -2×10^{-11} /s^2. The processes are small scale in nature within 100-350 km diameter, and are

found to be induced as a result of baroclinic instability arising owing to the westward propagating Rossby wave, semi-annual mode with phase speed of 0.20 m/s for CE1 and CE2 may be induced by Kelvin and the instability occurs due to the Ayeyarwady-Salween flow. While CE2 is associated with the process of convective mixing process occurring in the region due to cold dry continental air from north east. The study concludes that, in addition to the mesoscale processes, the convective mixing occurring along the northwest coast of Andaman is taking a substantial role in triggering the biological production of Andaman waters. Considerable increases in the regional surface biological production indicates the complementary role of such processes in bringing up the quality of production in Andaman waters. The role of convective mixing and eddies in the dynamics of the Andaman waters are explained for the first time.

Chapter 4

SPATIO-TEMPORAL VARIATION OF FORCING FACTORS REGULATING THE UPPER LAYER DYNAMICS

Contents

4.1 Introduction

The Indian Ocean is distinct from other oceans because of semiannual reversal of monsoon winds and the associated variations in the ocean currents and processes. Number of studies has come out regarding AS and BoB circulation, heat budget and its variability in various scales, while the circulation in Andaman Sea remains less elucidated. Unlike AS and BoB, Andaman waters are not showing any seasonal processes such as upwelling, convective mixing and occurrence of mesoscale eddies. Hence the water in this region is oligotrophic in nature. The average primary production during fall inter monsoon is 283.19 mg C/m^2/ day followed by spring inter-monsoon (249 mg C/m^2/ day), summer monsoon (238.98 mg C/m^2/ day) and winter monsoon (195.47 mg C/m^2/ day) [Sanjeevan et al., 2011]. Major fishery activities

associated with the region are based on the reef systems indicating the ocean realm as a desert. However, this region is having a substantial role in triggering the monsoon over the subcontinent and in the North Indian Ocean, monsoon hits the Andamans 12 days before the onset over Kerala. The currents in Andaman waters reverse with seasonally reversing monsoon winds. The region experiences southwesterly winds during summer monsoon and northeasterly during winter monsoon (Wyrtki, (1973) and Potemra et al. (1991)).

During the winter monsoon, the region experiences strong evaporation due to cold dry continental air that blow from the northern region (Wang et al., 2006). In summer monsoon, northeastern part of the sea is highly stratified due to the heavy fresh water discharge ($379 \pm 47 \times 10^9$ m^3/year) from the Ayeyarwady-Salween and Sittang rivers (Furuichi et al., 2009) and makes the region highly stratified. The sea is connected with South China Sea and Pacific Ocean through Malacca Strait at southeast (Rama Raju et al., 1981). He also reported that there is an ingress of low saline water through Malacca strait during NEM. In general Sestina the southern region is comparatively higher (>28°C) than that of the other regions and it always maintains the threshold value (28°C) for the active generation of depressions and cyclones in this region (Varkey et al., 1996). The stratification causes nutrient depleted layer in the upper water column resulting oligotrophy. In addition to this, the reduced upwelling and vertical turbulent mixing processes eradicates the existence of nutrient enriched water from the subsurface water to the

surface layer. The low primary productivity values observed for this region support these statements (Salini et al., 2018).

Different mechanisms controlling the upper ocean dynamics is suggested by many researchers. Among these, the major forcing mechanisms are wind and planetary waves (Shankar et al., 1996, McCreary et al., 1993, Vinayachandran et al., 1996). According to Yu et al. (1999), long Rossby wave excited by the remotely forced Kelvin wave contribute substantially to the variability of the local circulation in the ocean. Coastal Kelvin wave propagating northward along the eastern boundary of BoB (the western side of Andaman Nicobar Islands) excites westward propagating Rossby waves into the interior of BoB (McCreary et al., 1993, Iskandar et al., 2009, Paul et al., 2009). Potemra et al. (1991) reported the presence of an upwelling Kelvin wave, characterised by low upper layer thickness during early winter traveling east along the equator and hits the Sumatra coast and reflects back as a downwelling westward propagating Rossby wave. According to him, partial energy from the Kelvin wave move along the coast and bifurcates into two; one flowing northward and the other flowing southward.

However, no detailed attempts have been made so far to address the seasonal hydrodynamics of the upper column during winter season. In a recent study by Salini et al. (2018) brought out the upper layer dynamics and circulation pattern based on ship observations around the island chain and highlighted that geostrophy dominates over local wind forcing in driving the upper layer dynamics. During the winter months of 2009 and 2011, the upper 80 m are observed with uniform current

structure, while the Ekman influence was noted only up to 57m. The strong continental air mass from northeast is identified as the forcing factor for strong seasonal processes in the AS. But the role of the wind in the heat budget of eastern counterpart especially in Andaman waters is least addressed.

The Andaman waters are characterised by the presence of long island chain and its mass effects, heavy fresh water discharge, presence of sills and frequent impacts of geologic adjustments etc. These factors which may have a major influence in the oceanographic processes governing the ecosystem are least explored. Chatterjee et al., 2017 explained that the mean coastal circulation within the Andaman Sea and around the islands is primarily driven by equatorial forcing. However, spatial variation in the forcing both due to Kelvin and Rossby and its dominance over wind to regulate the regional upper layer dynamics are to be explored in detail. The present work is aimed to study the spatio-temporal variability of forcing factors in the winter process of the Andaman waters based on satellite SSHA, SST and wind.

4.2 Data and Methodology

SSHA data from satellite altimetry was acquired from Archiving Validation and Interpretation of Satellite Oceanographic (AVISO) with a 7-day temporal resolution on a 1/4°x1/4° Cartesian grid over the time period from January 2003 to December 2013. Winds from Quik Scatterometer (QuikSCAT) and Advanced Scatterometer (ASCAT) winds products are processed by NOAA/NESDIS utilizing measurements from the Scatterometer instrument aboard the EUMETSAT Metop satellites with

25km resolution. The MODIS Aqua Level 3 Mapped climatology SST and chl a data were derived from the NASA MODIS sensor on board the Aqua satellite.

Parameters such as shortwave radiation (SWR), net heat flux (NET), long wave radiation (LWR),sensible heat flux (SHF) and latent heat flux (LHF) were analysed using the monthly data from recently developed new global Tropical air-sea heat Fluxes (TropFlux) data products (Praveen Kumar et al., 2012a). This product was derived from the ECMWF Interim re-Analysis [ERA-I; Dee and Uppala, 2009] and the turbulent fluxes such as latent and sensible heat flux were obtained from the Coupled Ocean-Atmosphere Response Experiment (COARE3) bulk flux algorithm (Fairall et al., 2003), using ERA-interim SST, air temperature, specific humidity and wind speed.

Bulk formulae used to compute air-sea fluxes (Curry et al., 2004) are

$$LHF = \rho L_e C_e U(Q_s - Q_a) \quad \text{.....(1)}$$

$$SHF = \rho C_p C_h U(SST - T_a) \quad \text{.....(2)}$$

$$LWR_{net} = \varepsilon \sigma T_s^4 - LWR_{down} \quad \text{.....(3)}$$

$$SWR_{net} = (1 - a) SWR_{down} \quad \text{.....(4)}$$

$$NET = SWR_{net} - (LWR_{net} + LHF + SHF) \quad \text{.....(5)}$$

where ρ is the density of air, L_e is the latent heat of evaporation, C_e and C_h are the turbulent exchange coefficients for latent and sensible

fluxes respectively, C_p is the specific heat capacity of air at constant pressure, U is the wind speed relative to sea surface, Q_s and Q_a are saturation specific humidity at sea surface temperature and near-surface atmospheric specific humidity respectively. SST and T_a are sea surface and air temperature respectively, α is the surface albedo, ε is the surface emissivity (0.97) and σ is the Stefan–Boltzman constant.

For generating the climatology of air-sea flux, all the raster files of parameters from 2003 to 2014 were stacked individually. From each stacks the months representing January, February, November and December were extracted, stacked and then averaged to single raster layer of each parameter for each months. These parameters were then plotted as overlay maps.

Wavelet Comp (version 1.1) is an R package used for the continuous wavelet analysis of univariate and bivariate time series. It examines the frequency structure of uni and bivariate time series using the Morlet wavelet. Wavelet Comp make use of Fast Fourier Transform algorithms following Torrence and Compo (1998) methodology.

This analysis is carried out to study the seasonality of the temperature, wind and remote effects at four different boxes in Andaman regions (Fig. 4.1). These boxes are chosen at locations with direct effects of remote forcing, reversing winds and other water masses. The boxes are

1) Lat. 4-6°N and Long. 92-95°E (B1)
2) Lat. 8-10°N and Long. 92-94°E (B2)

3) Lat. 8-10°N and Long. 95-97°E (B3)

4) Lat. 14-16°N and Long. 91-94°E (B4)

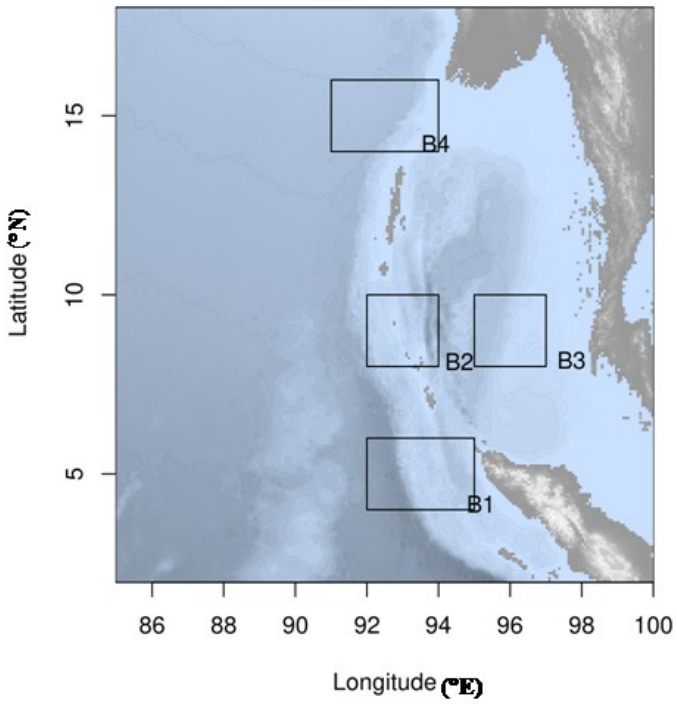

Fig. 4.1: Box location.

4.3 Results and Discussion

4.3.1 Sea Surface Height Anomaly (SSHA)

4.3.1.1 Temporal analysis

Surface indication of planetary waves can be well captured in the SSHA pattern-the positive SSHA or high in sea level evince downwelling mode Kelvin/ Rossby and negative SSHA or low in sea level indicate upwelling mode waves. The propagation of such waves of different

characteristics are ubiquitous in ocean and its seasonality, propagation and genesis in the equator have significant role in different physical processes of the ocean. The wind energy in the equatorial Indian Ocean generates these types of planetary waves with upwelling and downwelling mode as a wave guide along the equator (Potemra, 1991, Yu et al., 1991, McCreary et al., 1993). In the Equatorial Indian Ocean, the zonal winds in semiannual nature remotely generate corresponding semiannual sea level fluctuations near the eastern equator (Clark and Liu, 1993). Wavelet analysis of SSHA gives dominant wave period, energy and their interannual variations at different locations. At Box B1, signals are not present in every year. The semiannual signals are found during the years 2004, 2005, 2006, 2008, 2009, 2011, 2012 & 2013. It displays quarter annual signals during 2006. Dominant signal in B1 is semiannual (Fig. 4.2a). However, at B2 the semiannual signal is present during 2005, 2008 and 2013.Quarter annual signals are not prominent in this box compared to B1 (Fig. 4.2b). At box B3 the signal is semiannual in2005, 2008 and 2011. There is a weak annual signal during 2005 and 2012 (Fig. 4.2c). The box B4 shows the same condition of B3 in the case of semiannual signal. The annual signal is observed during 2004 and 2009, but the significant level of the signal is very less in 2004. Quarter annual signals are present during 2006 and 2009 (Fig. 4.2d).

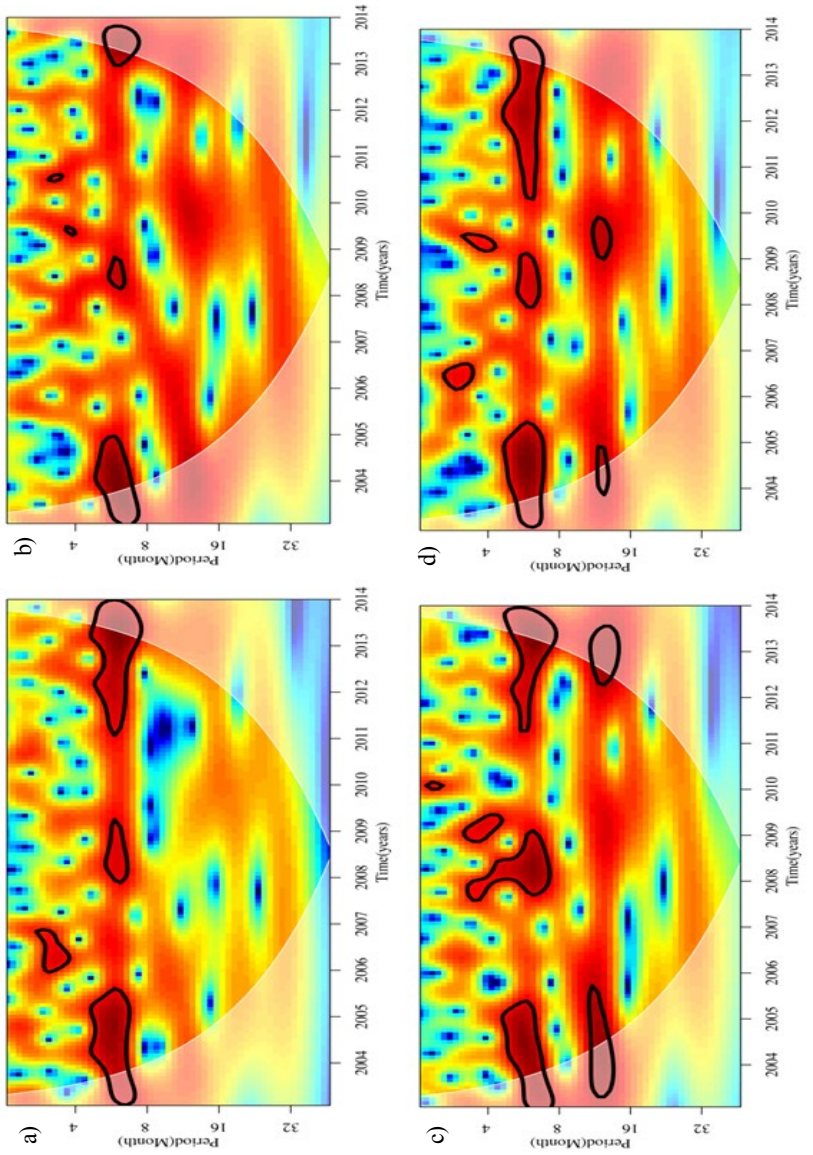

Fig. 4.2: Interannual variability of SSHA (m) at box location
a) B1 (4-6°N and 92-95°E) b) B2 (8-10°N and 92-94°E)
c) B3 (8- 10°N and 95-97°E d) B4 (14-16°N and 91-94°E) from 2003-2013

The boxes B1 and B2 show semiannual signals, whereas the signals at B3 and B4 are fluctuating in annual and semiannual period. The semiannual and quarter annual signals are dominant in all the boxes. Present observations corroborate the results from Potemra et al. (1991) and Chatterjee et al. (2017) that the planetary waves after hitting the Sumatra coast propagates through the eastern periphery of Andaman Sea. The semiannual and quarter annual period are mainly due to the westward propagating Rossby wave generated by the coastal Kelvin wave (Nienhaus et al., 2012) in the region. While comparing annual signals, it is seen that the energy associated with quarter annual and semiannual signals are more. The biennial periods (1-2 years) are always associated with ENSO and IOD years. But in the present analysis, the biennial signals are not observed in all the four selected boxes which indicate that the ENSO and IOD are not influential in regulating the upper layer dynamics of the selected region.

4.3.1.2 Spatial analysis

The climatology of SSHA fields exhibit −0.05 to 0.15m during November with peak positive value in the Ayeyarwady-Salween region but with negative SSH anomalies in the western part up to 90°E (Fig. 4.3a). During December, the negative anomaly dominates in western side of Island chain compared to east and it is also observed in eastern periphery of Andaman Sea (Fig. 4.3b). In January, negative anomalies enter into Andaman Sea through Great Channel (6°N) and travel through the entire periphery of eastern Andaman Sea and enters BoB via Preparis channel (Fig. 4.3c). This observation is comparable

with the result of Chatterjee et al. (2017). During February, negative SSHA remains in eastern side while it is replaced by positive SSHA in western side of Island chain (Fig. 4.3d).

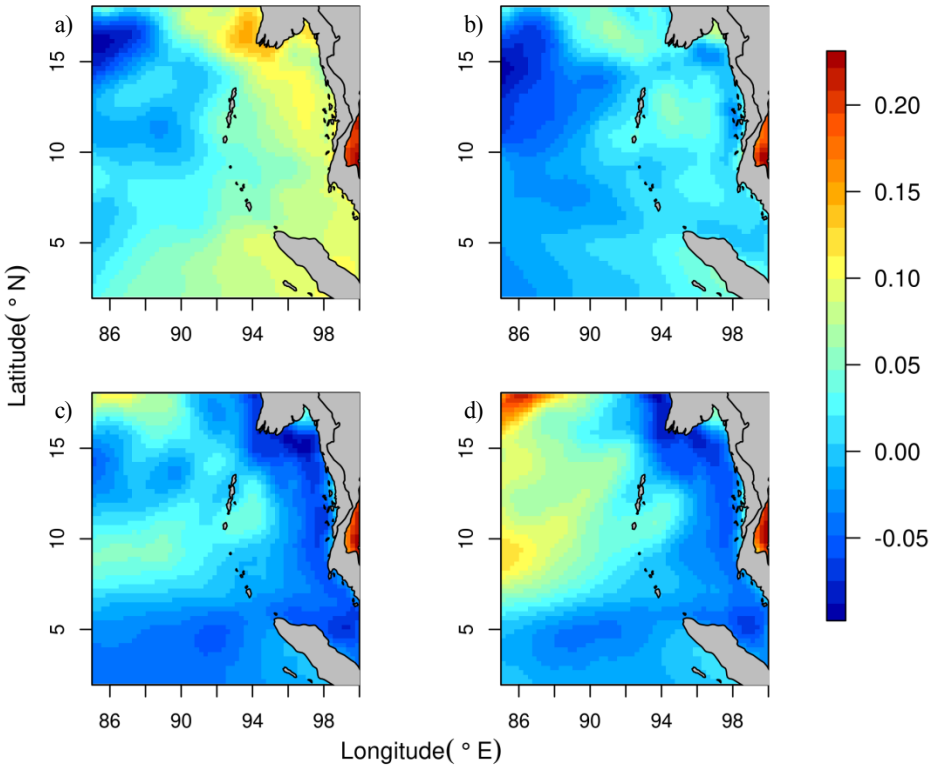

Fig. 4.3: Climatology of SSHA(m) in Andaman waters during a) November b) December c) January and d) February

4.3.2 Sea Surface Temperature (SST)

4.3.2.1 Temporal analysis

SST plays an important role in modulating the air-sea processes over a region thereby exchanging energy between atmosphere and ocean and have a great significance in the genesis of cyclones too. Thus it is considered as avital indicator used to address the processes linking ocean-atmosphere coupling and its variability like current flow, precipitation, upwelling and biological production.

The wavelet analysis of SST shows annual signal during2004 to 2013 in the box B1, whereas semiannual signal is observed only during 2012-2013 (Fig. 4.4a). In B2 there are signals in 2004, 2005, 2008, 2011 and 2012.Weak quarter annual signal exists in 2006 (Fig. 4.4b). The strong annual and semiannual signals are predominated in box B3. Semiannualsignals are observed during 2004-2006, 2008 and 2012. Annual signal is prominent during 2006-2012 (Fig. 4.4c). B4is dominated by semiannual signal over the whole time period; while the annual signal subsist in 2005-2008, 2009-2010 (Fig. 4.4d). The strong annual signals are found in the boxes B1, B3 and B4 except B2.It is seen that the semiannual signal dominates in all the boxes. The SST variability increases in the northern region with largest variations appearing near the northwestern region. The wavelet analysis of SST portrays that the long term SST of Andaman waters are influenced both by semiannual and annual forcing. It is reported that the annual forcing in the BoB have more control on the SST, but the Arabian Sea SST is influenced by both semiannual and annual forcing (Dinesh Kumar et al., 2016).

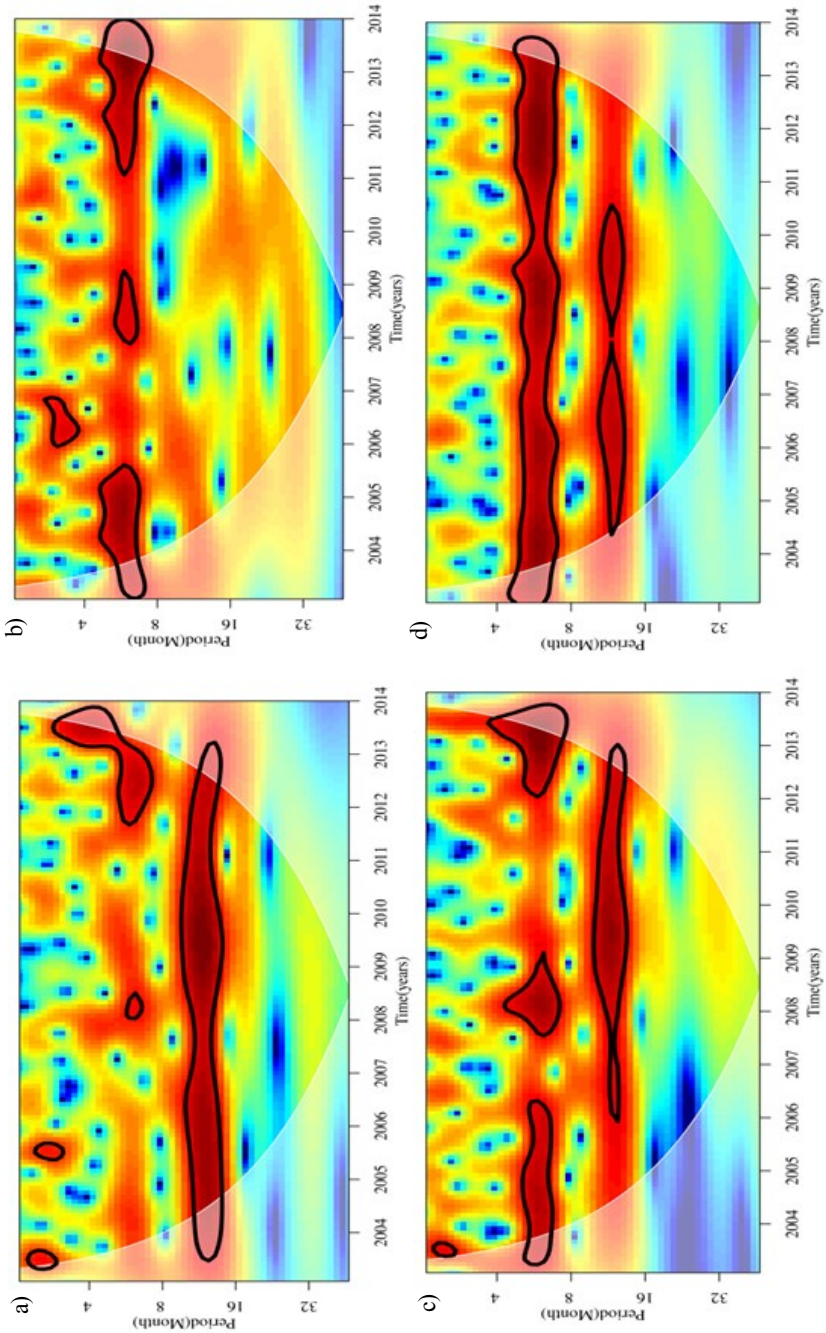

Fig. 4.4: Interannual variability of SST (°C) at box location
a) B1 (4-6°N and 92-95°E) b) B2 (8-10°N and 92-94°E)
c) B3 (8-10°N and 95-97°E) d) B4 (14- 16°N and 91-94°E) from 2003-2013

4.3.2.2 Spatial analysis

The spatial variation of SST shows the existence of warmer water (28.4°C-28.6°C) during November (Fig. 4.5a). But in December, SST decreases in the north (27.4°C) compared to south (Fig. 4.5b). During January, the water at north is cooler (26.0-27.0°C) than the south (28.6-28.8°C) (Fig. 4.5c). The same pattern exists during February also (Fig. 4.5d). The analysis reveals that the seasonal warming is observed in the entire Andaman waters during November and northern cooling during December-February (Fig. 4.5.b-d).

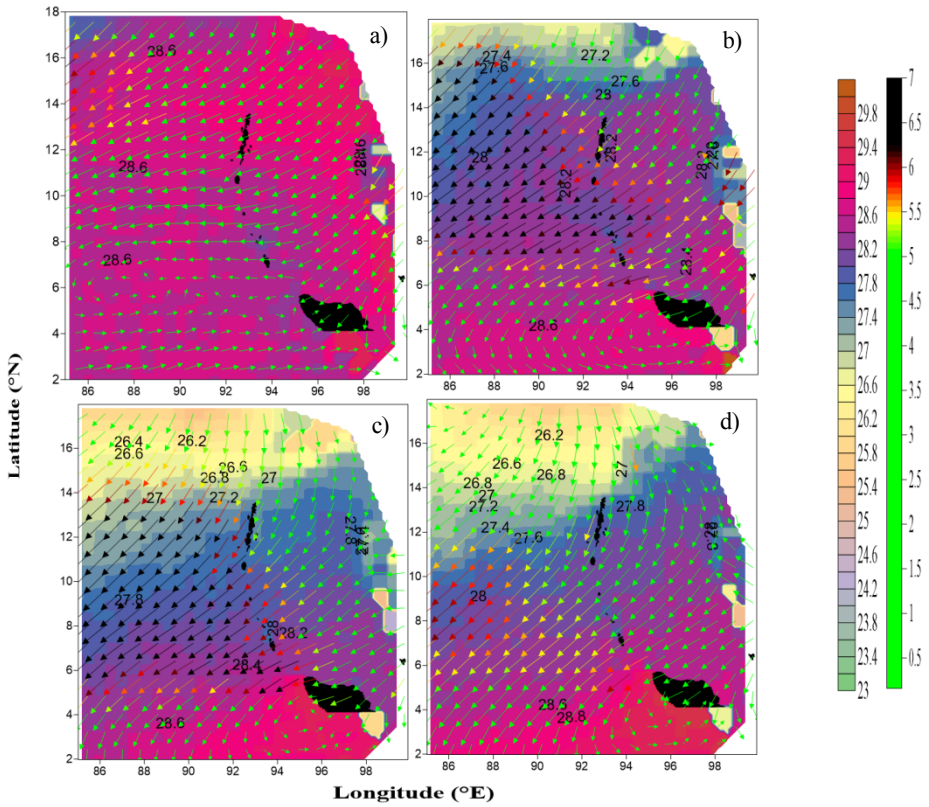

Fig. 4.5: Climatology of SST (°C) and wind (m/s) in Andaman waters during a) November b) December c) January and d) February

4.3.2.2.1 Heat Budget

To determine the causes of the higher SST in the Andaman waters, we analysed the heat budget components in the upper ocean like net heat flux, latent heat of evaporation, sensible heat, short wave and long wave radiations. Net heat flux is the total heat gain or loss from/to the ocean. Latent heat flux indicates the evaporation rate from the ocean surface and shows the rate of cooling. Similarly, sensible heat arises from the difference between air-ocean temperatures and indicate the movement of heat towards/from the ocean. Shortwave radiation is the total energy from the sun reaching the ocean, while those reflected back from the ocean is attributed to long wave radiation.

Variation of shortwave flux in November is between 165-185 W/m^2 with higher values in the northeastern region (Fig. 4.6a). While in December, it is between 155-175 W/m^2 and increased short wave radiation obtained in the southwest and north east region (Fig. 4.6b). From Fig. 4.6c, it is seen that there is an increase in short wave radiation 185-205 W/m^2 in January and 210-235 W/m^2 in February (Fig. 4.6d). Longwave radiation is generally negative over the Andaman waters with high negative values of -160 W/m^2 along 15°N and comparatively smaller negative values (-120 to -140 W/m^2) south of 15°N in all the winter months (Fig. 4.6a-d). Sensible heat flux also shows smaller negative values (-5 W/m^2) in the eastern Andaman waters in comparison with the western region (-5 to -15 W/m^2) (Fig. 4.8a-d). The northern region displays a higher negative value (-10 to -15 W/m^2) during December and January. This observations reveal that the longwave and sensible heat fluxes contribute comparatively less to the net heat flux.

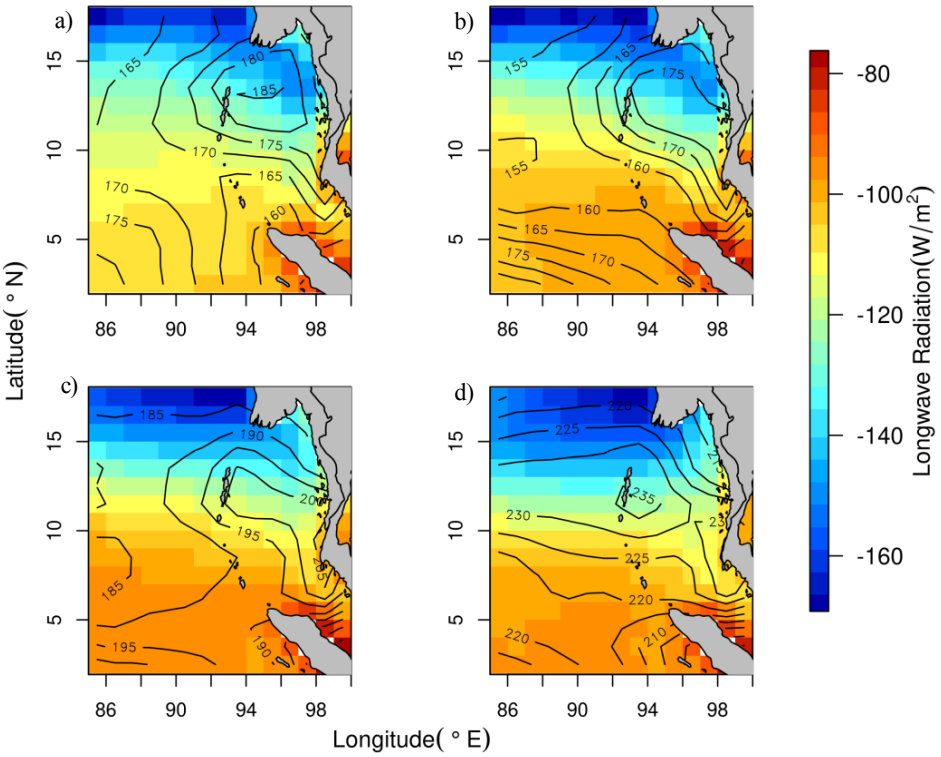

Fig. 4.6: Overlap map of climatological Short wave radiation (W/m^2) and Long wave radiation (W/m^2) during a) November b) December c) January and d) February

During November, maximum latent heat loss of about -160 W/m^2 is observed at northwest and it decreases to -110 W/m^2 at south and east (Fig. 4.7a). December and January show same pattern as November (Fig. 4.7b, c). But in February higher heat loss of -160 W/m^2 is observed between 7°-14° N in the western side of Andaman Islands (Fig. 4.7d). During all winter months, latent heat flux in the north is higher (-160 to -170 W/m^2) than south.The spatial distribution of wind speed varies from 5-7 m/s and the speed is low (5 m/s) in November (Fig. 4.5a) and it increases to 7 m/s for the northern region in December and January

(Fig. 4.5b, c). In February wind speed reduces to 5-5.5 m/s in Andaman waters (Fig. 4.5d). The highest latent heat flux is due to the combined effect of relatively strong winds and the dry continental air which descends from aloft towards the ocean causes strong humidity gradient. This ultimately contribute the cooling at north as reported by Shenoi et al., 2002. The weaker winds in the south compared to north increase the stratification and prevent turbulent mixing which lead to a shallow mixed layer. This causes the heat flux from the atmosphere to trap within the mixed layer and explains the higher SST of greater than 28°C.

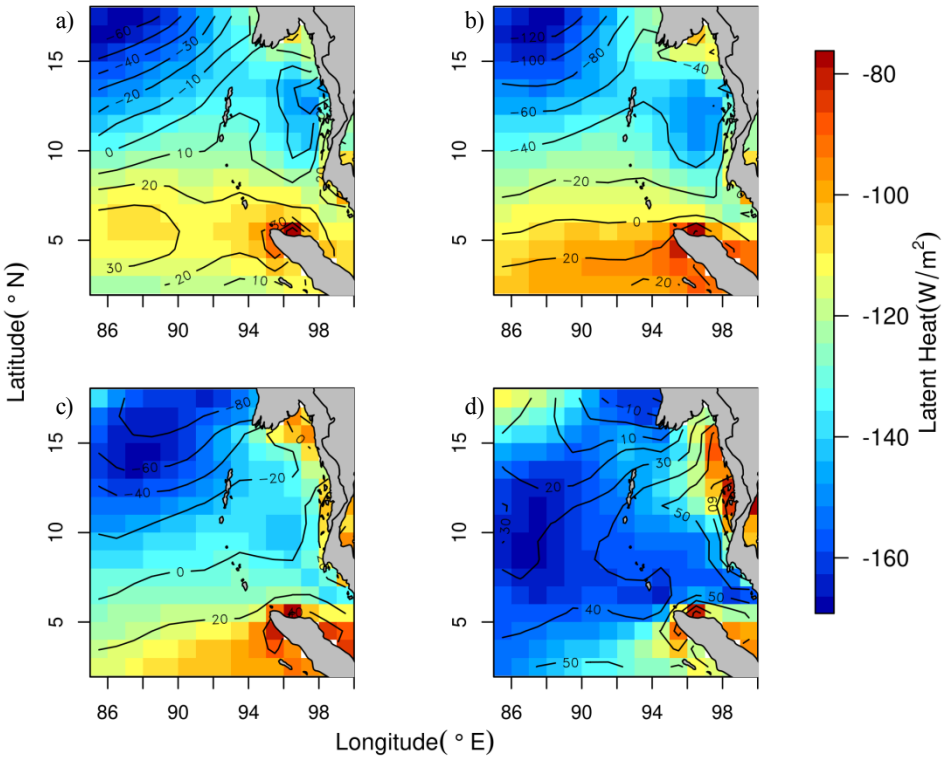

Fig. 4.7: Overlap map of climatological Net heat flux (W/m^2) and Latent heat flux (W/m^2) during a) November b) December c) January and d) February

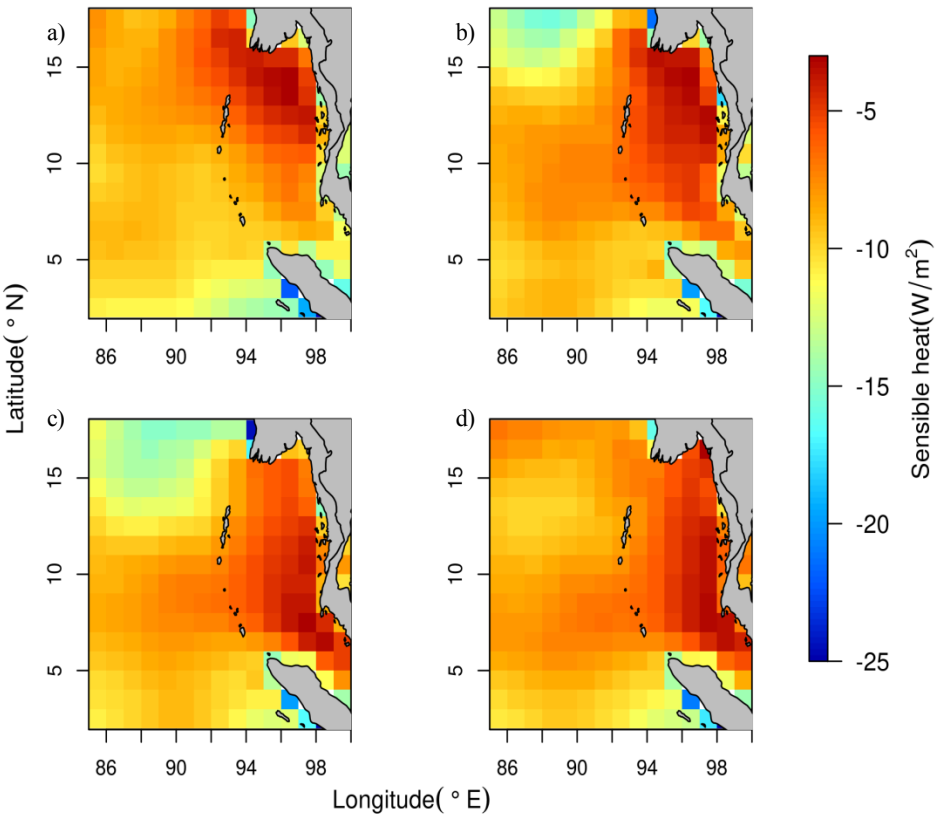

Fig. 4.8: Climatology of Sensible heat flux (W/m^2) in Andaman waters during a) November b) December c) January and d) February

During November, the northern region experiences with a net heat loss of -10 to -60 W/m^2 compared to the heat gain of 10 to 50 W/m^2 at south (Fig. 4.7a). The pattern follows in December also with heat loss of -20 to -120 W/m^2 in northern part up to 7° N (Fig. 4.7b). In January, the northern part of Andaman waters experience a net heat loss of -20 to -80 W/m^2 and net heat gain of 20 to 40 W/m^2 in the southern part (Fig. 4.7c). During February, the entire Andaman waters show heat gain

of 10-60 W/m^2 (Fig. 4.7d). The net heat loss in the north is resulted from the increasing trend of latent heat flux in the winter months compared to south. The observed heat loss accompanied with increased latent heat flux leads to SST cooling in the north resulting convective mixing in the upper layers as explained in Chapter 3. While in BoB, the variation of latent heat flux contributes to the net heat flux [Hiroyuki Tomita & Masahisa Kubota (2004)]. Heat flux variations drive most of the intraseasonal SST variability in the Bay of Bengal (Vialard et al., 2012). Duncan and Han (2009), suggest that latent heat flux variations in BoB have a stronger influence on SST than upwelling and advection induced by wind stress. SST variability attribute to changes in net heat flux associated with the active and weak phase of the summer monsoon (Sen Gupta et al., 2006). From this study it is inferred that the dominant heat fluxes in the Andaman waters are shortwave radiation and latent heat flux. This corroborate the findings of Hiroyuki Tomita & Masahisa Kubota (2004) in BoB, that the contributions of longwave radiation and sensible heat flux to net heat flux are very small compared to other fluxes.

4.3.3 Wind

Coupled ocean-atmosphere dynamics is important not only for annual and semiannual variability of the Indian Ocean but also plays an important role in the interannual variability (Huang and Kinter, 2002). The wind field over the Indian Ocean has a different pattern compared to other oceans. An important difference from the other tropical oceans is the absence of sustained easterly winds along the equator. Instead, the near equatorial winds have an easterly component

during the late winter/early spring, a semi-annual westerly component during both inter monsoons, and weak easterly annual mean (Schott et al., 2009).

4.3.3.1 Temporal Analysis

In box B1, quarter annual signals are prominent in the middle months of 2013 and the semiannual signal are observed during the years 2005, 2008, 2011 and 2012. Annual signals exist in 2005, 2009, 2010 and 2011 respectively (Fig. 4.9a & b). B2 shows weak quarter annual signals in 2003 and middle months of 2004. Semiannual signals exist during 2004, 2005, 2008, 2010 to 2012 and the annual signals occur in 2004 and 2005 (Fig. 4.9c & d). Box B3 exhibits quarter annual signals in 2003 and semiannual signal during 2010 to 2013. Annual signals are persistent from 2008 to 2013 (Fig. 4.9e & f). B4 comprises weak semiannual signals in 2005 and 2006 and it is strong in 2010 to 2012 (Fig. 4.9g & h). Annual signals exhibit in the whole period and is strong in almost all the boxes. It resembles the study of Vinayachandran et al. (1996) where the periodicity of winds in BoB is mainly annual.

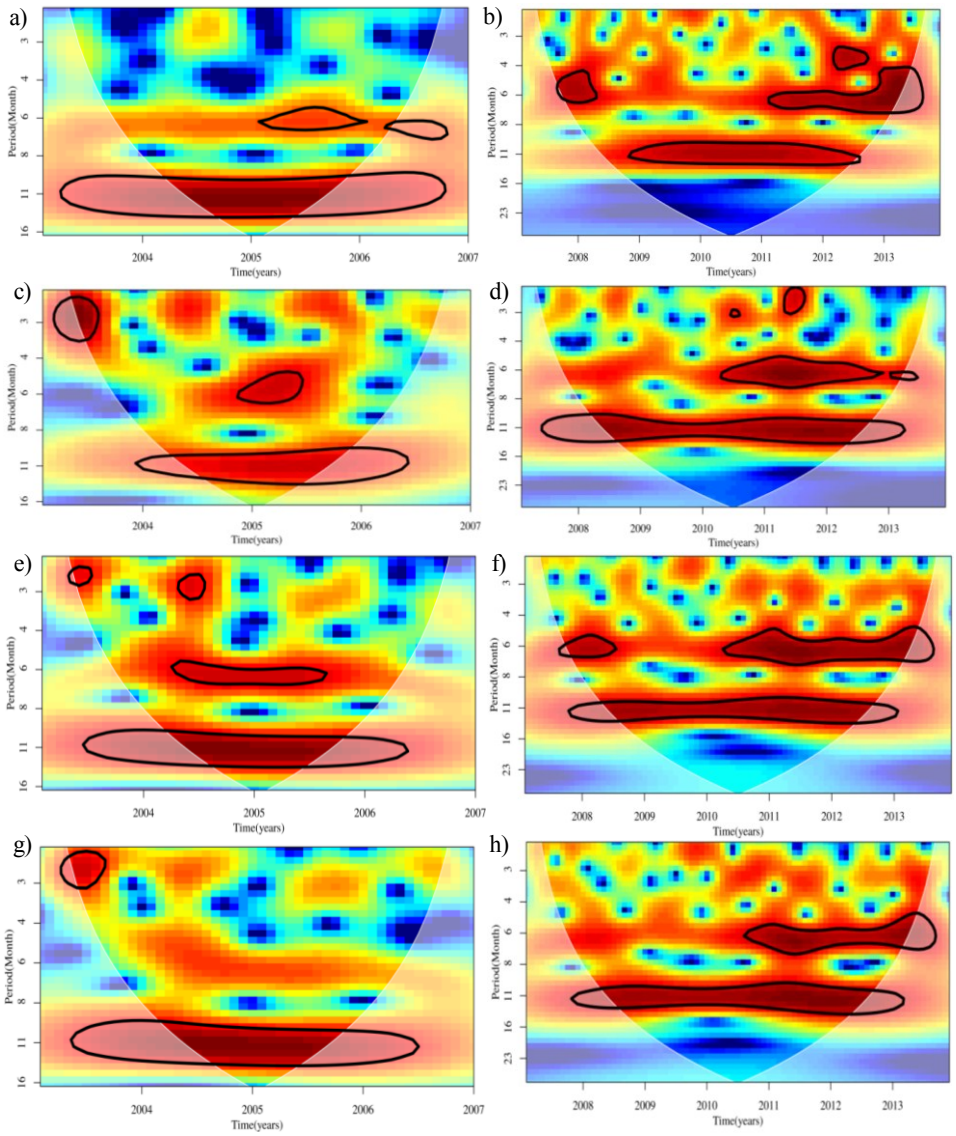

Fig. 4.9: Interannual variability of wind (m/s) at box location
a) B1 (4-6°N and 92-95°E) from 2003-2007
b) B1(4-6°N and 92-95°E) from 2008-2013
c) B2 (8-10°N and 92-94°E) from 2003-2007
d) B2 (8-10°N and 92-94°E) from 2008-2013
e) B3 (8- 10°N and 95-97°E) from 2003-2007
f) B3 (8-10°N and 95-97°E) from 2008-20013,
g) B4 (14-16°N and 91-94°E) from 2003-2007
h) B4 (14-16°N and 91-94°E) from 2008- 2013

4.3.3.2 Spatial Analysis

The surface distribution of climatological wind during the northern winter monsoon months of November shows that the flow is northeasterly with a speed of 5m/s from 6°N-18°N. Below 6°N, the winds exhibit a strong westerly component with similar speed of 5m/s and are zonal towards the east (Fig. 4.5a). During December, the winds are northeasterly up to 4°N with a speed of 5-7 m/s and higher speed of 7 m/s are present in the western side of Island chain between 8°-16°N (Fig. 4.5b). In the peak stage of winter monsoon (January), the wind is northeasterly with a speed of 5-7 m/s and the maximum speed exists between 6°-14°N, i.e. west of the Island chain (Fig. 4.5c). During February, the same pattern follows with a speed change of 5-6 m/s (Fig. 4.5d). Below 8°N, the line of anticyclonic wind shear exists during November. This shear pattern moves south as the season progresses.

4.3.4 Chlorophyll a

In the spatial chl a distribution pattern, high chl a concentration is observed around Ayeyarwady-Salween region (10 mg/m^3), Andaman Nicobar Island chain, Malacca Strait, northern side of North Andaman Island and the south of Great Nicobar (0.4 mg/m^3) in November (Fig. 4.10a). The high chl a concentration extend to the west of Great Nicobar Island in December (Fig. 4.10b). The same pattern follows in January and February also (Fig. 4.10c & d). The high chl a in the northwest is associated with the Ayeyarwady Salween river system and in the south, it is due to the influence of high productive Malacca Strait water (Salini et al., 2018 and Tan et al., 2006). It is obvious that, the

high chl a in the monthly climatology is not correlated with any of the upper layer mesoscale processes which we explained in Chapter 3. This indicates that the mesoscale processes are not a recurring phenomenon. Mild increase in biology (chl a- the range of 0.4 mg/m^3) at the north is influenced by the convective mixing, which is explained in the previous section 4.3.2.2.1. Figs. 4.10a-d shows the enhancement of the biology of the region through which the coastal Kelvin wave propagates in its upwelling mode as described by Potemra et al., 1991 and Chatterjee et al., 2017.

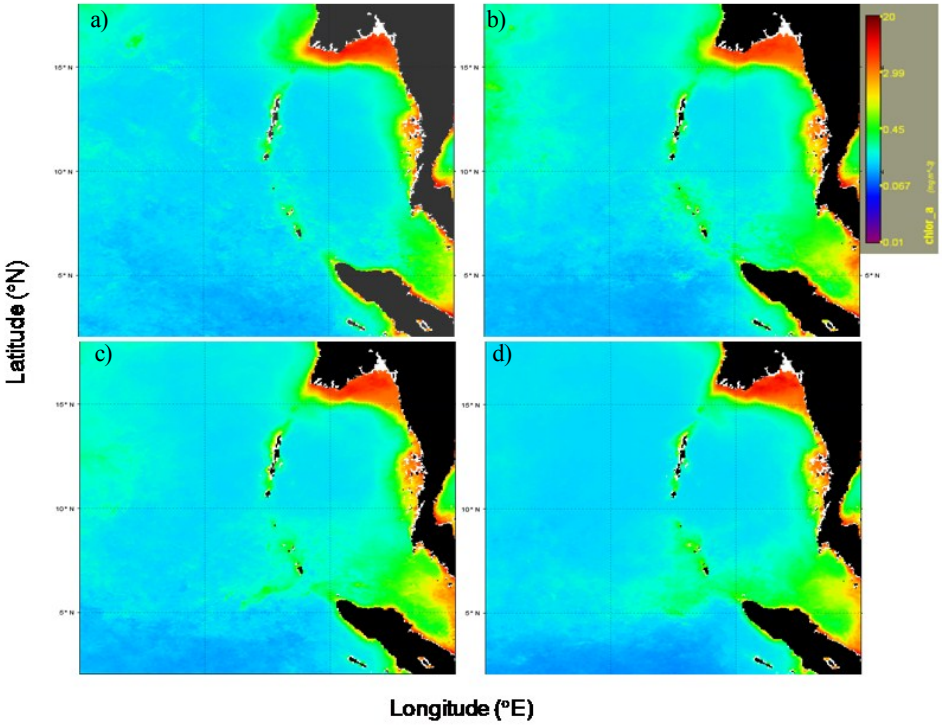

Fig. 4.10: Climatology of chl a (mg/m^3) in Andaman waters during a) November b) December c) January and d) February

4.3. Conclusion

The winter monsoon characteristics of the Andaman waters are explained based on the spatio-temporal variations in SSHA, SST, wind and the response variable chl a. The spatial variation as explained in the sub regional scale, based on the wavelet explains the various forcing that regulate the upper layer dynamics. For the forcing factors like wind, SSHA and SST the annual mode is dominated for B1 (near equatorial region), the sub region associated with the B2 (Ten degree Channel), B3 (eastern) and B4 (northern) show semiannual characteristics. In addition, SSHA observed in the quarter cycle during some years in the regions except for the sub-region B2, indicates the presence of two phases of upwelling and downwelling modes in the region. Temporal variation of SSHA shows semi-annual signal due to the westward propagating Rossby wave generated by the coastal Kelvin wave. The heat budget components clearly bring out the occurrence of convective mixing process at north (latent heat flux of $^{-}150$ W/m^2 and net heat flux of $^{-}70$ W/m^2). Spatial variations in SST, wind and heat flux are associated with convective mixing. Spatial variation of heat flux shows SST cooling in the north compared to south due to the increased latent heat flux and net heat loss. Also the study indicates that, unlike the Arabian Sea and Bay of Bengal, the southern Andaman is not responding to the reversing monsoons. The region associated with the Ten degree Channel is influenced by the island/topographic effect to experience a modulated atmospheric and oceanic processes. Generally Andaman waters are oligotrophic in nature, however the convective mixing and the mesoscale processes influence the biology of this region in a significant scale.

.....ൠ.....

Chapter 5

SUMMARY AND CONCLUSION

Hydrography, circulation, mesoscale processes, spatio-temporal variations in forcing factors and its response to upper layer biology of the Andaman waters during winter monsoon were investigated using in situ, satellite and climatological datasets. The hydrography and vertical current structure presented in this study is based on the data collected onboard FORV *Sagar Sampada* during January 2009 and November-December 2011.

The salient features observed in the hydrography, circulation and biological response of the region includes

- The northeasterly winds influence the upper layer dynamics of the region.
- Hydrography of the region demarcates the area into three, typical BoB waters at west, riverine influence due to Ayeyarwady-Salween input at northeast and the presence of South China Sea water intruded through Malacca strait at south east.

- In situ real time vertical current profiles show uniform flow pattern up to 96m. Whereas, the Ekman influence is restricted within the upper 55m, indicating the combined influence of Ekman and geostrophy in regulating the upper layer dynamics.
- The temperature inversion observed in the entire Andaman waters is a prominent characteristic during winter.
- The barrier layer formation is conspicuous in Andaman waters during winter due to the peculiar circulation pattern and the distribution of low saline BoB, Ayeyarwady-Salween and South China Sea waters.
- The region is oligotrophic in nature due to the stratified surface water.
- The southern Andaman water is comparatively productive which is associated with the influence of Malacca Strait.

Mesoscale processes regulating the upper layer dynamics explain the presence of two cold core eddies, their generation mechanism and the response in biology. The important features are

- Cyclonic eddies are tracked using negative SSHA, geostrophic current pattern and Okubo-Weiss parameter. The two eddies observed are at 8°N and 93°E (CE1) and 13°N and 93°E (CE2). The threshold value of Okubo-Weiss parameter ($^{-}2\times10^{-11}/s^{2}$) indicates CE1 is strong compared to CE2.
- The vertical temperature structure at CE1 shows upsloping as reflected in the MLD pattern, which shifts from 47 m to 19 m

with a relative abundance of surface chl a (0.5 mg/m^3). CE2 is characterized with a surface temperature of 26.5 °C and chl a of 0.4 mg/m^3.

- Negative wind stress curl at CE1 and CE2 indicates that wind is not a forcing factor in the eddy generation.
- Low Richardson's number (<0.0001), which measures the instability due to the vertical shear in the horizontal flow over stratified layers indicates the role of Baroclinic instability in triggering eddy formation and sustenance.
- The baroclinic instability is in concurrence with the semi-annual Rossby wave radiated from the coastally trapped Kelvin wave with a speed of 0.20 m/s causes the eddy formation at CE1.
- The generating mechanism of CE2 is Kelvin. The instability owing to the flow from Ayeyarwady-Salween river system is supposed to be the reason for CE2 origin.
- CE2 is associated with low incoming solar radiation and high latent heat flux which causes SST cooling and this region is evidenced with convective mixing due to cold dry continental air from north.

The Andaman water characteristics are addressed in a synoptic scale to explain the spatial and temporal variations of forcing factors using satellite and climatological data sets. The biological response is also explained in a spatial scale. The main features observed include

- Temporal variations in SST, wind and SSHA as reflected in the wavelet analysis indicate a dominant annual cycle in the equatorial sub region. The northern and eastern boxes are observed with semiannual and annual mode forcing. Whereas, the forcing signal in 10°N Channel box is semiannual in nature and is influenced by the regional dynamics.
- Semiannual SSHA signal is due to the westward propagating Rossby wave from the coastally trapped Kelvin wave. The quarter annual SSHA signal observed in the equatorial, northern and eastern boxes except the 10 degree Channel is associated with the two upwelling and downwelling planetary waves. Spatial variation of SST, SSHA and wind explain the regional processes viz convective mixing and mesoscale eddies.
- Increased latent heat and net heat fluxes cause more surface cooling at north compared to southern Andaman waters and thus result in convective mixing at north. The response of the same is well evident in the upper layer hydrodynamics and the present study reports this processes for the first time in this region.
- Generally, Andaman water is oligotrophic in nature but the winter processes like convective mixing, Malacca intrusion and Ayeyarwady Salween run off enhances the biological characteristics of Andaman waters.

5.1 Future scope of study

Located in the eastern part of the North Indian Ocean, this region is less explored to explain the Oceanography, the prevailing forcing and its response in different ecosystem levels. There was no major scientific programmes reported in addressing the features of the region so far since the observational network is scarce. As far as the air-sea coupling is considered, it is critical to have a basic understanding of the seasonal behavior of the basin including the roles in monsoons and cyclogenesis. Studies with a focused or integrated approach to explain the complex dynamics and functional interaction between various components both in small/large scale processes, including the coral ecosystems has to be attempted to. A better classification on seasons is proposed in this study by taking into consideration of the rate of precipitation (dry and wet season), climatological characteristics of sea surface temperature, salinity, sea surface height anomaly and other oceanographical parameters which drive the upper layer dynamics. Even though the present study attempted to bring out the winter characteristics especially the physical setup, based on in situ, satellites and climatological data sets, it is suggested to explore and expand the studies with high resolution data sets including vertical profiles. The biological response explained in the study are based on satellite derived ocean color imagery, which could only give the surface/optical depth representation. The study emphasises that it is essential to undertake more column sampling on organisms at various trophic levels to explain the biological responses associated with the physical forcing. Also there is a need to explore more on the reported mutli-scale processes like mesoscale eddies, convective mixing, Malacca

intrusion and Ayeyarwady-Salween river system etc. to explain how these processes influence the basin scale hydrodynamics and biological characteristics. It is suggested that a high resolution bio-physical model setup supported with seasonal insitu/ satellite measurements may unveil the upper layer processes to a great extent.

.....ഌ൹.....

References

Agarwal, N., Sharma, R., Parekh, A., Basu, S., Sarkar, A. & Agarwal, V.K., (2012). Argo observations of barrier layer in the tropical Indian Ocean. *Advances in Space Research*, 50, 642-654.

Alpers, W., Wang-Chen, H. & Hock, L., (1997). Observation of internal waves in the Andaman Sea by ERS SAR," *Proc. 3rd ERS Symposium on Space at the Service of our Environment*, Florence Italy, 1287-1291.

Amiruddin, A.M., Ibrahim, Z.Z. & Ismail, S.A., (2011). Water Mass Characteristics in the Strait of Malacca using Ocean Data View. *Research Journal of Environmental Sciences*, 5, 49-58.

Anderson, S. P., Weller, R. A. & Lukas, R. B., (1996). Surface buoyancy forcing and the mixed layer of the western Pacific warm pool: Observations and 1D model results. *Journal of Climate*, 9, 3056–3085.

Bakun, A., (2006). Fronts and Eddies as Key Structures in the Habitat of Marine Fish Larvae: Opportunity, Adaptive Response and Competitive Advantage. *Scientia Marina*, 70 (S2), 105–122.

Behrenfeld, M.J. & Falkowski, P.G., (1997). Photosynthetic rates derived from satellite-based chlorophyll concentration. *Limnology and Oceanography*, 42, 1–20.

Bhattathiri, P.M.A. & Devassy, V.P., (1981). Primary productivity of the Andaman Sea. *Indian Journal of Marine Sciences*, 10, 243-247.

Biju, A., Honey U.K. Pillai, Jayaraj, K.A., Sabu, P. & Muraleedharan, K.R., (2010). Influence of environmental parameters on the vertical distribution and abundance of mesozooplankton in the Andaman waters during spring intermonsoon. In: *Indian Ocean Marine Living Resources*, Book of Abstracts, Centre of Marine Living Resources and Ecology, Ministry of Earth Sciences, Kochi, 21.

Buranapratheprat, A., Laongmanee, P., Sukramongkol, N., Prommas, R., Promjinda, S. & Yanagi, T., (2010). Upwelling Induced by Mesoscale Cyclonic Eddies in the Andaman Sea. *Coastal Marine Science*, 34 (1), 68–73.

Chatterjee, A., Shankar, D., McCreary, J.P., Vinayachandran, P.N. & Mukherjee, A., (2017). Dynamics of Andaman Sea circulation and its role in connecting the equatorial Indian Ocean to the Bay of Bengal. *Journal of Geophysical Research: Oceans*, 122, 3200-3218.

Chen, X., Pan, D., Bai, He, X., Chen, C.A. & Hao, Z., (2013). Episodic Phytoplankton Bloom Events in the Bay of Bengal Triggered by Multiple Forcings. *Deep Sea Research Part I: Oceanographic Research Papers*, 73, 17–30.

Clarke, A.J. & Liu, X., (1993). Observations and dynamics of semiannual and annual sea levels near the eastern equatorial Indian Ocean boundary. *Journal of Physical Oceanography*, 23, 386–399.

Curray, J.R., (2005). Tectonics and history of the Andaman Sea region. *Journal of Asian Earth Sciences*, 25, 187–232.

Curry, J. A., Bentamy A., Bourassa, M.A., Bourras, D., Bradley, E.F., Brunke, M., Castro, S., Chou, S.H., Clayson, C.A., Emery, W.J., Eymard, L., Fairall, C.W., Kubota, M., Lin, B., Perrie, W., Reeder, R.A., Renfrew, I.A., Rossow, W.B., Schulz, J., Smith, S.R., Webster, P.J., Wick, G. A. & Zeng, X., (2004). SEAFLUX. *Bulletin of American Meteorological Society*, 85 (3), 409–424.

de Boyer Monte´gut, C., Vialard, J., Shenoi, S.S.C., Shankar, D., Durand, F., Ethe, C. & Madec, G., (2007b). Simulated seasonal and interannual variability of mixed layer heat budget in the northern Indian Ocean. *Journal of Climate*, 20, 3249– 3268.

Dee, D.P. & Uppala, S., (2009). Variational bias correction of satellite radiance data in ERA-interim reanalysis. *Quarterly Journal of the Royal Meteorological Society,* 135, 1830–1841.

Dinesh Kumar, P.K., Steeven, Y.Paul, Muraleedharana, K. R., Murty, V.S. N. & Preenu, P.N., (2016). Comparison of Long-term variability of Sea Surface Temperature in the Arabian Sea and Bay of Bengal. *Regional Studies in Marine Science,* 3, 67-75.

Dong, C., McWilliams, J.C., Liu, Y. & Chen, D., (2014). Global heat and salt transports by eddy movement. *Nature Communications*, 5, 3294.

Duncan, B. & Han, W., (2009). Indian Ocean intraseasonal sea surface temperature variability during boreal summer: Madden–Julian oscillation versus sub monthly forcing and processes. *Journal of Geophysical Research*, 114, C05002.

Durand, F., Shetye, S.R., Vialard, J., Shankar, D., Shenoi, S.S.C., Ethe, C.´ & Madec, G., (2004). Impact of temperature inversions on SST evolution in the South-Eastern Arabian Sea during the pre-summer monsoon season. *Geophysical Research Letters*, 31, 1-4.

Fairall, C.W., Bradley, E.F., Hare, J.E., Grachev, A.A. & Edson, J.B., (2003). Bulk parameterization on air-sea fluxes: updates and verification for the COARE algorithm. *Journal of Climate,* 16, 571–591.

Fousiya, T.S., Parekh, A. & Gnanaseelan, C., (2015). Interannual variability of upper ocean stratification in Bay of Bengal: observational and modeling aspects. *Theoretical Applied Climatology*, 126, 285–301.

Furuichi, T., Win, Z. & Wasson, R.J., (2009). Discharge and suspended sediment transport in the Ayeyarwady River, Myanmar: centennial and decadal changes. *Hydrological Processes.* 23, 1631–1641.

Garg, J.N., Murty, C.B. & Jayaraman, R., (1968). Vertical distribution of oxygen in the Bay of Bengal and the Andaman Sea during February-March 1963. *Bulletin of National Institute of Sciences of India*, 38, 40-48.

Geetha, A., Kurup, K.N., Naomi, T.S., Soloman, K. & Mathew, K.J., (1997). Zooplankton abundance and secondary production in the seas around Andaman-Nicobar Islands. *Indian Journal of Fisheries*, 44, 141-154.

Girishkumar, M.S., Ravichandran, M., McPhaden, M.J. & Rao, R.R., (2011). Intraseasonal variability in barrier layer thickness in the south central Bay of Bengal. *Journal of Geophysical Research*, 116, C03009.

Hacker, P., Firing, E., Hummon, J., Gordon, A.L. & Kindle, J.C., (1998). Bay of Bengal Currents during the Northeast Monsoon. *Geophysical Research Letters*. 25 (15), 2769–2772.

Hiroyuki Tomita & Masahisa Kubota (2004). Variability of surface heat flux over the Indian Ocean, *Atmosphere-Ocean*, 42, 3, 183-199.

Hoegh-Gulberg, O., (1999). Climate change, coral bleaching and the future of the world's coral reefs. *Marine and Fresh water Research*, 50, 839-866.

Honey, U.K. Pillai., Shiju, C.K., Suja, D., Saramma, U.P., Vijayalakshmi, R.N., & Lalithambika Devi, C.B., (2006). Zooplankton composition and diversity in the Andaman waters during north east monsoon. *7th Asia Pacific Marine Biotechnology Conference*.

Huang, B. & Kinter III, J. L., (2002). Interannual variability in the tropical Indian. Ocean. *Journal* of Geophysical *Research*, 107, 3199.

Hyder, P., Jeans, D.R.G., Cauquil, E. & Nerzic, R., (2005). Observation and predictability of internal solitons in the northern Andaman Sea. *Journal of Applied Ocean Research*, 27, 1-11.

Hyrenbach, K. D., Veit, R.R., Weimerskirch, H. & Hunt, G.L., (2006). Seabird Associations with Mesoscale Eddies: The Subtropical Indian Ocean. *Marine Ecology Progress Series*, 324, 271–279.

Ibrahim, Z. & Yanagi, T., (2006). The Influence of the Andaman Sea and the South China Sea on Water Mass in the Malacca Strait. *Mer*, 43/44, 33-42.

Isern-Fontanet, J., García-Ladona, E. & Font, J., (2003). Identification of marine eddies from altimetric maps, *Journal of Atmospheric and Oceanic Technology*, 20, 772–778.

Iskandar, I., Masumoto, Y. & Mizuno, K., (2009). Subsurface equatorial zonal current in the eastern Indian Ocean, *Journal of Geophysical Research*, 96, C11, 44920-45420.

Jeyabaskaran, R., (1999). Report on Rapid Assessment of coral reefs of Andaman & Nicobar Islands. GOI/UNDP/GEF Project on Management of Coral Reef Ecosystem of Andaman & Nicobar Islands.

Published by Zoological Survey of India, Port Blair, 110.

Jha, D.K., Vinithkumar, N.V., Santhnakumar, J., Abdul Nazar, A.K. & Kirubagaran, R., (2011). Assessment of post tsunami coral reef resource in Pongi Balu coast, south Andaman Islands. *Current Science*, 100, 530-534.

Kabanova, JU.G., (1964). Primary production and nutrient salts content in the Indian Ocean waters in October-April 1960-61. *Trud. Inst. Okeanol.*, 44, 85-93.

KameshRaju, K.A., Ramprasad, T., Rao, P.S., Rao, B.R. & Varghese, J., (2004). New insights into the tectonic evolution of the Andaman Basin Northeast Indian Ocean. *Earth and Planetary Science Letters*, 221, 145-62.

Kara, A.B., Rochford, P.A. & Hurlburt, H.E., (2000). An optimal definition for ocean mixed layer depth. *Journal of Geophysical Research*, 105, 803-821.

Kessler, W. S., (1990). Observations of long Rossby waves in the northern tropical Pacific. *Journal of Geophysical Research*, 95, 5183–5217.

Krey, J. & Babenard, B., (1976). Phytoplankton production. *Atlas of the International Indian Ocean Expedition*. Inst. Meer. Kiel Univ., 1-10.

Krishnan, P., Dam Roy, S., George, G., Srivastava, R.C., Anand, A., Murugesan, S., Kaliyamoorthy, M., Vikas, N. & Soundararajan, R., (2011). Elevated sea surface temperature during May 2010 induces mass bleaching of corals in the Andaman. *Current Science, 100*, 111–117.

Kurien, P., Ikeda, M. & Valsala, V.K., (2010). Mesoscale variability along the east coast of India in spring as revealed from satellite data and OGCM simulations, *Journal of Oceanography*, 66, 273–289.

Lalithambika Devi, C.B., Rosamma Stephen, Aravndakshan, P.N. & Meenakshikunjamma, P.P., (1996). Ichthyoplankton from Andaman and Nicobar seas. *Proceedings of Second Workshop Scientific Results of FORV Sagar Sampada*, 239-248.

LaViolette, P.E., (1967). Temperature, Salinity and Density of the World's Seas: Bay of Bengal and Arabian Sea. *Informal Report No.67-57*, Naval Oceanographic Office, Washington D.C.

Levitus, S. & Boyer, T., (1994). World Ocean Atlas 1994, Vol 4: Temperature, NOAA Atlas NESDIS 4, U.S. Govt. Printing Office, 150.

Levitus, S., Burgett, R. & Boyer, T., (1994): World Ocean Atlas 1994, Vol 3: Salinity, NOAA Atlas NESDIS 3, U.S. Govt. Printing Office, 150.

LI Jian, YANG Lei, SHU Ye-Qiang &Wang Dong-Xiao, (2012). Temperature Inversion in the Bay of Bengal Prior to the Summer Monsoon Onsets in 2010 and 2011, A*tmospheric and Oceanic Science Letters*, 5, 290−294.

Lix, J. K., Venkatesan, R., Grinson, G., Rao, R. R., Jineesh, V. K., Arul, M.M., Vengatesan, G., Ramasundaram, S., Sundar, R. & Atmanand, M. A., (2016). Differential bleaching of corals based on El Niño type and intensity in the Andaman Sea, southeast Bay of Bengal. *Environmental Monitoring Assessment* 188, 175.

Lukas, R. & Lindstrom, E., (1991). The mixed layer of the western equatorial Pacific Ocean. *Journal of Geophysical Research*, 96, 3343-3357.

Madhu, N.V., Jyothibabu, R., Ramu, K., Sunil, V., Gopalakrishnan, T.C. & Nair, K.C., (2003). Vertical distribution of mesozooplankton biomass in relation to oxygen minimum layer in the Andaman Sea. *Indian Journal of Fisheries*, 50, 533-538.

Madhupratap, M., Achuthankutty, C.T., Sreekumaran Nair, S.R. & Vijayalakshmi, R. Nair., (1981). Zooplankton Abundance of the Andaman Sea. *Indian Journal of Marine Sciences*, 10, 258-261.

Madhupratap, M., Prasanna Kumar,S., Bhattathiri, P.M.A., Dileep kumar, M., Raghukumar, S., Nair., K.K.C. & Ramaiah, N., (1996). Mechanism of the biological response to winter cooling in the northeastern Arabian Sea. *Nature*, 384, 549 – 552.

Manickasundaram, M. & Ramaiyan, V., (1989). On some fish eggs and larvae from the Andaman and Nicobar seas. *Proceedings of First Workshop Scientific Results of FORV Sagar Sampada*, 193-199.

Manikiam, B., (1988). Remote Sensing Techniques for Ocean-related studies. *Current Science*, 57, 764–767.

Masson, S., McCreary, P. & Kohler, K., (2002). A model study of the seasonal variability and formation mechanisms of the barrier layer in the eastern equatorial Indian Ocean. *Journal of Geophysical Research*, 107, 18-20.

McCreary, J.P., Kundu, P.K. & Molinari, R.L., (1993). A numerical investigation of dynamics, thermodynamics and the mixed layer processes in the Indian Ocean. *Progress in Oceanography*, 31, 181-244.

Meyers, S. D., Kelly, B.G. & O'Brien, J.J., (1993). An introduction to wavelet analysis in oceanography and meteorology: With application to the dispersion of Yanai waves. *Monthly Weather Review*, 121, 2858–2866.

Miles, J.W. (1961). On the stability of heterogeneous shear flows. *Journal of Fluid Mechanics*, 10, 496-508.

Morel, A. & Berthon, J., (1989). Surface pigments, algal biomass profiles, and potential production of the euphotic layer: Relationships reinvestigated in view of remote-sensing applications. *Limnology and Oceanography*, 34, 1545 – 1562.

Muley, E.V., Subramanian, B.R., Venkataraman K. & Wafar, M., (2000). Status of coral reefs of India. *9th International Coral Reef Symposium*, Bali Indonesia Abstract, 360.

Murty, C.S., Das, P.K. & Gouveia, A.D., (1981). Some Physical aspects of the waters around the Little Andaman Island. *Indian Journal of Marine Sciences*, 10, 221-227.

Naik, S., & Reddy, C.V.G., (1983). Calcium phosphate saturation in sea water around the Andaman Island. *Indian Journal of Marine Sciences*, 12, 112-114.

Nienhaus, M. J., Subrahmanyam, B. & Murty, V.S. N., (2012). Altimetric observations and model simulations of coastal Kelvin Waves in the Bay of Bengal, *Marine Geodesy*, 35(1), 190–216.

Nuncio, M. & Prasanna Kumar, S., (2012). Life cycle of eddies along the western boundary of the Bay of Bengal and their implications, *Journal of Marine Systems*, 94, 9-17.

Okubo, A., (1970). Horizontal dispersion of floatable particles in the vicinity of velocity singularities such as convergences. *Deep Sea Research*, 17, 445-454.

Osborne, A.R., (1990). The generation and propagation of internal solitons in the Andaman Sea. *In Soliton Theory: A Survey of Results*. A.P. Fordy (ed.) Manchester: Manchester University Press, 152-173.

Osborne, A.R. & Burch, T.L., (1980). Internal Solitons in the Andaman Sea. *Science*, 208, 451-460.

Pant, A., (1992). Primary productivity in coastal and offshore waters of India during two southwest monsoon, 1987 and 1989. In: *Oceanography of the Indian Ocean*, B. N. Desai (Ed.), Oxford and IBH Publ. Co.

Paul, S., Chakraborty, A., Pandey, P.C., Basu, S., Satsangi, K. & Ravichandran, M., (2009). Numerical Simulation of Bay of Bengal Circulation Features from Ocean General Circulation Model, *Marine Geodesy, 32*, 1 - 18.

Pillai, H.U.K, Jayaraj, K.A., Rafeeq, M., Jayalakshmi, K.J. & Revichandran, C., (2011). Mesozooplankton distribution near an active volcanic island in the Andaman Sea (Barren Island). *Environmental Monitoring and Assessment*, 176, 239-250.

Pond, S. & Pickard, G.L., (1983). *Introduction to Dynamical Oceanography*; 2nd Edition. Butterworth-Heinemann Ltd: Woburn, MA.

Potemra, J.T., Luther, M.E. & O'Brien, J.J., (1991). The seasonal circulation of the upper ocean in The Bay of Bengal. *Journal of Geophysical Research*, 96, 667-683.

Prasanna Kumar, S. & Prasad, T.G., (1996). Winter cooling in the northern Arabian Sea. *Current Science*, 71, 834-841.

Praveen Kumar, B., Vialard, J., Lengaigne, M., Murty, V.S.N. & McPhaden, M.J., (2012a). TropFlux: Air-sea fluxes for the global tropical oceans – description and evaluation. *Climate Dynamics*, 38, 1521-1543.

Qasim, S.Z. & Ansari, Z.A., (1981). Food Components of the Andaman Sea, *Indian Journal of Marine Sciences*, 10, 276-279.

Rama Raju, D. V., Gouveia, A. D., & Murthy, C. S. (1981). Some physical characteristics of Andaman Sea Waters during winter. *Indian Journal of Marine Sciences*, 10, 211–218.

Ramaswamy, V., Rao, P.S., Rao, K.H., Thwin, S., Rao, N.S. & Raiker, V., (2004). Tidal influence on suspended sediment distribution and dispersal in the northern Andaman Sea and Gulf of Martaban. *Marine Geology*, 208, 33–42.

Rama Raju, D.V., Gouveia, A.D. & Murthy, C.S., (1981). Some physical characteristics of Andaman Sea Waters during winter. *Indian Journal of Marine Sciences*, 10, 211–218.

Ramesh Babu, V. & Sastry, J.S., (1976). Hydrography of the Andaman Sea during late winter. *Indian Journal of Marine Sciences*, 5, 179-189.

Rao, D.V., (2010). Field Guide to Coral and Coral Associates of Andaman and Nicobar Islands: (Published by the Director, Zool. Surv. India, Kolkata), 1-283.

Rao, R.R & Sivakumar, R., (2003).Seasonal variability of sea surface salinity and salt budget of the mixed layer of the north Indian Ocean. *Journal of Geophysical Research*, 108, 1-13.

Rao, R.R., Girish Kumar, M.S., Ravichandran, M., Rao, A.R., Gopalakrishna, V. V. & Thadathil, P., (2010). Interannual variability of Kelvin wave propagation in the wave guides of the equatorial Indian Ocean, the coastal Bay of Bengal and the southeastern Arabian Sea during 1993–2006. *Deep Sea Research I*, 57, 1–13.

Riley, J.P & Chester, R., (1971). Introduction to marine chemistry. London: Academic Press. Inc. Ltd, 465.

Robinson, R.A.J., Bird, M.I., Oo, N.W, Hoey, T.B., Aye, M.M.D., Higgitt, L., Lud, X.X., Swe, A., Tun, T. & Win, S.L., (2007). The Irrawaddy river sediment flux to the Indian Ocean: the original nineteenth-century data revisited. *Journal of Geology*. 115, 629–640.

Rosamma, S. & Meenakshikunjamma, P.P., (1996). Ostracods of Andaman Sea. *Proceedings of Second Workshop Scientific Results of FORV Sagar Sampada*, 197-203.

Salini, T.C., Fanimol, C.L., Smitha, B.R., Jayalakshmi, K.J., Asha Devi, C.R., Sanjeevan, V.N., Saravanane, N. & Sajeev, R., (2010). Oceanography of the Andaman Waters: Physico-chemical and biological characteristics during January 2009. In: Indian Ocean Marine Living Resources, Book of Abstracts (Ed. G.V.M.Gupta et al), Centre for Marine Living Resources and Ecology, Ministry of Earth Sciences, Kochi, 29.

Salini, T.C., Smitha, B.R., Sajeev, R. & Sanjeevan, V.N., (2018). Upper layer circulation, hydrography, and biological response of the Andaman waters during winter monsoon based on in situ and satellite observations. *Ocean Dynamics*, 68, 801-815.

Sanjeevan, V.N., Smitha, B.R., Ashadevi, C.R., Abdul Jaleel, K.U. & Jayalalshmi, K.J., (2011). Revalidation of Potential Yield from Indian EEZ: A trophodynamic approach, in: Report of the Working Group for revalidating the potential of fishery resources in the Indian EEZ, (Ministry of Agriculture, New Delhi), 50-60.

Sarma, V.V.S.S. & Narvekar, P.V., (2000). A study on inorganic carbon components in the Andaman Sea during the post monsoon season. *Oceanologica Acta*, 24 (2), 125-134.

Sarojini, Y. & Sarma, N.S., (2001). Vertical distribution of phytoplankton around Andaman and Nicobar Islands, Bay of Bengal. *Indian Journal of Marine Sciences*, 30, 65-69.

Sarupriya, J.S. & Bhargava, R.M.S., (1993). Seasonal Primary Production in different sectors of the EEZ of India. *Mahasagar*, 26, 139-147.

Schott, F. A., Xie, S.P. & McCreary Jr., J.P., (2009). Indian Ocean circulation and climate variability, *Reviews of Geophysics*, 47, RG1002.

Sengupta, D., Bharath Raj, G.N. & Shenoi, S.S.C., (2006). Surface freshwater from Bay of Bengal runoff and Indonesian throughflow in the tropical Indian Ocean, *Geophysical Research Letters*, 33, L22609.

Sengupta, R., Moraes, C., George, M.D., Kureishy, T.W., Noronha, R.J. & Fondekar, S.P., (1981). Chemistry and Hydrography of the Andaman Sea. *Indian Journal of Marine Sciences*, 10, 228-233.

Sewell, R.B.S., (1929). Geographic and oceanographic research in Indian waters, Part V. Temperature and salinity of surface waters of the Bay of Bengal and Andaman Sea, with references to the Laccadive Sea. *Memoirs of the Asiatic Society of Bengal*, 9, 207-355.

Shankar, D., McCreary, J.P., Han, W. & Shetye, S.R., (1996). Dynamics of the East India Coastal Current. *Journal of Geophysical Research*, 101, 13975-13991.

Shenoi, S.S.C., Shankar, D. & Shetye, S.R., (2002). Differences in heat budgets of the near- surface Arabian Sea and Bay of Bengal: Implications for the summer monsoon. *Journal of Geophysical Research*, 107, C6, 3052.

Shetye, S.R., Gouveia, A.D., Shankar, D., Shenoi, S.S.C., Vinayachandran, P.N., Sundar, D., Michael, G.S. & Nampoothiri, G., (1996). Hydrography and circulation in the western Bay of Bengal during the northeast monsoon, *Journal of Geophysical Research*, 101, 14011–14026.

Sindhu, B., Suresh, I., Unnikrishnan, A.S., Bhatkar, N.V., Neetu, S. & Michael, G S., (2007). Improved bathymetric datasets for the shallow water regions in the Indian Ocean. *Journal of Earth System Sciences*, 116(3), 261-274.

Sprintall, S.R. & Tomczak, M., 1993. Evidence of the barrier layer in the surface layer of the tropics. *Journal of Geophysical Research*, 97: 7305-7316.

Sreenivas, P., Gnanaseelan, C. & Prasad, K. V. S. R., (2012). Influence of El Niño and Indian Ocean Dipole on sea level variability in the Bay of Bengal. *Global and Planetary Change*, 80, 215-225.

Subrahmanyam, B., Robinson, I.S., Blundell, J.R. & Challenor, P.G., (2001). Indian Ocean Rossby waves observed in TOPEX/POSEIDON altimeter data and in model simulations. *International Journal of Remote Sensing*, 22, 1, 141-167.

Suwannathatsa, S., Wongwises, P., Wannawong, W. & Vongvisessomjai, S., (2012). The Coastal Current of the Andaman Sea Revealed by Reprocessed Observations. *American Journal of Applied Sciences*, 9 (7), 1079-1084.

Syamsul Rizal, Peter Damm, Mulyadi A. Wahid, Jurgen Sundermann, Yopi Ilhamsyah, Taufiq Iskandar & Muhammad, (2012). General Circulation in the Malacca Strait and Andaman Sea: A Numerical Model Study. *American Journal of Environmental Science*, 8 (5), 479-488.

Tan, C.K., Ishizaka, J., Matsumura, S., Yusoff, FMd. & Mohamed, M.I.H. (2006). Seasonal variability of SeaWiFS chlorophyll a in the Malacca Straits in relation to Asian monsoon. *Continental Shelf Research*, 26, 168-178.

Thadathil, P., Muraleedharan, P.M., Rao, R.R., Somayajulu, Y.K., Reddy, G.V. & Revichandran, C. (2007). Observed seasonal variability of barrier layer in the Bay of Bengal. *Journal of Geophysical Research*, 112.

Tikader, B.K., Daniel, A. & Subba Rao, N.V., (1986). Sea shore Animals of Andaman & Nicobar Islands. Zoological Survey of India, Culcutta: 1-188.

Torrence, C. & Compo, G.P., (1998). A Practical Guide to Wavelet Analysis, *Bulletin of the American Meteorological Society*, 79, 61-78.

Unnikrishnan, A.S. & Bahulayan, N., (1991). Simulation of barotropic wind-driven circulation in the Bay of Bengal and Andaman Sea during premonsoon and postmonsoon seasons. *Indian Journal of Marine Sciences*, 20, 97-101.

Varkey, M.J., Murty, V.S.N & Suryanarayana, A., (1996). Physical oceanography of Bay of Bengal and Andaman Sea. *Oceanography and Marine Biology: An annual Review.* University College London Press, 1-70.

Vijayalakshmi R. Nair & Gireesh, R., (2010). Biodiversity of chaetognaths of the Andaman Sea. Indian Ocean. *Deep Sea Research II*, 57, 2135-2147.

Vialard, J., Jayakumar, A., Gnanaseelan, C., Lengaigne, M., Sengupta, D. & Goswami, B. N. (2012). Processes of 30–90 day sea surface temperature variability in the Northern Indian Ocean during boreal summer, *Climate Dynamics*, 38, 1901-1916.

Vialard, J., Shenoi, S.S.C., McCreary Jr, J.P., Shankar, D., Durand, F., Fernando, V., & Shetye, S.R. (2009). Intraseasonal response of the northern Indian Ocean coastal waveguide to the Madden-Julian Oscillation, *Geo Physical Research Letters*, 36.

Vinayachandran, P.N., Shetye, S.R., Sengupta, D. & Gadgil, S. (1996). Forcing mechanisms of the BoB circulation, *Current Science*, 71, 10, 753-763.

Vinayachandran, P.N., Murty, V.S.N. & Ramesh Babu, V., (2002). Observations of barrier layer formation in the Bay of Bengal during summer monsoon. *Journal of Geophysical Research,* 107.

Wang, B., Webster, P., Kikuchi**,** K., Yasunari, T. & Qi, Y., (2006). Boreal summer quasi-monthly oscillation in the global tropics. *Climate Dynamics*, *27*, 661-675.

Weiss, J., (1991). The dynamics of enstrophy transfer in two-dimensional hydrodynamics. *Physica D*, 48, 273-294.

White, W. B., (1977). Annual forcing of baroclinic long waves in the tropical North Pacific. *Journal of Physical Oceanography*, 7, 50–61.

Wyrtki, K., (1961). Physical oceanography of the Southeast Asian waters. 1st Ed. University of California, California, 195.

Wyrtki, K., (1971). Oceanographic atlas of the International Indian Ocean Expedition. NSF, Washington, DC.

Wyrtki, K., (1973). Physical Oceanography of the Indian Ocean. London: Chapman and Hall Ltd. 18-37.

Yang, J., Yu, L., Koblinsky, C.J. & Adamec, D., (1998). Dynamics of the seasonal variations in the Indian Ocean from TOPEX/POSEIDON sea surface height and an ocean model. *Geophysical Research Letters*, 25, 1915–1918.

Yu, L., (2003). Variability of the depth of the 20°C isotherm along 6°N in the BoB: its response to remote and local forcing and its relation to satellite SSH variability. *Deep Sea Research II*, 50, 2285–2304.

Yu, L. S. & Rienecker, M.M., (1999). Mechanisms for the Indian Ocean warming during the 1997-98 El Nino. *Geophysical Research Letters*, 26735738.

Yu, L., O'Brien, J.J. & Yang, J., (1991). On the remote forcing of the circulation in the BoB, eastern Indian Ocean, *Journal of Geophysical Research*, 114.